UNIVERSITAT POLITÈCNICA
DE CATALUNYA

Ph.D. Thesis

Contribution to the Optimization of 4G Mobile Communications by Means of Advanced Carrier Aggregation Strategies

Author: María Angel Lema Rosas

Advisor: Mario García-Lozano, Ph. D.
Associate Professor
Universitat Politècnica de Catalunya (UPC)

Wireless Communications and Technologies Research Group
Department of Signal Theory and Communications
Universitat Politècnica de Catalunya

Barcelona, May 2015

Abstract

Mobile broadband subscriptions and data traffic have increasingly grown in the past few years with the deployment of the 3G and 4G technologies and the massive use of mobile devices. In this sense, Long Term Evolution Advanced (LTE-A) has been presented as the next step in wireless communications where higher data rates are targeted and fully packet switched services are held. The ultimate goal of 4G and the forthcoming 5G technology is to increase the Quality of Experience (QoE) of users. In this context, several challenges open up to face the increased bandwidth demands in both uplink and downlink. To this end, LTE-A has proposed the use of Carrier Aggregation (CA) which allows the simultaneous data transmission in two separated pieces of spectrum, thus constituting a wise solution that facilitates the use of the fragmented spectrum and allows to increase the transmission bandwidth.

The improvements brought by CA in the downlink can be almost straightforward appreciable, since the evolved Node B (eNB) is in charge of transmissions, and where power availability is not typically an issue. Conversely, the uplink presents many open challenges to introduce aggregated transmissions, since it relies on the user terminal for transmission procedures. Lower transmission power and increased interference variability turn the uplink into a more complex framework than the downlink. For this reason, this Ph.D. thesis provides a contribution to the field of CA for uplink mobile systems. The novelties here presented address the main limitations the uplink encounters when introducing CA; new methods and strategies are proposed with the final objective of enhancing the uplink communications with the use of increased bandwidth transmissions, thus reducing the unbalanced data rate between the uplink and downlink.

Throughout an exhaustive literature review, the main research opportunities and potential improvements to successfully implement CA in the uplink were identified. In particular, three main blocks can be recognized. First, the need for introducing intelligent Radio Resource Management (RRM) procedures that provide the user with increased QoE especially in the cell edge, where users are more likely to be power limited, and aggregated transmissions are typically discarded. Consequently, the first part of this dissertation places emphasis on topics related to resource scheduling and the user power limitation to face the increased bandwidth transmissions. Two relevant contributions are presented in this line, first, a scheduler capable of allocating aggregated resources based on the user specific power capabilities; second, a CA

eligibility method that selects users not only based on their power availability but also considering the intrinsic gain brought by wider bandwidth allocations. Results show that significant improvements can be obtained especially in the cell edge, where it is encouraged to introduce CA.

Indeed, both strategies strongly rely on an accurate improved Channel State Information (CSI), it is of utmost importance to possess precise CSI to effectively support these assessments. In this line, the second part deals with the imperfect CSI where the efficient use of reference signals provides a high value. The potential constraints that impact the CSI are studied, and several strategies to reduce the imperfect CSI are evaluated. In particular, channel prediction techniques have been proposed with the use of the splines method. However, the increased variability of interferences and the high delay in measurements still impairs the CSI accuracy. Thus, interference cancellation is introduced to support the prediction method, however, results show that increased channel reporting intervals are as detrimental as the interferences. In this manner, two well-known inter-cell interference methods are studied with a twofold objective: first, to control the interference generated, and second, to reduce the delay in CSI reporting by limiting the available bandwidth. Results show that improvements can be obtained with inter-cell interference coordination schemes as long as the scheduling flexibility is not voided by limiting in excess the available bandwidth.

Finally, since CA constitutes the most transverse topic of the new features added to the 4G standard, the last block of research focuses on the opportunities that emerge with the use of CA in the context of heterogeneous networks, and new system designs are addressed. It is proposed to use dual connectivity in the form of decoupled uplink and downlink connections in a CA context, where aggregated carriers may have different coverage footprints. An analysis of two different cell association cases has been driven. Stochastic geometry is used to study the system analytically, propagation conditions in the different tiers and frequencies are considered and the different association cases are compared to a classical downlink received power association rule. Conclusions show that decoupling the uplink provides the system with outstanding gains, however being connected to the cell that receives the highest received power may not always be profitable, since issues like interferences or load conditions shall be also considered.

Resumen

El número de usuarios móviles y el tráfico de datos generado han aumentado en los últimos años con el despliegue de redes 3G y 4G y el uso masivo de dispositivos móviles. De este modo, *Long Term Evolution Advanced* (LTE-A) surge como el siguiente escalón de las comunicaciones móviles, dónde se apunta a mayores velocidades de transmisión y los servicios ofrecidos se basan en la conmutación de paquetes. El objetivo principal de las redes 4G y de la inminente red 5G es aumentar la calidad de la experiencia del usuario. En este contexto, se presentan nuevos retos para hacer frente a las demandas de incrementar el ancho de banda en ambos enlaces: ascendente y descendente. Por ello, LTE-A propone el uso de portadoras agregadas, en inglés *Carrier Aggregation* (CA), una tecnología que permite la transmisión simultánea en dos regiones separadas del espectro, proporcionando así una solución vital al problema del uso del espectro fragmentado, y además, permitiendo incrementar el ancho de banda de transmisión.

Las mejoras que aporta CA en el enlace descendente son casi inmediatas dado que las transmisiones corren a cargo del evolved Node B (eNB), el cual no sufre la falta de potencia disponible. Al contrario, en el enlace ascendente se presentan más retos para introducir CA, ya que es el terminal quién se encarga de los procedimientos de transmisión. La baja disponibilidad de potencia y la alta variabilidad de las interferencias convierten al enlace ascendente en un entorno mucho más complejo. Por ello, esta disertación presenta una contribución al campo de CA para enlaces ascendentes en sistemas de comunicaciones móviles. Las novedades presentadas en este documento tratan las principales limitaciones para incorporar CA; se proponen nuevos métodos y estrategias con el objetivo final de mejorar las comunicaciones en el enlace de subida mediante el uso de transmisiones agregadas, todo ello, para reducir el desajuste que existe entre la velocidad de transmisión de subida y la de bajada.

Mediante una extensa revisión de la literatura, se han detectado las principales líneas de investigación y potenciales mejoras para incorporar CA de manera exitosa. Se han identificado tres grandes bloques de investigación. Primero, la necesidad de introducir estrategias de asignación de recursos radio inteligentes, que proporcionen al usuario una mejora de la experiencia, especialmente en el límite de la celda. Es allí donde los usuarios tienen una mayor probabilidad de estar limitados en potencia, razón por la cual normalmente se les aparta de CA. Consecuentemente, la primera

parte de esta tesis pone énfasis en temas relacionados con la asignación de recursos, y las limitaciones en potencia por parte del usuario para hacer frente a un incremento del ancho de banda. En concreto, se presentan dos contribuciones principales, la primera, un método de repartición de recursos capaz de asignar anchos de banda no contiguos a usuarios, basándose en la disponibilidad de potencia de estos; en segundo lugar, un método de elección de usuarios para CA que no solamente considera las limitaciones en potencia, sino que también, cuenta con las ganancias intrínsecas de transmitir en anchos de banda mayores.

En efecto, para apoyar el funcionamiento de estas estrategias de asignación, y para asegurar su máximo rendimiento, es necesario un método que proporcione un conocimiento del estado del canal preciso y fidedigno. De este modo, la segunda parte de la investigación lidia con la información del estado del canal, en inglés *Channel State Information* (CSI), donde el uso eficiente de las señales de referencia son de gran importancia. Se estudian los principales condicionantes que impactan a la obtención del CSI, y se evalúan diferentes propuestas para reducir el error en las medidas. Particularmente, se proponen técnicas de predicción de señal mediante el uso de Splines. Sin embargo, la alta variabilidad de las interferencias y el gran retardo en las medidas del canal perjudican la precisión. De este modo, se introducen métodos de cancelación de interferencias para ayudar a las predicciones; no obstante, los resultados reflejan que los retardos en las medidas pueden llegar a ser tan perjudiciales como las interferencias. Por ello, se estudian dos mecanismos de control de interferencias con un doble objetivo: controlar la interferencia generada en la celda, y reducir el retardo limitando el ancho de banda disponible. Los resultados muestran mejoras siempre y cuando la flexibilidad de la asignación de recursos no se vea afectada por la reducción excesiva del ancho de banda.

Finalmente, dado que CA es una de las funciones más transversales de las introducidas por el estándar 4G, la última parte de investigación se centra en las oportunidades que surgen con su uso en el contexto de redes heterogéneas. Se propone el uso de la conectividad dual, concretamente desacoplando el enlace ascendente del descendente con el uso de CA, donde el área de cobertura de las portadoras agregadas puede ser diferente. Se analizan dos escenarios de asociación posibles en este entorno. Mediante el uso de geometría estocástica se lleva a cabo el modelado del sistema, considerando diferentes condiciones de propagación en los distintos tipos de celda y frecuencias; los diferentes escenarios de asociación se comparan a un escenario tradicional en el cual los usuarios se asocian en función de la potencia recibida de las bases. Las conclusiones destacan que el desacoplo aporta mejoras en el enlace ascendente. Sin embargo, temas como interferencias o carga deben también considerarse.

Resum

El nombre d'usuaris mòbils i el tràfic de dades generat han augmentat en els últims anys amb el desplegament de les xarxes 3G i 4G i l'ús massiu de dispositius mòbils. D'aquesta manera, *Long Term Evolution Advanced* (LTE-A) sorgeix com el següent graó de les comunicacions mòbils, on s'apunta a majors velocitats de transmissió i els serveis oferts es basen en la commutació de paquets. L'objectiu principal de les xarxes 4G i de la imminent xarxa 5G és augmentar la qualitat de l'experiència de l'usuari. En aquest context, es presenten nous reptes per fer front a les demandes d'incrementar l'ample de banda en tots dos enllaços: ascendent i descendent. Per això, LTE-A proposa l'ús de portadores agregades, de l'anglès *Carrier Aggregation* (CA), una tecnologia que permet la transmissió simultània en dues regions separades de l'espectre, proporcionant així una solució vital al problema de l'ús de l'espectre fragmentat, i a més, permetent incrementar l'ample de banda de transmissió.

Les millores que aporta CA a l'enllaç descendent són gairebé immediates atès que les transmissions són a càrrec del evolved Node B (eNB), el qual no sofreix la falta de potència disponible. Al contrari, a l'enllaç ascendent es presenten més reptes per introduir CA, ja que és el terminal qui s'encarrega dels procediments de transmissió. La baixa disponibilitat de potència i l'alta variabilitat de les interferències, converteixen a l'enllaç ascendent en un entorn molt més complex. Per això, aquesta dissertació presenta una contribució al camp de CA per a enllaços ascendents en sistemes de comunicacions mòbils. Les novetats presentades en aquest document tracten les principals limitacions que es troben per incorporar CA; es proposen nous mètodes i estratègies amb l'objectiu final de millorar les comunicacions a l'enllaç de pujada mitjançant l'ús de transmissions agregades, tot això, per reduir el desajustament que existeix entre la velocitat de transmissió de pujada i la de baixada.

Mitjançant una extensa revisió de la literatura, s'han detectat les principals línies de recerca i potencials millores per incorporar CA de manera reeixida. S'han identificat tres grans blocs de recerca. Primer, la necessitat d'introduir estratègies d'assignació de recursos radio intel·ligents, que proporcionin a l'usuari una millora de l'experiència, especialment en el límit de la cel·la. És aquí on els usuaris tenen una major probabilitat d'estar limitats en potència, raó per la qual normalment se'ls aparta de CA. Conseqüentment, la primera part d'aquesta tesi posa èmfasi en temes relacionats amb l'assignació de recursos, i les limitacions en potència per part de l'usuari per fer front a un increment de l'ample de banda. En concret, es presenten

dues contribucions principals, la primera, un mètode de repartició de recursos capaç d'assignar amples de banda no contigus a usuaris, basant-se en la disponibilitat de potència d'aquests; en segon lloc, un mètode d'elecció d'usuaris per a CA que no només considera les limitacions en potència, sinó que també, compta amb els guanys intrínsecs de transmetre en amples de banda majors.

No obstant això, per recolzar el funcionament d'aquestes estratègies d'assignació, i per assegurar el seu màxim rendiment, és necessari un mètode que proporcioni un coneixement de l'estat del canal precís i fidedigne. D'aquesta manera, la segona part de la recerca brega amb la informació de l'estat del canal, de l'anglès *Channel State Information* (CSI), on l'ús eficient dels senyals de referència són de gran importància. S'estudien els principals condicionants que impacten a l'obtenció del CSI, i s'avaluen diferents propostes per reduir l'error en les mesures. Particularment, es proposen tècniques de predicció de senyal mitjançant l'ús de Splines. No obstant això, l'alta variabilitat de les interferències i el gran retard en les mesures del canal perjudiquen la precisió. D'aquesta manera, s'introdueixen mètodes de cancel·lació d'interferències per ajudar a les prediccions; amb tot, els resultats reflecteixen que els retards en les mesures poden arribar a ser tan perjudicials com les interferències. Per això, s'estudien dos mecanismes de control d'interferències amb un doble objectiu: controlar la interferència generada a la cel·la, i reduir el retard limitant l'ample de banda disponible. Els resultats mostren millores sempre i quan la flexibilitat de l'assignació de recursos no es vegi afectada per la reducció excessiva de l'ample de banda.

Finalment, atès que CA és una de les funcions més transversals de les introduïdes per l'estàndard 4G, l'última part de la recerca es centra en les oportunitats que sorgeixen amb el seu ús en el context de xarxes heterogènies. Es proposa l'ús de la connectivitat dual, concretament desacoblant l'enllaç ascendent del descendent amb l'ús de CA, on l'àrea de cobertura de les portadores agregades pot ser diferent. S'analitzen dos escenaris d'associació possibles en aquest entorn. Mitjançant l'ús de geometria estocàstica es duu a terme el modelatge del sistema, considerant diferents condicions de propagació en els diferents tipus de cel·la i freqüències; els diferents escenaris d'associació es comparen a un escenari tradicional en el qual els usuaris s'associen en funció de la potència rebuda de les bases. Les conclusions destaquen que el desacoblo aporta millores en el UL. No obstant això, temes com les interferències o la càrrega a la cel·la han de considerar-se també.

Acknowledgements

Con estas líneas cierro el que, hasta ahora, ha sido el capítulo más importante de mi corta vida. Un camino de constantes subidas y bajadas, duro, pero sobretodo, muy gratificante. Quiero expresar mi más sincera gratitud a Silvia Ruiz, por abrirme las puertas del mundo de la investigación. Gracias por confiar en mí, la motivación que un día me regalaste, se ha convertido en una verdadera vocación.

Un enorme Gracias a mi director de tesis, Mario García-Lozano. Gracias por tus ánimos, por la motivación y por siempre indicarme el camino hacia la excelencia. De tí he aprendido a no dejarme llevar por los momentos buenos, ni a derrumbarme en los malos, a siempre buscar la respuesta correcta, o la pregunta correcta.

Agradezco a Joan Olmos por toda la ayuda brindada en el soporte técnico de esta tesis, y extiendo mi gratitud a todo el equipo de Wicomtec, por la oportunidad de realizar esta tesis dentro del proyecto de la CICYT.

I would like to express my gratitude to Prof. Mischa Dohler, for receiving me at King's College London, where I have learned so much. Thank you for encouragement and support, you have made my stay in London really motivating and very fruitful. Also, thanks to all the people in the CTR for such a warm welcome.

Gracias a mis amigos, por acompañarme durante todo este proceso, por el interés, por los momentos de desconexión que me habéis dado, habéis sido un gran apoyo.

Y, finalmente, quiero dedicar esta tesis a las personas más importantes de mi vida: mis padres y mis hermanos, gracias por animarme a perseguir mis sueños, por ser mi modelo a seguir, *Persevera y triunfarás...* resuena siempre en mi cabeza; y a mi otra mitad, Mathew, gracias por caminar a mi lado, por extenderme tu mano cuando me quedo por detrás, por tu paciencia ... por millones de razones más.

Contents

Acronyms

3GPP	Third Generation Partnership Project
4G	Fourth Generation
5G	Fifth Generation
ABS	Almost Blank Subframes
AC	Admission Control
BCD	Both Carrier DUDe
BLER	BLock Error Rate
CA	Carrier Aggregation
CC	Component Carrier
cdf	Cumulative Distribution Function
CDM	Code Division Multiplex
CoMP	Cooperative Multi-Point
CQI	Channel Quality Indicator
CSI	Channel State Information
DFT-S-OFDM	Discrete Fourier Transform - Spread - OFDM
DL	DownLink
DLRP	DownLink Received Power
DTX	Discontinuous Transmission and Reception
DUDe	DownLink-Uplink Decoupling
eICIC	enhanced ICIC
eNB	evolved Node B
EPB	Extended Pedestrian B
FD	Frequency Domain
FDD	Frequency Division Duplex
FDM	Frequency Division Multiplex
FFR	Fractional Frequency Reuse

FPC	Fractional Power Control
HARQ	Hybrid Automatic Repeat Request
HetNet	Heterogeneous Network
IC	Interference Cancellation
ICIC	Inter-Cell Interference Coordination
ICS	Independent Carrier Scheduling
IoT	Interference over Thermal
ISD	Inter Site Distance
ITU-R	International Telecommunications Union - Radio
JCS	Joint Carrier Scheduling
LMS	Least Mean Square
LTE	Long Term Evolution
LTE-A	Long Term Evolution-Advanced
MAC	Medium Access Control
MCell	Macro Cell
MCS	Modulation and Coding Schemes
MIMO	Multiple Input Multiple Output
MMSE	Minimum Mean Square Error
MMSE-IRC	MMSE-Interference Rejection Combining
MPR	Maximum Power Reduction
MSE	Minimum Square Error
MU-MIMO	Multi User MIMO
OFDMA	Orthogonal Frequency Division Multiple Access
OLPC	Open Loop Power Control
PA	Power Amplifier
PAPR	Peak-to-Average Power Ratio
PCC	Primary Component Carrier
PCD	Per Carrier DUDe
PDCCH	Physical Dlownlink Control Channel
PDCP	Packet Data Convergence Protocol
pdf	Probability Density Function
PF	Proportional Fair
PHR	Power Headroom Report
PPP	Poisson Point Process

PRB	Physical Resource Block
PSD	Power Spectral Density
PUSCH	Physical Uplink Shared Channel
QoE	Quality of Experience
QoS	Quality of Service
RAT	Radio Access Technology
RE	Range Expansion
RLC	Radio Link Control
RR	Round Robin
RRC	Radio Resource Control
RRH	Radio Remote Head
RRM	Radio Resource Management
RSRP	Reference Signal Received Power
RSRQ	Reference Signal Received Quality
RTT	Round Trip Time
RU	Resource Utilization
SCC	Secondary Component Carrier
SCell	Small Cell
SC-FDMA	Single Carrier Frequency Division Multiple Access
SFR	Soft Frequency Reuse
SI	System Information
SINR	Signal-to-Interference-plus-Noise-Ratio
SIR	Signal-to-Interference-Ratio
SNR	Signal-to-Noise-Ratio
SRS	Sounding Reference Signal
TD	Time Domain
TTI	Transmission Time Interval
UE	User Equipment
UL	UpLink
UTM	Universal Transverse Mercator

List of Tables

List of Figures

Chapter 1

Introduction

1.1 Background and Motivation

Nowadays society has settled to immediate broadband access everywhere. It relies on its mobile connectivity and generates greater traffic demands on the wireless network. During the past years, the overall infrastructure has been forced to evolve and meet the demands of a new type of user: data-centric. This evolution has made the research community and standardization organisms increase their efforts in creating new standards of communications, capable of evolving from one technology to another, with the aim of increasing the data rate and improving users Quality of Service (QoS). From the operator's perspective it is mandatory to provide the best user experience and also user differentiation. To this purpose, it is essential that networks are deployed spectrally efficient and offer QoS to users. All this must be accomplished while assuring a reduced energy consumption and economic cost.

Long Term Evolution (LTE) rises as the evolution of Third Generation Partnership Project (3GPP) radio technologies towards the Fourth Generation (4G). However, LTE requirements defined in [1] and system performance [2] do not fulfill the terms established by the International Telecommunications Union - Radio (ITU-R) for the 4G standards [3]. In particular, those regarding data bit rate, spectral efficiency and available bandwidth were far from being achieved. In fact, one of the key requirements is the support for variable badwidths up to 100 MHz. For this reason, 3GPP evolved the first standardized version of LTE, Release 8, into LTE-Advanced (LTE-A), a novel technology which based on the foundations of the previous one, is the 3GPP technology for the 4G.

The deployment of a feasible high speed spectral efficient network needs a variety of innovative features given that link level solutions have evolved to near Shannon limit capacity with advanced Modulation and Coding Schemes (MCS) [4]. Given this, LTE-A addresses the major LTE gaps by offering pioneering solutions or improved versions of earlier releases proposals. Some of them are introduced in the following.

Enhanced Multiple Input Multiple Output (MIMO) techniques improve spectral efficiency of inner users in the cell; cooperative strategies, such as Cooperative Multi-Point (CoMP in 3GPP) boosts the spectral efficiency in the cell edge by entailing the coordination of transmissions or receptions. Inter-cell Interference Coordination (ICIC) techniques have been also recognised as a means to improve the edge performance, indeed the 3GPP includes within the LTE standard mechanisms that help to the deployment of innovative ICIC schemes. To increase spectral efficiency and fairness in the entire cell, it is necessary to move on to denser topologies. In the 3GPP context it is introduced the concept of heterogeneous networks, which are macro or micro cells together with small cells (Pico, femto, Radio Remote Heads (RRH), relays) that are used to enhance the cell performance. Note that this definition is different to that of classic Heterogeneous Networks understood as a composition of multiple RATs (Radio Access Technologies), for this reason the 3GPP nomenclature HetNet is preferred in the following.

Indeed, the mentioned techniques are useful for increasing the spectral efficiency and fairness. However, these do not contribute to the large bandwidth demand to achieve high data rates. With this purpose, LTE-A introduces Carrier Aggregation (CA), technique that allows the simultaneous transmission on different carriers, named Component Carriers (CC), extending the accessible bandwidth. Given the rare availability of large portions of spectrum, it facilitates an efficient use of the fragmented parts and so allows the operator to make the most of its usable bandwidth. As a matter of fact, the idea of having more than one CC for a single evolved Node-B (eNB) enables a high number of design options besides the increased capacity or flexible usage of spectrum. Bandwidth extension provides extra assets when combined with other 3GPP new features, such as HetNets or CoMP, improving load balancing or interference coordination. It is said, that CA is the most transverse topic of the new features added to the 4G standard.

CA is almost directly applicable in the Downlink (DL) since the use of Orthogonal Frequency Division Multiple Access (OFDMA) already facilitates the transmission of non contiguous resources. Also, power availability to face increased bandwidth allocations is not an issue, given that the eNB is in charge of the transmission. The most restrictive link is always the Uplink (UL), as it relies on the user terminal for transmission procedures. Given this, an extension in the transmitted bandwidth may not be beneficial owing to the User Equipment (UE) power limitations. In early releases of LTE it was agreed the use of Single Carrier - FDMA (SC-FDMA) as the technology for the UL. The main reason was the low Peak-to-Average Power Ratio (PAPR) generated in localized (contiguous) allocation of resources. Non-contiguous allocation generates higher PAPR which increases the difficulty in allocations, since cheap components must be considered when building the UE to make the device affordable. Lower transmission power and increased interference variability results in a poorer data rate. Altogether, as it is further discussed in the following chapters, there are increasingly more open challenges in the UL to implement CA.

This Ph.D. dissertation provides a contribution to the field of CA for UL cellular systems. In the main, original Radio Resource Management (RRM) algorithms in 4G/LTE-A networks for the UL have been investigated and proposed. Several open

issues in this field have been addressed and new methods, guidelines and strategies are proposed. Throughout the research process, emphasis was placed in coming up with realistic and applicable solutions to each problem, with the main objective of reducing the unbalanced data rate between UL and DL by:

- introducing smart decisions in the RRM processes, and assure that the UE capabilities of transmitting over the aggregated spectrum are considered;
- improving the UE Channel State Information (CSI) acquisition in the CA context to further enhance the UL performance;
- allowing novel cell association rules in heterogeneous deployments, where energy saving and constant user satisfaction along the cell radius are pursued.

The specific aspects that have been covered concerning this general objective are detailed in the next section.

1.2 Scope of the Dissertation and Structure

The main objective of this Ph.D. dissertation is the design of new and advanced CA strategies, mainly in the form of RRM procedures, so that UL communications in realistic deployments are enhanced. All this, with the final objective of contributing to the study of the theory and state-of-the-art of CA in the UL to reduce the existing imbalance between both UL and DL. With this aim, challenges and research efforts have been derived by studying the existent literature.

This document is composed of seven chapters and one appendix. After this introduction, the next five chapters comprise the core of the Ph.D dissertation. The final chapter closes this document with the conclusions and future research lines.

The first part of this document, chapter 2, is devoted to provide the reader with the background knowledge and clarifies the motivation and relevance of the research carried out in this work. In general terms, this part aims at pointing out the needs of improving the UL data transmissions in the context of mobile communications, and also explains the requirement of introducing new strategies in the UL to include CA achieving the highest gains.

Chapters 3, 4 and 5 deal with the improvement of Medium Access Control (MAC) and Radio Resource Control (RRC) layers procedures to maximize the gain of CA in the UL. It starts with a background description of the UL power control, followed by the new challenges that scheduling and CC selection procedures must face. Bearing in mind the UL power scarcity, the MAC layer scheduling process and the RRC layer CC selection process are configured to obtain the maximum spectral efficiency, conclusions of this study highlight the need for enhanced CSI to support it. This part ends with the proposal of novel techniques to address the CSI improvement. The last part of this dissertation, chapter 6, conducts an analytical study of UL data transmission improvement from a network perspective. Based on

HetNet deployments, this study includes the effect of changing the cell association rule to provide a more fair UL data rate with respect to the one in the DL. In the CA context several association opportunities arise, which are evaluated for the different possible aggregation scenarios.

The innovations, guidelines and new methodologies of study were obtained by means of studies based on practical engineering considerations, mathematical analysis and system level simulations. A dynamic UL LTE-A system level simulator fully programmed in C# has been developed during the period of the Ph.D. A complete description of this platform is given in appendix A. Next, a summary of each chapter is provided.

Chapter 2 starts with a generic overview of the CA technology, where special attention is paid to the system level issues and the RRM novelties that arise with the inclusion of this innovative feature. It justifies the need for improvements in the UL to successfully implement CA. Given the UE limited power and the strong variability of the interference map generated, emphasis must be placed on improving the RRM to achieve not only spectral efficient transmissions, but also reliable CSI. This chapter describes the most relevant RRM strategies that can be addressed to get the utmost gain out of bandwidth extension. Along with this, a detailed state of the art review is provided and comparisons among the contributions are done to detect the main challenges and potential improvements to be developed in the next sections. The chapter is divided into three main blocks. First, topics related to MAC and RRC layers procedures are addressed, where scheduling and UL power control are topics of major interest. Here, the literature review pays special attention to the contributions that consider the user capability of transmitting in CA. The second block is focused on the CSI acquisition, where Sounding Reference Signals (SRSs) are of paramount importance. References regarding this topic are centered on contributions that propose CSI improvements to support data scheduling decisions. The last block continues with the improvement of UL transmissions from a network perspective, by means of the new Fifth Generation (5G) features recently devised. In this part, the state of the art review aims at detecting which strategies have been proposed to reduce the UL and DL imbalance, especially important in heterogeneous deployments. Inter-site CA has proven to improve communications in this context owing to the flexibility that provides, for such reason, it has gained a lot of importance lately. Inter-node RRM with the use of CA is one of the topics of interest in this block. Each of these parts provides a technical overview of the functionalities of LTE-A that are relevant to this dissertation. Altogether, this chapter describes the interesting challenges that were identified from the review processes, as well as the research objectives and potential improvements that are further developed in the research parts of this thesis.

Chapter 3 addresses the problem of the Fractional Power Control (FPC), specifically the Open Loop Power Control (OLPC). The adjustment of the OLPC parameters have a significant impact on the UE and network performance. Two scenarios have been studied, a synthetic deployment and a realistic one. Detailed results are provided, where differences between both networks arise when selecting the optimal configuration of parameters. When considering CA, recent releases of LTE-A

account for the use of a different transmission mode, in which the localized allocation constraint is broken, and up to two discontinuous clusters of consecutive sub-carriers per CC are possible. As a result, when transmitting in separated pieces of spectrum further considerations to power settings must be taken into account. Maximum Power Reduction (MPR) is introduced as a means to reduce the out of band emissions and yet allow multi carrier transmissions. This MPR may limit even more the UL communications and it may also cause a strong misalignment between the CSI and the data transmissions. All this, in overall, is translated into a jeopardized UL performance. These results allow deriving guidelines to design enhanced scheduling and CC selection processes that overcome these limitations.

Given the UL limitations that were pointed out in chapter 3, chapter 4 proposes novel scheduling and CC selection techniques that intend to cope with them. Two types of scheduling processes are detected when using CA, first, the Joint Carrier Scheduling (JCS) and second, the Independent Carrier Scheduling (ICS). JCS considers a single scheduling entity and one resource pool with all the available carriers. Therefore, non-contiguous and multi-CC allocations must be evaluated in a per-UE basis on each scheduling interval. The algorithm presented, proposes the use of SRSs and Power Headroom Reports (PHRs) to perform smart decisions in the frequency resource allocation. On the contrary, ICS allows for the use of one scheduler per CC, and each allocation entity is in charge of managing its own resources. In this context, the proposed method uses the SRSs of UEs to select which of them are eligible for CA transmission. This eligibility is measured in terms of estimated throughput; CA is compared to single carrier transmission, and the solution that provides the best performance is the one selected. Results show significant improvements in both cell edge and average throughput, however, conclusions drawn highlight the need for improved CSI, given that the algorithm strongly relies on it to estimate the UE capabilities.

According to the UL CSI acquisition problematic exposed in chapter 2, together with the conclusions derived in chapter 4, chapter 5 proposes further enhancements to scheduling decisions by improving the CSI. The misalignment of the CSI with data transmissions is a problem that has several degrees of freedom. For instance, interference variability, delay in SRS reception, Round Trip Time (RTT), are variables that have a paramount impact in the UE channel measurement. Results regarding this impact are provided and are also a useful starting point for designing the strategies for improvement. First, channel prediction techniques are proposed. With the use of Splines, the eNB can predict the UE Signal-to-Interference-plus-Noise-Ratio (SINR) at the time of reception. Results show that when both, average interference and its variability increase, predictions are no longer reliable and the use of Interference Cancellation (IC) strategies must be considered to contain its impact. Moreover, the delay in SRS reception is addressed with the inclusion of two well-known ICIC techniques: Soft Frequency Reuse (SFR) and Fractional Frequency Reuse (FFR). These techniques are applied in the SRSs allocation process by limiting the available bandwidth to the cell edge UEs. The benefits of this approach are twofold: first, the delay is reduced simply because the available sounding bandwidth does so, and the time needed to measure the entire band is consequently lower; second, the interference variability reduces in the cell-edge, given that a smaller number of UEs

are potential interferers. Results show significant improvement in CSI acquisition with respect to the case in which no ICIC is considered. Less misalignment between the sounded SINR and the data SINR occurs, which leads to Block Error Rate (BLER) reduction with its consequent throughput improvement.

All the previous chapters have addressed the UL spectral efficiency and data transmission improvement by proposing strategies in the MAC and RRC layers. Chapter 6 proposes an improvement of the UL transmission but, from a network perspective. In the context of HetNets, different cell types (Small and Macro) transmit at different power levels. As a consequence, the cell that provides the best received power in the DL may not be the same that receives the highest power in the UL. Traditional cell association schemes, based on DL received power, result in a sub-optimal association solution for the UL. Therefore, this chapter proposes to introduce the idea of DL and UL Decoupling (DUDe), where each link is connected to the cell from which (or to which) receives the highest power, into the inter-site CA context. This chapter specifies the use of inter-band CA, in which CCs of different frequency bands are aggregated. Considering different frequency propagation conditions on every cell type, several association cases arise. The proposal is to decouple in two manners: first, allowing full flexibility, each UL carrier is connected to the eNB that receives its higher power, second, both UL carriers are decoupled at the same time. With the use of stochastic geometry this novel proposal is analyzed and compared against a classical DL received power association rule. Results include the analytical derivation, a Poisson Point Process (PPP) simulation that verifies the mathematical part, and also system level simulations under realistic considerations. All three methods agree to the same conclusion: DUDe provides the system with outstanding gains.

1.3 Research Contributions

The different novelties of this Ph.D. dissertation have been disseminated through several research contributions, and the author has also collaborated in other topics not directly related to this thesis during the doctoral period. In particular, 1 book section, 1 lecture notes, 4 journal papers and 13 conference papers.

Chapter 3: 1 book section, 1 lecture notes and 2 conference papers,

- **[B1]** N. Cardona (ed.), *Cooperative Radio Communications for Green Smart Environments: COST IC1004 Action - Final Book*, To be published in 2015. Section entitled: *Power Control and Power Saving.*
- **[LN1] M. Lema**, M. García-Lozano, J. Olmos, S. Ruiz, "On the Performance LTE UL Power Control in Realistic Conditions," in *Lecture Notes of the Institute for Computer Sciences, Social-Informatics and Telecommunications Engineering (LNICST)*. 58 - XIII, pp. 142 - 155. Springer, 07/05/2013. ISSN 1867-8211.
- **[C1] M. Lema**, M. Garcia-Lozano, S. Ruiz, J. Olmos,"On the performance

of LTE UL power control in realistic conditions," in *Proceedings of the 4th International Conference on Mobile Networks and Management (MONAMI 2012)*. pp. 142 - 155. Hamburg (Germany) 2012.

- **[C2] M. Lema**, M. García-Lozano, S. Ruiz, J. Olmos, "LTE UL Power control evaluation in a system level simulation for synthetic and realistic scenarios," COST IC1004-Cooperative radio communications for green smart environments: 2nd Scientific Meeting, Lisbon (Portugal), 2011.

Chapter 4: 1 journal paper and 4 conference papers,

- **[J1] M. Lema**, M. García-Lozano, S. Ruiz,, "MPR-Aware Scheduler for Carrier Aggregation Transmissions in LTE Uplink," *Accepted for publication in Wireless Personal Communications (Springer)* ISSN: 0929-6212.

- **[C3] M. Lema**, M. García-Lozano, S. Ruiz, D. González, "Improved Component Carrier Selection Considering MPR Information for LTE-A Uplink Systems,"in *Proc. of International Symposium on Personal, Indoor and Mobile Radio Communications (PIMRC)*, London (UK), Sep. 2013.

- **[C4] M. Lema**, M. García-Lozano, S. Ruiz, J. Olmos, "Improved Scheduling Techniques for Efficient Uplink Communications with Carrier Aggregation,"in *Workshop on SON Algorithms for Energy Efficiency*, Ilmenau (Germany), May. 2013.

- **[C5] M. Lema**, M. García-Lozano, S. Ruiz, D. González, "Introduction of MPR Information for Enhanced Multi-Cluster Scheduling in LTE-A Uplink," *Proc. of Wireless and Mobile Networking Conference (WMNC)*, Dubai (UAE) Apr. 2013.

- **[C6] M. Lema**, M. García-Lozano, S. Ruiz, J. Olmos, "Improved Scheduling Decisions for LTE-A Uplink Based on MPR Information ," COST IC1004-Cooperative radio communications for green smart environments: 6th Scientific Meeting, Malaga (Spain), Feb. 2013.

Chapter 5: 1 journal paper and 2 conference papers,

- **[J2] M. Lema**, M. García-Lozano, S. Ruiz, "Cubic Spline Extrapolation for Uplink Channel Quality Prediction in LTE-A with Carrier Aggregation", *Accepted for publication in Transactions on Emerging Telecommunications (Wiley)* ISSN: 2161-3915.

- **[C7] M. Lema**, M. García-Lozano, S. Ruiz, "Sounding Reference Signals Management for CSI Improvement in LTE-A UL with Carrier Aggregation," COST IC1004-Cooperative radio communications for green smart environments: 11th Scientific, Krakow (Poland) Sep. 2014.

- [**C8**] **M. Lema**, M. García-Lozano, S. Ruiz, "Interference Coordination Method for CSI Improvement in LTE Uplink with Carrier Aggregation," Accepted for oral presentation in *European Conference on Networks and Communications (EuCNC)*, Paris (France) Jul. 2015.

Appendix A: 1 conference paper

- [**C9**] **M. Lema**, M. García-Lozano, S. Ruiz, "Uplink System and Link Level simulator of 3GPP LTE Rel. 8," COST IC1004-Cooperative radio communications for green smart environments: 1st Scientific meeting, Lund (Sweden) June 2010.

During the development of this thesis the author has supervised one Master Thesis in the topic of UL Admission Control (AC) under realistic conditions. As a result, one conference paper published:

- [**C10**] **M. Lema**, S. Ramón-Ferran M. García-Lozano, S. Ruiz, "Admission Control in LTE Uplink Systems with Sounding Reference Signals based Channel State Information," COST IC1004-Cooperative radio communications for green smart environments: 3rd Scientific Meeting, Barcelona (Spain) Feb. 2012.

Finally, the following publications are indirectly related to the specifics of this dissertation:

- [**J3**] M. García-Lozano, **M. Lema**, S. Ruiz, F. Minerva, "Metaheuristic procedure to optimize transmission delays in DVB-T single frequency networks,"in *IEEE transactions on broadcasting, 57, 876 - 887* ISSN: 0018-9316
- [**J4**] D. González, M. García-Lozano, S. Ruiz , **M. Lema**, DongSeop Lee, "Multiobjective Optimization of Fractional Frequency Reuse for Irregular OFDMA Macrocellular Deployments," *Accepted for publication in Telecommunication Systems (Springer)* ISSN: 1018-4864.
- [**C11**] D. González, M. García-Lozano, S. Ruiz , **M. Lema**, DongSeop Lee, "Adapting fractional frequency reuse to realistic OFDMA cellular networks,"in *Proc. of Wireless and Mobile Networking Conference (WMNC)*, Dubai (UAE) Apr. 2013.
- [**C12**] A. Serra, J. J Olmos **M. Lema**, "Modelling Channel Estimation Error in LTE Link Level Simulations" IC1004-Cooperative radio communications for green smart environments: 3rd Scientific Meeting, Barcelona (Spain) Feb. 2012.
- [**C13**] M. García-Lozano, S. Ruiz, **M. Lema**, E. Torras, J. J Olmos, F. Minerva, "Metaheuristic Proposal to minimize self-interference in Single Frequency Networks" COST2100 - Pervasive Mobile & Ambient Wireless Communications, 11th Management Committee Meeting, Aalborg (Denmark) June 2010.

Chapter 2

Strategies for Uplink Enhancement with CA

2.1 Introduction

In the previous chapter it was summarized how the requirements for the 4G mobile communications have led to the inclusion of new original features. In particular, requirements regarding data bit rate, spectral efficiency and bandwidth allocation have motivated the 3GPP to allow simultaneous transmission in more than one part of the spectrum. In the case of LTE-A systems, this is referred to as CA, and consists of aggregated transmissions across multiple CCs. The close relationship between maximum data rate capacity and available bandwidth allows for a direct increase in the UE throughput, however, CA does not provide an immediate solution for the spectral efficiency. In this sense, further efforts must be considered to improve spectral efficiency with the use of CA. An efficient use of the spectrum depends on the link adaptation process, and also on the UE external factors such as inter-cell interference, or path-losses. The RRM processes that are executed across the radio access network are typically designed with the aim of improving the spectral efficiency. The inclusion of CA may modify some of these processes, and also some new RRM procedures are identified.

This chapter starts, in section 2.2, with a generic overview of the CA technology, where the main aspects of the system level are described. Special attention is paid to the modified RRM processes: CC selection and resource scheduling; both have a great impact in the CA performance. Given this, section 2.3 analyses the existing strategies for CC selection and scheduling as well as their impact in the system performance. Both RRM procedures can be configured to attend different objectives in the cell or network. Three main goals can be identified: CC selection strategies that pursue load balancing improvement with the use of CA, selection strategies that consider frequency propagation conditions and UE capabilities of transmitting

over the aggregated spectrum, and last, resource scheduling strategies that aim for UE throughput maximization. An extensive literature review concludes that the UL is the most attractive research line, given the research challenges and open issues identified. Based on this, this Ph.D dissertation is focused on the UL performance improvement with the use of CA.

The UL improvement is not only related to the scheduling or the CC selection process; the link itself presents several challenges to improve the spectral efficiency, and it is seriously aggravated with the introduction of CA. Given this, section 2.4 studies the impact of the imperfect CSI in the UL, where interference variations and delays in measurements are great handicaps when aiming for a precise link adaptation. It provides a review of the most relevant strategies that the literature has proposed to improve the CSI, and a set of research guidelines is listed based on the conclusions drawn. These guidelines aim at designing accurate CSI acquisition techniques, while considering the use of realistic reference signals.

Despite all the enhancements introduced by the CSI reliability or the efficient resource allocation, macro-only networks may not be sufficient to meet the requirements. Therefore, the next step is to introduce additional Small Cells (SCells) to complement the Macro Cells (MCells) and improve the system performance by getting the network closer to the UE. In this line, section 2.5 addresses the topic of further UL enhancements with the use of HetNet deployments, where several design options arise with the use of CA. Several open challenges in this context are detected. Particular attention is paid to those specific strategies that the literature has proposed to improve the UL, which are compared and discussed in terms of suitability in CA networks. Finally, work items in this line are derived and justified.

2.2 CA technology: Overview

In mobile communications context, there is a rare availability of large portions of spectrum. Operators usually have a very fragmented spectrum allocation, and the need for new carriers is continuously increasing. These usable allocations may be in the same or different bands. Hence, to achieve the requested peak data rates for the 4G, LTE-A has came with a mechanism that allows the simultaneous transmission of data in more than one CC. With this, an efficient use of the fragmented spectrum is pursued by supporting the aggregation of:

- each CC can use a paricular bandwidth from the original ones defined for LTE Release 8: 1.4, 3, 5, 10, 15 or 20 MHz,
- adjacent or non-adjacent CCs in the same or different frequency bands.

In Frequency Division Duplex (FDD) the number of UL and DL CCs aggregated can be different, although the number of CCs in the DL must be always equal or higher than the ones in the UL, [5, 6]. This dissertation considers only FDD.

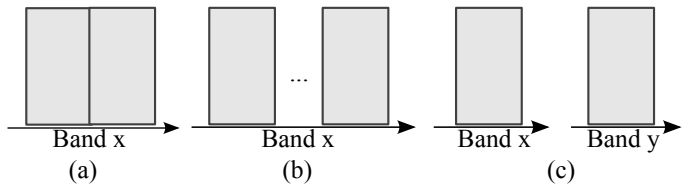

Figure 2.1: Aggregated Scenarios: (a) intra-band contiguous; (b) intra-band non-contiguous; (c) inter-band

To provide for smooth network migration and future updates of the standard, CA must be configured assuring full backward compatibility with its predecessor, LTE. From a high-layer point of view, each CC appears as a separate cell, it has a unique cell identifier and it broadcasts its own specific System Information (SI). A device supporting CA executes a generic access process as in LTE in the so-called Primary CC (PCC). Depending on the network load, QoS requirements and the UE capabilities [7] a set of Secondary CCs (SCCs) can be configured. Each SCC is considered as additional resources.

2.2.1 Aggregation Scenarios

CC Aggregation Forms

Figure 2.1 pictures the available aggregated spectrum scenarios. Three different combinations are identified:

- Intra-band contiguous CA: The center frequency of both aggregated CCs must be a multiple of 300 kHz, to preserve backward compatibility with the 100 kHz raster of LTE Release 8, and also, to preserve the orthogonality of the subcarriers with 15 kHz spacing. Large bandwidth aggregations are less likely in this scenario given the actual frequency allocations in the mobile communications bands, figure 2.1(a).

- Intra-band non-contiguous CA: Multiple CCs belonging to the same band are used but not in a contiguous manner, figure 2.1(b).

- Inter-band non-contiguous CA: In this case, multiple CCs belonging to separated bands are aggregated, figure 2.1(c). This type of aggregation may improve mobility robustness in HetNets, by exploiting the different propagation characteristic of the frequency bands.

Based on the user device complexity, cost and power consumption, the most easy scenario to implement in the UL is the contiguous CA scheme, given that the radio frequency front-end must not be changed. However, non-contiguous approach provides a practical way to fully utilize the spectrum resources, and inter-band schemes provide extra flexibility to the RRM. Radio channel characteristics and

transmission performance changes from one band to another, particularly propagation losses and Doppler shifts. In such cases, it is interesting to apply multidimensional resource allocation and management techniques to further improve spectral efficiency and maximize gains of CA [4].

System Deployment

Several network deployment options arise with the use of CA. The most efficient deployment of carriers will depend on several factors, for example: the area in consideration, the type of antennas, the hot-spots location, among others. Based on the aggregation forms explained in the previous section, CCs can be:

- Co-located and overlaid in the same frequency band. In this system design all CCs provide the same coverage region, all UEs may access all CCs and CA main functionality is to enhance the UE throughput by providing bandwidth extension.
- Co-located and overlaid with different frequency band. This design provides coverage extension owing to the difference in propagation conditions. It is useful to boost the cell edge performance. Antenna configurations may be changed to increase efforts in the cell edge. Simultaneous transmission in both carriers is reserved to those overlapped areas.
- Not co-located. One CC (or all) provides macro cell coverage and RRHs are set along the cell to improve throughput at traffic hotspots with other CCs, connected to the macro-cell or not. Frequency selective repeaters can be deployed so that coverage is extended for one of the carrier frequencies

It is evident that CA allows for flexible network layouts that can easily adapt to the operator's needs.

2.2.2 Protocol Architecture

Control Plane

In the context of LTE-A, UEs establish the cell connection by following the usual Release 8 procedure: cell search and selection, SI acquisition and initial random access. As all CCs broadcast the SI and synchronization signals, the cell search is sped up. During connection establishment, the PCC is configured and initiates the RRC connection, only one connection per UE is allowed and is carried out in the PCC. Once the network is aware of the CA capabilities of the device, RRC performs reconfiguration, addition and removal of SCCs. PCC connection is to say the most robust the UE must have, and it must be chosen so that it provides the best signal quality. Note that the selection of the PCC is not cell-based, all UEs in one eNB can have different PCC connections. With this, load balancing, specific QoS and

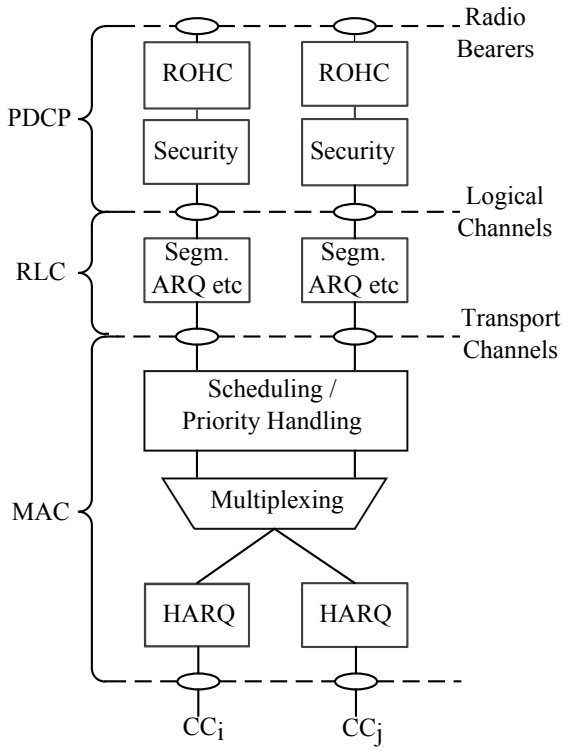

Figure 2.2: Protocol layers for CA

propagation conditions must be considered when configuring the PCC. During RRC CONNECTED state the network may decide to change the PCC to a UE, which is done via handover procedure [8].

User Plane

From the perspective of the data plane, the multiple CCs are transparent to Packet Data Convergence Protocol (PDCP) and Radio Link Control (RLC) layers. Figure 2.2 summarizes the protocol structure for CA. The first and simplest option regarding the scheduler would be to use a single entity that covers all UEs and CCs, this is defined as JCS. There are several studies focused on the per-CC scheduling, known as ICS, or the globally optimized scheduler. This is one of the active items of discussion addressed in the following sections. Dynamic scheduling is performed every subframe, by means of grants transmitted in the Physical Downlink Control Channel (PDCCH). Two ways of transmitting the grants are considered in CA:

- The allocation can be transmitted in the same CC as the assigned resources.
- All grants are transmitted in one CC despite they belong to the same CC, this is called cross-carrier scheduling and it is depicted in figure 2.3.

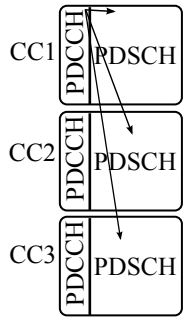

Figure 2.3: Cross-carrier scheduling

Semi-persistent scheduling may only be performed in the PCC. Note that even though the scheduler might be unique, each CC has its own independent Hybrid Automatic Repeat Request (HARQ) entity at the MAC layer.

2.2.3 System Level Design

The RRM in wireless communications carries out all functions that are related to the assignment and the sharing of resources among the users in the network, in both UL and DL. In LTE-A, the RRM presents many similarities with the previous Release 8 and 9 functionalities, Figure 2.4 depicts a flowchart of the main tasks recognised in LTE-A. The AC is done based on the corresponding QoS associated to each UE specific service. QoS parameters are the same for LTE and LTE-A, and therefore are totally independent to the CA feature.

CA introduces the new functionality of CC selection, which aims at configuring a set of CCs for each user. In this case, the CC set, will be composed of those frequencies in which the user may be scheduled. Indeed, the CC selection functionality added to the RRM is a very important operation for both, the optimization of the system performance and the energy saving. In fact, the number of CCs allocated to a user is directly related to the power consumption: as the number of carriers increases, required power will do so. To decide the optimal configuration of the CCs, the eNB evaluates several factors such as those UE-specific (QoS parameters or terminal capability), or those specific to the eNB (cell load or availability of resources) [9].

The traditional task of the layer 2 scheduler is to allocate frequency resources to UEs, one Physical Resource Block (PRB) is the smallest allocable transmission unit. To allow broadband transmissions and a better load parity among the different CCs, UEs are allowed to be scheduled across multiple CCs. Thus, scheduling functionalities are very much related to CA. In fact, the scheduler decides whether the UE is allowed to transmit in all the previously configured SCC, providing an additional control tool for optimizing the UE power consumption. The scheduling process can be configured to satisfy different system requirements, as for example the maximization of the cell throughput, cell edge user throughput or cell fairness.

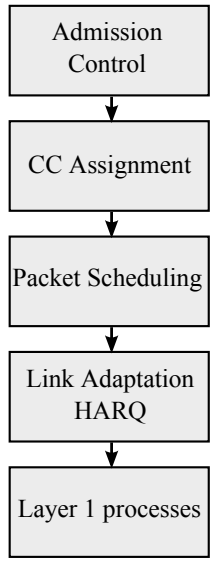

Figure 2.4: RRM tasks in LTE-Advanced

2.3 Schemes for CC Selection and Scheduling

As explained in section 2.2, CC selection and scheduling are the most important RRM procedures concerning the resource allocation. Strategies to perform the assignment are designed with multiple objectives, but in general, the improvement of the cell throughput is pursued. Along with data rate requirements, the eNB may introduce first CC selection and then scheduling strategies that aim for other simultaneous objectives such as better load balancing among carriers, cell edge improvement, fairness maximization, or contention of the energy consumption.

This section describes the main strategies the research community has proposed so far with regard to this topic. The schemes here presented are differentiated based on the main objective the scheduler or CC selection process aims to achieve:

- CC selection strategies that pursue load balancing improvement with the use of CA. Schemes include solutions in which UEs transmit in all carriers, and also solutions in which dedicated CCs are assigned for resource allocation.
- CC selection strategies that consider frequency propagation and UE capabilities. In both, UL and DL, transmitting in more than one CC may imply an extra effort from the transmitter side, in terms of coverage or power limitation. Solutions included consider inter-band CA with different propagation conditions, and also the limited power availability in the UL.
- Resource scheduling strategies. Both JCS and ICS schemes are included. Some differences arise in the scheduling process of both techniques and topics like fairness and scheduler complexity are of major interest.

2.3.1 CC Selection: Load Balancing

In the literature, there are several contributions that propose load balancing methods to avoid the aggregated transmission. The main argument against the simultaneous allocation of resources in several CCs is the high signal processing complexity at the UE side. The following references consider different load balancing strategies that are compared to JCS. The joint scheduling scheme allows the allocation of PRBs of all the aggregated CCs, which are integrated together in a common resource pool and UEs can access them with a single level of scheduling, skipping the CC selection process.

Authors in [10] propose a dual-scheduling process: first, traffic packets are allocated a CC following load balancing policies, and then resources on each CC are allocated, this process is named as disjoint queue scheduler. In [11] two schemes are compared with JCS: Round Robin (RR) and mobile hashing load balancing. Also [12] proposes a CC selection procedure in which the load balancer allocates one CC to each UE in a random fashion known as separate random user scheduling. All these references arrive to the same conclusion: aggregated transmission always performs better. It provides higher frequency selective gain as users can camp on the PRBs that are better for their transmission conditions. However, as results show, this gain is inconspicuous when traffic load is high.

Given the previous conclusions, some authors propose the use of hybrid methods. Work in [13] compares two different schemes, alternate allocation, in which the same number of users are allocated on each CC, and join the shortest queue which considers the queue state when assigning CCs. A novel traffic load balancing method is proposed based on coupling CCs together. Initially each UE is transmitting in one CC but, if a given CC is set to idle (meaning that there is no user in the queue) it can complement other CCs to help with the transmissions. Authors remark that the coupling method can achieve optimal performance, in the same manner as the aggregated transmission, irrespective of the traffic intensity. JCS always performs better than the load balancing techniques, however, the novel contribution can perform equal than the first. In the same line than the previous, [14] argues that the separate random user scheduling load balancing scheme presents lack of efficiency and has low spectrum utilization. Therefore, authors present semi-joint user scheduling, a CC allocation strategy in which traffic load is dynamically balanced at a burst level. The main goal of this contribution is to improve the random allocation and at the same time keeping low complexity when compared to JCS. Results show that the solution presented is better than random allocation, however solutions in which users are able to access all CCs still present better results.

Immediate outcomes

A straightforward conclusion is drawn after the analysis of the load balancing techniques: CA is the best way to improve the system throughput. To take the utmost profit out of multiple carriers, transmission in aggregated channels is mandatory. However, as it is going to be detailed further on in this chapter, load balancing

techniques in the CC selection process are necessary to assure an even traffic load among carriers, as well as improving cell edge performance.

2.3.2 CC Selection: Transmission Conditions

The evaluation of a UE as eligible for multi carrier transmission accounts for different issues. First of all, there is the terminal capability of CA, pre-Release 10 terminals are directly withdrawn from CA. Other points with high impact in CC selection are: the UE path-loss, especially in inter-band CA deployments, the UE power headroom, which is the power availability to cope with the higher bandwidth, and also the already mentioned load balance, which impacts the carrier occupancy and therefore the subsequent resource allocation. The following references consider part, or all, of these issues when designing CC selection schemes.

References tackling the CC selection can be easily found in the DL with inter-band CA deployments, where carriers have different radio electric propagation conditions. In [15] it is proposed a geometry factor based algorithm. Users far from the eNB transmit in the carrier that provides larger coverage, and the rest are allocated following load balancing policies. Results show that the CC selection process can improve coverage performance at the expense of marginal average throughput loss. Another related work is [16] where the decisions are based on the Reference Signal Received Power (RSRP) and also the average rate of past transmissions, which increases fairness. Authors in [17] develop a CC selection process based on both: propagation conditions and load balancing policies. Results show that the system performance is improved as more dimensions are considered. Linked to the previous, [18] introduces a per-UE weight variable per CC based on the user path-loss and the occupancy of the CC. With this, both problems are tackled: radio electric propagation and load balancing. All these works consider that there are UEs who are not capable of transmitting in more than one carrier, and the scheduler considers these as pure Release 8 UEs. However, in the DL the main reasons to deprive one UE from being allocated in more than one carrier is congestion and coverage; whereas in the UL there are more variables to evaluate.

UL CC selection must be different than the DL techniques, given that the throughput is ruled by the UE availability of power. Extending bandwidth to users not always results in a performance gain. In maximum power transmission situations an increased bandwidth may jeopardize the UE capacity. Usually, when intra-band contiguous CCs are aggregated, the transmitter uses the same Power Amplifier (PA) for all carriers. The PAs used in radio transmitters have non-linear characteristics, which cause significant distortion in the signals whose instantaneous power fluctuations come too close to saturation level. MPR is introduced as a power de-rating solution when non adjacent transmissions are carried out [19]. With this, non-linearities on the PA are contained and the spectrum emission mask is respected, it ensures a lower working point of the PA, which guarantees linearity. This topic is addressed in detail in chapter 3.

Gains brought by adopting CA in the UL are analyzed in [20]. A power back-off

factor is introduced to limit the power among the different CCs, however no MPR is reckoned within this study. No gain is perceived in the cell-edge coverage because power limited LTE-A users are treated as LTE users, that is to say allocating contiguous PRBs in one CC. Reference [21] is probably the most representative and relevant work dealing with UL CA selection of UEs. Here, users are allocated one or multiple CCs based on their path-loss. A threshold is calculated to distinguish between power limited and non-power limited LTE-A users. This value must be fine tuned to assure the maximization of both, cell-edge and average throughput. Besides, the optimum value depends on the Inter Site Distance (ISD) and might be quite different in rural or high dense urban environments. This study does not consider non-adjacent allocations in one CC, and also MPR is set to be the same value regardless the allocated bandwidth. Moreover in [22] the same path-loss threshold is applied with multi-user MIMO (MU-MIMO) techniques. This work considers the MPR and also non-adjacent allocations in one CC. However, access to CA and multi cluster transmission is limited to those users that succeed the aforementioned path-loss threshold. Meaning that both CA and non-contiguous resource allocation is limited to the inner UEs. In the same line there is [23], in which inter-band CA is considered. Here, authors claim that UEs in the cell edge have less CCs with good channel quality than those of the cell centre. If both types of users have the same traffic requirements, then the assignment of equal number of CCs may result unfair. So, users with similar channel conditions are grouped, and the cell edge groups are prioritized in the CC assignment. This cell edge oriented CC selection algorithm is compared to RR and opportunistic CC assignments showing improvements in the cell edge.

Immediate outcomes

DL studies are mainly centered in the inter-band CA, which is a feasible deployment because the entire transmitter complexity is placed on the eNB part. In here, challenges addressed are mainly congestion and coverage. On the other hand, the UL presents more open challenges in terms of the eligibility criteria. In the majority of the UL works cell edge UEs are not considered for spectrum aggregation, which are basically treated as LTE UEs and the new capabilities brought by LTE-A are not exploited. Power de-rating is not included in most of the UL works, and realistic CSI with the use of sounding reference signals is never mentioned.

2.3.3 Resource Scheduling Schemes

Traditional scheduling algorithms aim at maximizing the overall cell throughput, provide higher fairness, or improve cell-edge performance. All this by distributing the frequency resources among UEs in an intelligent manner. When it comes to the inclusion of CA, these same issues are pursued, but in a new framework which adds an extra degree of freedom. The related literature described in this section gathers the works that investigate scheduling in the CA and non-adjacent resource allocation context, topics like fairness and coverage maximization are of major interest.

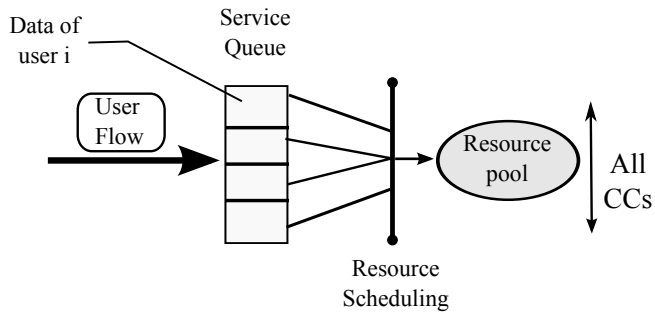

(a) Cross or Joint carrier scheduling

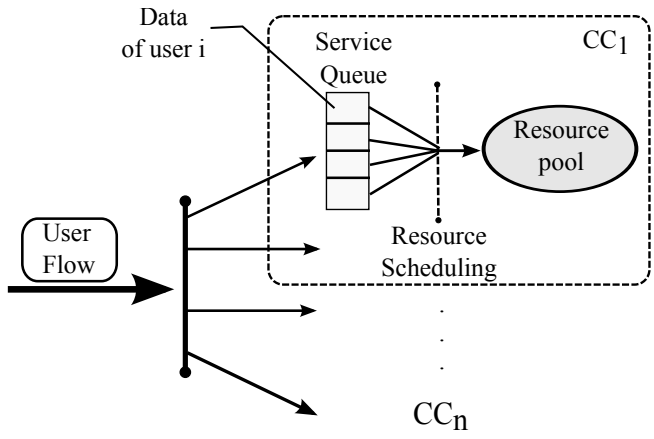

(b) Independent carrier scheduling

Figure 2.5: Independent and joint scheduling strategies

In general terms, two different scheduler positions are identified: Joint scheduling, in which all CCs are managed by the same entity, this strategy is also known as cross carrier scheduling; individual scheduling, in which every CC is managed by an independent scheduler, as it is shown in figure 2.5 [13].

Works in [24] and [25] present two approaches of scheduling. The first one, investigates the performance of schedulers operating in a per-CC basis, so information about throughput in other CCs remains unknown and proportional fairness is impaired. The second work evaluates the gains of cross-carrier scheduling and sharing past throughput information from all CCs. Results of this contribution do not present such a gain in terms of average throughput, however it presents an important increase of coverage gain. The same results are obtained analytically in [26], which proves that the cross CC Proportional Fair (PF) scheduler maximizes the network utility. It also improves fairness by increasing the scheduler priority of users that cannot access all CCs. Authors in [27] also deal with independent versus cross-CC scheduling. After quantifying the benefits of the latter in different

scenarios, they observe that users with diverse performance in available CCs are not uniformly scheduled among them. Hence, they propose a Layer-3 management scheme that configures a particular number (and choice) of CCs to specific users, thus obtaining the same results as joint scheduling but with less complexity.

All these scheduling discussions are centered in the DL, in which CA is not exploited in the same manner as in the UL. Authors in [28] tackle the scheduling problem in the UL from an energy efficiency point of view. A dynamic scheduler is proposed, in which each CC can collaborate with the others to assure that the total capacity of all CCs is fully utilized; two different cooperation approaches are presented. Results show that the same average throughput as in joint scheduling can be obtained with an efficient reduction in power consumption. Also, the balancing capacity is improved. All UEs can use multiple CCs simultaneously and it does not consider power de-rating when simultaneous transmission across more than one CC occurs. Work in [29] studies the system performance of clustered Discrete Fourier Transform - Spread - OFDM (DFT-S-OFDM). No CA is considered but sparse allocation of PRBs along one carrier is. Due to frequency selective gain and scheduling flexibility UL transmissions improve. Authors propose two methods of MPR, one with a fixed value and another one in which the power de-rating varies depending on the bandwidth allocated, solution that is quite close to the conclusions drawn by 3GPP in [19].

Immediate outcomes

In general, joint scheduling enhances fairness among CA and non-CA users, given that scheduling priority in all CCs is referred to the past throughput transmitted along the entire system bandwidth. However, if average transmitted throughput metrics are considered in all CCs, performance with independent scheduling can be similar, and the scheduler complexity is lower

2.3.4 Remarks from the State of the Art

This section has presented a detailed review of the strategies the literature has proposed so far when dealing with CA CC selection and resource scheduling. From the results reported in the literature, some guidelines and conclusions can be drawn.

Table 2.1 shows a comparative analysis of the solutions presented showing their main features. The vast majority of proposals are centered in solving DL issues where the gain of applying CA is more directly viewed. Here, authors deal with topics of coverage, load balancing and selection in both intra and inter-band CA. In the UL this is more challenging, there are more constraints regarding the UE capability which results in less straightforward gains when applying CA. In the majority of the UL works cell edge UEs are not considered for spectrum aggregation, and are essentially treated as LTE UEs, therefore, the new capabilities brought by LTE-A are not exploited. In this context, table 2.2 provides a more specific comparison for the UL. At a glance, it is noted that power de-rating is hardly included in most of

Table 2.1: Summary of CC selection and resource scheduling strategies

Ref #	Link	Load Balancing	Transmission Capabilities	CA	Aggregation Scenario	Cell Edge
[10]	DL	✓	✘	✓/✘	Intra	✓
[11]	DL	✓	✘	✓/✘	Intra	✓
[12]	DL	✓	✘	✓/✘	Intra	✓
[13]	DL	✓	✘	✓/✘	Intra	✘
[14]	DL	✓	✘	✓	Intra	✓
[15]	DL	✓	✘	✓	Inter	✓
[16]	DL	✓	✓	✓	Inter	✘
[17]	DL	✓	✓	✓	Inter	✘
[18]	DL	✓	✓	✓	Inter	✓
[20]	UL	✘	✘	✓	Intra	✘
[21, 22]	UL	✘	✓	✓	Intra	✓
[23]	UL	✘	✓	✓	Intra	✓
[24–26]	DL	✘	✘	✓	Intra	✘
[27]	DL	✘	✓	✓	Intra	✘
[28]	UL	✘	✓	✓	Intra	✘
[29]	DL	✘	✓	✘	Intra	✓

Table 2.2: Summary of references dealing with UL

Ref #	CA	MPR	Cell-edge	SRS
[28]	✓	✘	✘	✘
[29]	✘	✓	✓	✘
[22]	✓	✓	✘	✘
[20]	✓	✘	✘	✘
[21]	✓	✘	✘	✘
[23]	✓	✘	✓	✘

the strategies, and realistic CSI with the use of SRSs is never mentioned. Both are crucial in the correct functioning of the opportunistic scheduling. With the aim of increasing spectral efficiency, it is necessary to perform an accurate scheduling of the sounding resources mainly in the CA environment, where bandwidths can be highly extended. This can also be applied for the DL Channel Quality Indicator (CQI) reports from the UE side to the eNB.

There are still open challenges to address for the UL improvement in order to reduce UL and DL imbalance. The popularity of social networking services outcomes in a rise of the UL traffic due to the increased user generated contents. To fully exploit CA in the UL it is necessary to devise selection strategies that consider the radio electric conditions of the UE to maximize the spectral efficiency. Also, CA implies a strong overhead in power limited users because of the higher bandwidth. It is worth analysing the feasibility and applicability of CA in such conditions, as

well as assessing the performance gains or losses. All these topics are addressed in this thesis in chapter 4.

2.4 Impacts of CSI in the UL

So far, the literature review from section 2.3 has proposed strategies to enhance coverage, throughput, fairness and energy efficiency of both UL and DL. However, this increase is mainly based on an important assumption: all channels between the eNB and the UE are accurately known. One of the aspects that allows to increase spectral efficiency is the existence of reliable up-to-date CSI. This information can be used at the discretion of the scheduler, which will select the best transmission scheme opportunistically. In the UL of LTE systems, the CSI is obtained by the eNB after receiving and processing the SRSs sent by the UE [30].

In a system operating with several aggregated carriers, the bandwidth to be sounded increases for UEs transmitting in more than one CC. So, given the power limitations in the UE, the SRS cannot be transmitted occupying all the bandwidth. Distributing the available power among all subcarriers might lead to very poor SINR and so poor channel estimation. LTE allows the SRSs to be allocated in smaller pieces of spectrum so that UEs perform a frequency sweep. This allows sounding the complete bandwidth effectively but it also rises the time delay between measurements at the same frequency block.

A second problem the UL CSI must deal with, is the intrinsic rapid variations of the interference levels. This is not only due to short term fading, but also because of scheduling decisions. With every Transmission Time Interval (TTI), allocated resources are updated and so the sources of interference in each PRB are changed. This implies fast SINR variation and reduces the sounding reliability, eventually generating errors in the link adaptation and reducing the UE throughput.

This section provides an overview of the SRS process, followed by a description of the main strategies the literature has proposed so far to improve the channel estimation. Note that the term *channel estimation* may also refer to the CSI estimation using the combined knowledge of the transmitted and received signal; assuming the channel affects like a filter, these techniques aim at recovering the received signal by estimating the filter coefficients. In this dissertation *channel estimation* refers to the knowledge of the SINR of the UE at the eNB side, with the aim of improving MAC layer procedures.

2.4.1 CSI through SRS transmission

Sounding signals are sent by the UE and configured by the eNB with the main goal of achieving up-to-date and accurate CQI. This allows performing opportunistic frequency domain scheduling, since the best spectrum areas can be detected. Eventually it also contributes in the decision of the best MCS in the link adaptation process. All the sounding parameters such as: sounding bandwidth, frequency and

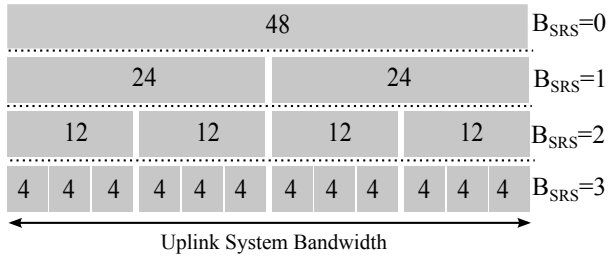

Figure 2.6: Sounding reference signal bandwidth configuration example for one C_{SRS}

time domain resource selection, are configured by the eNB on a cell-wide basis. Specific per-UE configuration parameters are: sounding periodicity, bandwidths, and hopping patterns.

Frequency domain

The maximum sounding bandwidth, C_{SRS}, is a cell-specific parameter signalled via RRC messages. A range of bandwidth configurations are available depending on the system bandwidth [31]. For each C_{SRS} selected by the eNB, four different UE specific assignments are possible, B_{SRS}. This allows the sounding region to be configured to span only in the resource blocks used, as for example, in those ICIC schemes in which UEs are restricted to transmit in certain parts of the spectrum. Also, narrow bandwidth soundings are desirable for power limited UEs, since an increase in bandwidth reduces its Power Spectral Density (PSD), which leads lo less accurate SINR measurements [32]. Figure 2.6 shows a graphical example of the different B_{SRS} values that can be configured for one C_{SRS}.

As said, the B_{SRS} of UEs placed at the cell edge should be selected considering their low power availability to assure the reliability of the measurement. But, if the sounding bandwidth is narrow, the time to measure the entire system bandwidth is larger, increasing the period between two consecutive measurements of the same piece of spectrum (T_{sound}), as shown in figure 2.7. This is particularly problematic in carrier aggregated systems making use of very wide bands.

Both Frequency and Code Division Multiplex (FDM and CDM) are used in LTE to support a higher number of users. FDM is done following a transmission comb structure and CDM is done using a base sequence with different cyclic shifts. Each frequency comb can be configured to support one sounding bandwidth B_{SRS}. Currently in LTE only two transmission combs are supported. For each sounding region up to eight UEs can be multiplexed via cyclic shifts, n_{SRS}. Based on this, both FDM and CDM allows to multiplex a total of 16 UEs in the same spectrum area. In practice, this number of UEs is not feasible since there are orthogonality and interference issues, so a more realistic estimate is to multiplex 6 to 8 UEs [32].

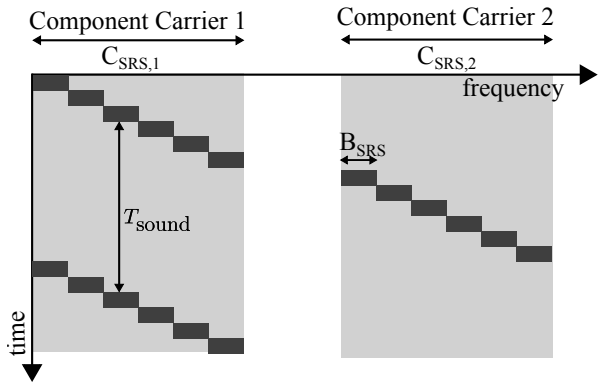

Figure 2.7: Sounding procedure all UEs in the scenario follow

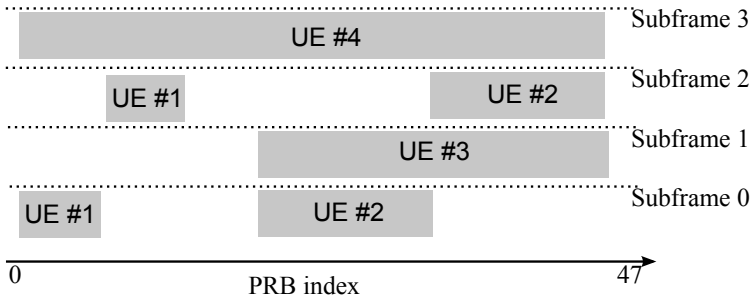

Figure 2.8: Example of SRS Management with 4 different UEs

Time domain

In the time domain, the SRS is transmitted in the last SC-FDMA symbol of the subframe. To avoid SRS overlapping with Physical UL Shared Channel (PUSCH) transmissions, UEs are not allowed to transmit PUSCH when the SRS takes place. The eNB configures cell-specific sounding offsets (T_{offet}) for each 10 ms radio frame, which defines the subframes containing a SRS transmission. LTE-A includes three types of sounding: *Single SRS*, in which the SRS transmission is done once, *Periodic SRS*, in which the UE transmits SRS continuously and *Aperiodic SRS*, which are SRS transmissions based on a trigger. The eNB configures the UE-specific sounding periods (T_{SRS}) that range from 2 ms to 320 ms. Figure 2.8 shows an example of the SRS configuration parameters, indexes of B_{SRS} are recalled from figure 2.6. For instance, UE 1 transmits a $B_{\text{SRS},1} = 3$ with a SRS periodicity $T_{\text{SRS},1} = 2\,ms$; UE 2 has the same periodicity but has a different sounding bandwidth configuration $B_{\text{SRS},2} = 2$; UE 3 in the example transmits with an offset of $T_{\text{offet},3} = 1$ and UE 4 $T_{\text{offet},3} = 3$, given that their first SRS transmissions in the 10 ms frame are held in those subframes.

2.4.2 Strategies to Improve CSI

Based on the existent limitations to obtain accurate CSI, and on the impact it has in the system performance, the literature has proposed several strategies to improve it. Some techniques directly tackle the CSI improvement by proposing specific solutions such as SINR prediction, cooperation among eNBs or per-UE SRS management. Other techniques may be useful to improve the interference variability in the UL, however they have not been yet used to address the CSI problem.

Prediction Techniques

The CSI prediction literature is substantial, however this section provides a review of the most relevant solutions with respect to the topic of this thesis.

The channel estimation error in the DL has been tackled by several authors. In [33], authors deal with the CQI delay. This CQI feedback delay is caused by CQI measurement at the UE side, CQI feedback and CQI processing at the eNB side. A polynomial extrapolation method is proposed to predict the CSI, where no second-order statistics of the SINR are required. The solution is evaluated for different UE speeds and results show that the proposed method works for UEs with low variant channels. Another strategy to overcome the performance loss brought by channel estimation error is presented in [34]. Authors propose two types of link adaptation algorithms. The first one performs a weighted average of different past received information of the UE, such as channel, SINR and MCS. The algorithm calculates the current channel, SINR or MCS by averaging the past information in a fixed time window. The performance of this last algorithm strongly depends on the time window size, therefore, authors propose the use of a dynamically adjusted time window. Link adaptation decisions based on the channel averaging shows to compensate better the channel estimation errors.

Other works that can be found in the literature undertake this problem by using prediction filters. In [35] it is proposed the use Least Mean Square (LMS) prediction method. In particular, a modified version of the normalized LMS is proposed in order to support wider CQI feedback delays. Improvements brought by predictions are very much dependent on the time difference of two consecutive CQI measurements. When the difference is low, the LMS proposed strategy shows significant improvement, however as it increases, the LMS solution degrades the instantaneous channel information. Results conclude that the prediction solution has the ability to improve throughput when the time delay is less than 5 ms. Wiener-based prediction filters are also widely found in the literature as a strategy to overcome the channel estimation errors, [36–38]. This solution has also been proposed for the UL [39, 40]. Practical Wiener filters are obtained using temporal averages to approximate the cross-correlation and auto-correlation functions involved in the solution and ergodicity therein is also assumed. Work in [41] compares two different approaches in the DL: Wiener filters with cubic spline extrapolation. The cubic spline method constitutes a near optimal solution in low speed UEs and it does not have the strong input/outpur correlation dependency the Wiener solution has. To adapt the cubic

spline solution to fast moving UEs, the authors propose a simple heuristic using the autocorrelation of past samples that, combined with the extrapolation output, provides an accurate prediction. Other authors consider Kalman filters for channel prediction in the DL [42, 43]. In the UL, work in [44] uses Kalman filtering to predict the interferences in a time division multiple access wireless network. In this context, multiple contiguous time slots are allowed to be used by the same terminal or base station for transmitting. As a consequence, the interference at a given receiver is correlated from one time slot to the next. To successfully implement this type of filters a well estimation of the process noise (and its variances) is crucial. Which, in this case, depends on the error characteristics of the interferences at the receiver.

Specific strategies for the UL may consider collaboration among different eNBs to provide a wider knowledge of the interference map generated, which depends on the resource allocation decision of the eNB. Work in [45] proposes to exchange scheduling decisions between the eNBs, incorporating a time delay that occurs for the information exchange. Each eNB predicts the channels of its own users using a Minimum Mean Square Error (MMSE) predictor and sends the scheduling information in two manners, a fixed allocation decision, or the probability of the scheduling decision. This new scheme provides better results for link adaptation decisions, and in particular, the interchange of probabilities is especially beneficial for fast moving UEs.

SRSs resource management

The 3GPP community has recognised that an adequate management of SRS configuration parameters in LTE-A UL can lead to improvements in the system performance. In [46] authors evaluate the gain of non-contiguous resource allocation in the UL considering two SRS bandwidth setups based on the UE SINR. Results show that a discontinuous allocation may be beneficial as it can exploit additional frequency diversity gains. However, SINR estimation errors provided by SRS inaccuracy or unavailability can lead to degrading effects. Other 3GPP contributions already mentioned the need for different sounding bandwidth options to avoid CQI measurement error. This necessity was already discussed in [47], where authors propose to adaptively control the sounding bandwidth. This solution allows reducing the number of wideband transmissions which assures lower MCS selection error due to decreased received signal power density. Results show that the adaptive control is especially effective in hyper dense scenarios with high volumes of traffic. Also, in [48] different schemes of configuring SRS across multiple CCs are discussed. Authors propose that sounding signals should be configured separately for the different CCs. This turns sounding more flexible, this can be useful in heterogeneous networks interference coordination. Another proposal is that UEs should transmit SRS symbols only in their active CCs, meaning the ones that are actively being used for data transmission.

Inter-Cell Interference Coordination

Other strategies that can be used to improve the CSI at the receiver site are based on interference management techniques. These are widely known in the literature, however, they have never been specifically applied to improve the SINR estimates. Following the classification done in [49], the techniques for interference management in the UL can be grouped in:

- FPC: Determines the UE transmitted power by partially compensating the UL path-loss, measured by the DL RSRP. UEs with higher losses will operate at lower SINR values and hence, fairness in the cell will decrease: the farther the UE is from the cell center, the lower the SINR target becomes. The open loop part of the FPC algorithm can be used to adjust fairness and interference, this issue is specifically tackled in chapter 3. The closed loop part provides UE-specific corrections to further improve the performance. Several contributions study the impact of FPC in the UL performance. In [50] authors analyse and compare the UL OLPC against two reference mechanisms. Results show that FPC is beneficial when compared to traditional full-compensation algorithms. Work in [51] present an accurate study of the FPC regarding the impact in the resulting SINR distribution and interference generated.

- Frequency reuse: ICIC techniques have been widely studied in the DL [52], where frequency reuse is applied in the cell edge to improve the performance of those UEs affected by severe interference. Some interesting works have also appeared in the UL [53–55], though there is far less literature. All these references have shown that ICIC improves the UL performance by reducing the interference impact.

- IC: The previous interference management techniques presented are not optimal in terms of spectral efficiency. An alternative, is to allow higher transmitted powers, and hence, higher interference levels while using techniques to reduce it at the receiver site. Network assisted IC and suppression [56] is proposed by the 3GPP to improve transmission performances by increasing the degree of knowledge about interfering transmissions. Also, some interference suppression receivers such as MMSE-Interference Rejection Combining (MMSE-IRC) have proved to improve DL UE throughput [57].

2.4.3 Remarks from the State of the Art

This section has gathered the most relevant proposals the literature has made so far to improve the CSI. Table 2.3 summarizes the prediction strategies described in the previous section in a comparative way, where the most important features are highlighted. Once more, the majority of the work is done in the DL, where the CSI acquisition problems may be similar at a first glance, but the UL indeed presents more challenges, mainly because of the interference variability. There are several proposals that suggest the use of Wiener filtering, which needs second

Table 2.3: Summary of prediction strategies to improve CSI

Ref #	Link	Strategy	Statistics	Interference	Delays
[33]	DL	Polynomial	✘	✓	✓
[34]	DL	Average	✘	✓	✓
[35]	DL	LMS	✘	✘	✓
[36]	DL	Wiener	S.O	✘	✘
[37]	DL	Wiener	S.O	✘	✘
[38]	DL	Wiener	S.O	✘	✘
[39]	UL	Wiener	S.O	✘	✓
[40]	UL	Wiener	S.O	✘	✘
[41]	DL	Polynomial	✘	✓	✓
[42]	DL	Kalman	L.O	✓	✓
[43]	DL	Kalman	S.O	✓	✓
[44]	UL	Kalman	L.O	✓	✓
[45]	UL	MMSE	S.O	✓	✓

S.O: Second Order L.O: Low Order

order statistics to compute the filter coefficients. In particular, Wiener estimators require a previous knowledge of the stochastic property of fading channels, the auto-correlation and cross-correlation channel statistics are difficult to obtain in a real wireless communications system, which is an added limitation for their application in realistic UL CSI prediction. Methods that require either low or high order statistics are not practical in the UL given the rapid variations caused by inter-cell interference. Among the other prediction filters proposed, there is the LMS, which can rule out any low or high order statistics, but however, requires a constant time difference between the past CQI samples and the prediction. In the UL, the SRSs in a particular piece of spectrum are only available after a complete bandwidth sweep, but the scheduler may need to decide about the suitability of those resources at any time. Thus, as it will be justified in chapter 4, a continuous time formulation for the prediction is ideally required, which is mathematically tricky for Wiener and LMS based solutions.

Interference management techniques have shown significant improvement in the PUSCH channels, and when carried out, ICIC in SRS should be considered as well. None of the references that tackle the UL interference issue with ICIC consider the impact of the CSI. Frequency domain scheduling and link adaptation decisions are supported by the SINR information provided by the SRS. Because of the interference variability, the time difference between the SRS and data reception, and UE transmit power considerations, there is a misalignment between the SINR measured from the SRS and the actual one measured at the PUSCH transmission. This concept of misalignment is widely invoked in this dissertation, and essentially refers to the difference that exists between the SINR used for resource allocation purposes and the SINR of the actual data transmission. When the misalignment is high the CSI is seriously impaired and impacts the UE performance. In this sense,

CSI acquisition techniques must place efforts in reducing the SINR misalignment and thereby improving the system performance.

Therefore, the main challenge to address is finding solutions that allow increasing the SRS reliability considering:

- Realistic interference generation. As pointed out earlier in this section, and also highlighted by the literature, the UL interferences variate with time mainly due to scheduling decisions.
- SRS delays. Not only because of hopping along the entire band, but also affected by the RTT.
- Low complex prediction methods. Strategies must be applicable under realistic conditions.
- IC techniques. Used in the eNB side to suppress the most dominant interference sources, and hence, reduce both the average interference and its variability.
- Accurate scheduling of the sounding resources that adapts to each UE specific needs by adopting ICIC strategies in the SRS allocation process.
- Accurately adjust FPC parameters to contain the generated interference while not jeopardizing UEs at the cell edge.

All these topics are addressed in this dissertation. A detailed analysis of the FPC is provided in chapter 3, and more specific strategies for CSI improvement are provided in chapter 5.

2.5 Further Improvements: Network Strategies

LTE-A has to face a non-constant Quality of Experience (QoE) within cells because of the difference in spectral efficiency depending on the UE position. Adding spectrum or improving the link adaptation provides faster connectivity, however, no homogeneous performance is actually met. One of the challenges 4G and further technologies such as the forthcoming 5G must meet are the new requirements of spectral efficiency over the cell and per user. This implies that performance metrics such as average SINR or BLER become less relevant, while metrics such as user rate distribution or area spectral efficiency are of major interest [58]. Further improvements in this line are possible by increasing the eNB deployment density. Nowadays, mobile networks are shifting from a single-tier homogeneous network approach to multi-tier HetNets, the so-called HetNets. It has become a popular approach in the past few years as an efficient and scalable solution to improve the network capacity in hot-spots; it is also a viable solution to improve fairness, since the network gets closer to the UE.

This section provides an overview of the HetNet concept and highlights the main opened challenges this network topology has to face. In particular, a study of the solutions and methods the literature has proposed to improve the UL is addressed, considering the potentials of CA over these new architectures.

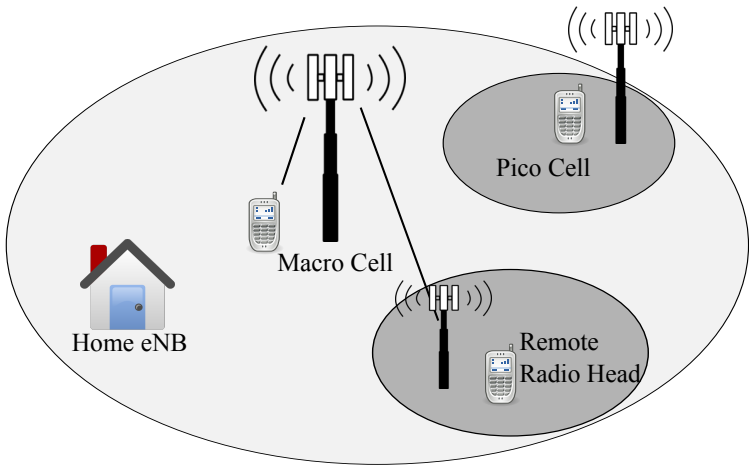

Figure 2.9: Example of HetNet deployment

2.5.1 3GPP Heterogeneous Networks: Main Challenges

A HetNet is a network deployment consisting of MCells and overlaid low-power nodes such as pico-cells, femto-cells, RRHs or relays, referred to more generally as SCells. The MCells are high power eNBs typically located along the geographical area with purposes like coverage maximization or interference reduction; SCells are in charge of eliminating coverage holes or improving capacity by off-loading the MCells at hot-spot areas, figure 2.9 shows a typical HetNet deployment. Based on the frequency deployment, two solutions arise: co-channel deployment where both MCells and SCells share the same frequency carrier; and dedicated deployment where each type of cell transmit at different frequencies. This new paradigm of network deployment potentially increases the spectral efficiency, as pointed out before; however, significant challenges are introduced to assure the correct operation of HetNets.

Authors in [59] classify the key challenges the HetNets have to face. Some of them are:

- Backhaul challenges: SCells need to be provided with energy efficient and low cost backhaul, and sometimes the deployment itself of the SCells can make this tricky. In this context, several architectural solutions are presented in [59–62].
- Mobility management challenges: Mainly in the form of inter-cell handovers. Topics of interest in here are mainly UE-idle mobility and increased handovers in high-speed UEs continuously triggered given the reduced SCell size addressed in [63–66]. In [58] challenging topics are listed for future work in this context: improved mobility modeling, handover optimization, and mobility-aware interference management.
- Interference mitigation challenges: especially in co-channel deployments the

inter-cell interference is an important limitation. In the DL a UE associated to the MCell may see increased interference from the SCells, and a terminal served by a SCell may see strong interferences in the cell edge from the MCell. In the UL, both association cases, MCell or SCells generate high number of interferences. Techniques like cell Range Expansion (RE) allow to reduce inter-cell interference in the UL, by allowing the UEs to associate to cells that do not provide the highest DL RSRP, increasing the SCell coverage region. However, this solution increases the interference in the DL, mainly in UEs placed in the expanded area. Enhanced ICIC (eICIC) techniques based on Almost Blank Subframes (ABS) are proposed, where the MCells almost mute transmissions on certain subframes, reducing the interference generated and allowing UEs connected to the SCells to transmit with better signal quality.

- Radio planning challenges: frequency deployment is an important issue, if capacity must be maximized or spectrum is scarce frequencies should be reused, on the other hand dedicated deployments are attractive in large bandwidth availabilities. Moreover, cellular networks have often been designed based on the DL; cell selection rules have a huge impact in the load imbalance and the UL performance. The DL/UL imbalance problem has been recognised by the 3GPP in [67, 68]. A UE is said to be in this situation if the best UL cell and the best DL cell are different based on received power metrics; this topic is addressed in detail in the following section.

The inclusion of CA in the HetNet context has been recognised by the literature as a feasible way of providing multi-site radio resource allocation, which allows improvements in mobility and interference management. Authors in [69] propose a centralized radio access network architecture with many RRHs and utilizes the LTE-A Release 10 functionality of CA between macro and small cells carriers. CA helps to maintain the basic connectivity and mobility along the MCell coverage, while SCells (also referred to as *Add on cells*) achieve higher throughput performance and larger capacity. A centralized entity is in charge of handling the processing for CA and handovers. In [70] insights of most of the opened challenges of heterogeneous networks using CA are presented. Authors agree with the previous reference and highlight that a centralized architecture allows for multi-site CA, which was first introduced in Release 11 [71]. Finally, [72] presents two different macro and small cell cooperation schemes, one for co-channel deployments and another for dedicated ones. In the same line with the previous contributions, authors propose to exploit collaborative inter-site CA in a centralized deployment.

2.5.2 HetNets Strategies for UL Improvement

One of the major design goals for HetNets listed in [67], is the use of radio resources across macro and small cells to achieve figures of per-user throughput and system capacity similar to ideal backhaul deployments. The 3GPP has introduced the *Dual Connectivity* concept in [67], where the user consumes radio resources provided by at least two different network points, also known as inter-site CA. It is one of the

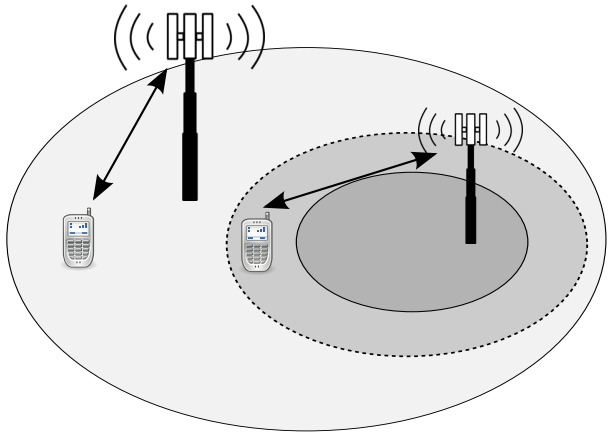

Figure 2.10: Example of HetNet with Range Expansion

3GPP potential solutions to improve user performance by combining the benefits of the MCell coverage and the SCell capacity [73]. To be able to design such inter-site techniques the SCells should be implemented as RRHs, given that the scheduler for the RRHs is implemented in the MCell and inter-site radio resource allocation is feasible in such a deployment [72]. Work in [74] addresses this topic in a DL scenario where MCells share resources with RRHs, where a CA window is proposed to determine if CA-capable UEs should be included in inter-site CA. A dedicated frequency deployment is considered. The benefit of aggregating resources from both cells is verified for different traffic patterns, as well as for different load situations. This topic has been addressed in the UL in [75] where results show improvement of UL throughput with the use of inter-site CA in low load situations due to larger bandwidth accessibility.

Cell selection based on the RSRP or the Reference Signal Received Quality (RSRQ) provides high imbalance problems, since the DL coverage of the MCell is much larger than that of the SCell. This type of cell association leads to UL/DL imbalance, since the UL coverage of both cells are much similar [72]. One strategy that tackles this problem and brings some fairness to the UL is RE, introduced in the previous section, shown in figure 2.10. The SCell range is expanded by adding a RE threshold to the RSRP or RSRQ measured from the SCell. However, recent studies [76, 77] have shown that using high offsets (greater than 3-6 dB) increases the DL interference levels, therefore eICIC techniques such as ABS have been developed to overcome this. Gains brought by CA in the context of DL using RE have been studied and verified in the literature [78, 79], where results conclude that co-channel deployment typically yields to the largest rate.

Both UL/DL power and Macro/Small cell load imbalance motivates the decoupling of both links, which is particularly beneficial for co-channel heterogeneous deployments, shown in figure 2.11. For Release 12, the 3GPP has included UL/DL split results for co-channel deployments in [67], where it shows improvement in the cell edge throughput. Results in [80] show a high improvement in the UL performance

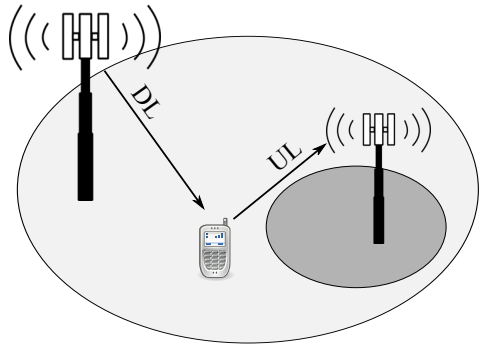

Figure 2.11: Example of HetNet with DL and UL decoupling

for both low and medium load scenarios; especially in cell edge UL UE throughput. The literature has tackled the power and load imbalance problem recently and some relevant references can be identified. Authors in [81] present the path-loss cell association solution to the power imbalance problem. Results in terms of gain that can be achieved in the UL capacity are very promising. A detailed analysis of the decoupled access in terms of association probability, coverage and capacity are presented in [82, 83]. Here, prior work is extended by adding the analytical evaluation using stochastic geometry and architectural considerations. Results show same trend between the stochastic geometry analysis and the real world experimental data. Work in [84] introduces cell load and the backhaul limitation into the cell association process. SINR variance is reduced with the enhanced DUDe solution presented; also, the interference-aware UL power control applied lets the system improve in terms of throughput. Finally, [85] contributes to the topic with the analysis of the UL SINR and rate distributions as a function of the association rules considering UL power control design parameters. Results show that minimum path-loss association leads to identical load distribution across all cells which is also optimal in terms of rate, irrespective of power control parameters. When both UL and DL joint coverage must be maximized, the decoupled association is the optimal solution. It is beneficial because it reduces the QoS imbalance between both links.

2.5.3 Remarks from Literature Review

This section has provided an overview of the context of HetNets which are useful to improve the system performance, however some challenges are still opened. The literature that has been so far proposed to improve the UL performance in this context has been reviewed. Proposals can be classified into three main groups:

- Dual connectivity or Inter-site CA. The literature has verified the UL improvements in dedicated deployments. However, there is yet no study that includes inter-site CA as a solution to the UL/DL imbalance problem, the association rules proposed in the prior art are based on the DL RSRP or RSRQ.

- Cell RE with eICIC. The literature has verified the UL improvement in co-channel deployments. This strategy helps to reduce the UL/DL imbalance, however, while the UL improvement is maximized the DL inter-cell interference is also increased. Therefore RE techniques must be always accompanied by eICIC solutions for the DL such as ABS. Nevertheless, the RE technique is limited to moderate offset values due to the harsh interference in the DL. Cell selection rules are based on DL RSRP and RSRQ with a RE offset added.
- UL/DL decoupling. There are verified improvements in the UL in co-channel deployments with the use of DUDe. The UL/DL imbalance problem is mitigated since both cell selections are optimal in terms of received power.

Based on this comparison, it is clear that DUDe brings the benefits of having very high RE offsets in the UL without the interference effects in the DL, since both links are separated, and connected to the best serving cell. There are still open research efforts in this novel strategy, since DUDe works presented so far consider only the use of one CC. When considering the aggregation of more than one carrier, other SCell enhancement challenges are identified, for example when two CCs operating at distant bands are aggregated. According to the existing literature, recent contributions that highlight potential 5G solutions consider the use of CA in a collaborative way in heterogeneous networks. Dual connectivity, or inter-site CA can provide further improvements to this strategy. Recent works in this line have been centered in dedicated HetNet deployments, where each tier uses only one CC; but, the literature review has proved that throughput increases when aggregated transmissions take place in co-channel deployments. Therefore research for improving the UL performance in HetNets, while not jeopardizing the DL should include:

- DUDe, to reduce the UL/DL imbalance, and not increase the DL inter-cell interference.
- Study of multi-tier propagation conditions. Since the UL and DL association rules are based on the received power, specific propagation conditions on each type of cell should be considered.
- Study of decoupled inter-site CA for inter-band scenarios, where frequency separation has a direct impact in the coverage footprint.
- Co-channel deployment and aggregated transmissions to maximize the system throughput.

All these topics are addressed in this thesis and are detailed in chapter 6.

Chapter 3

Uplink Power Control: Parameters Adjustment

3.1 Introduction

To provide QoS to the subscribers the design of mechanisms that accurately manage the radio resources is of utmost importance. Specifically, power efficient techniques that manage the interference generated with the aim of improving the spectral efficiency. In LTE-A, the particular UL medium access technique allows an almost null intra-cell interference; the use of SC-FDMA implies that the radio channels utilized by the different users are orthogonal. On the other hand, it is desirable to reuse all available channels in every cell to achieve high throughput levels. However, a high reuse factor increases the interferences between adjacent cells jeopardizing the performance of certain users. For this reason, the power control mechanism presented by the 3GPP plays an important role in maintaining the required SINR while reducing the interferences caused, by adding an original capability: the fractional path-loss compensation.

This chapter is devoted to the description and study of the UL power control mechanism. In particular, section 3.2 provides the OLPC algorithm description and expands the concept of FPC with simulation results, where the impact of the parameter configuration is studied. This power control mechanism constitutes a versatile way of adjusting the interference generated with respect to the UE experienced throughput. In this line, an interesting comparison is addressed in section 3.3, where the system performance of two different scenarios is studied. The optimal OLPC parameter configuration in a synthetic environment is compared to the optimal configuration in a realistic mobile communications network. Finally, this chapter ends with section 3.4, which addresses further considerations to the power control mechanism when considering CA. This provides an analysis required for the correct understanding of subsequent chapters and contributions.

3.2 UL Power Control in LTE

Traditional power control algorithms assure that users with the same service are received at the eNB with the same SINR. This approach fully compensates the particular path-loss of every UE, this is why it is known as Full Compensation power control. In this scheme cell edge users, who are making up for a high path-loss, must transmit higher power levels to meet the SINR requirements. In order to avoid this situation, the power control formula defined for the LTE UL enables the use of FPC. This means that the UE can compensate for a fraction of its path-loss and, as a result, UEs with higher losses will operate at lower power values generating less interference.

3.2.1 Standardized Power Control Mechanism

The power control scheme agreed by the 3GPP is divided into two main components: opened loop and closed loop. The UE establishes an operation point using the opened loop part, where it compensates the mean path loss and its slow variations. Additionally, this may be fine tuned by specific commands. The UE calculates its transmission power based on the path-loss estimation, broadcast system parameters, and dedicated signalling. Equation 3.1 from [30] establishes the criteria to adjust the power.

$$P = \min(P_{\max}, P_0 + 10 \log M + \alpha \cdot L + \Delta_{\mathrm{TF}} + \Delta_{\mathrm{i}}), \tag{3.1}$$

where,

- $P_{\max}$ (dBm): Maximum allowed transmission power for all UEs defined by the UE power class.
- M: is the number of PRBs allocated in the PUSCH.
- P_0 (dBm): This parameter is used to control the SINR target. A cell-specific value is broadcasted, and a UE-dedicated correction value is signaled, which aims at compensating inaccurate estimations of the path-loss. P_0 has an important impact on the system performance; intuitively, an increase in P_0 would provoke a rise in the transmitted power density with a subsequent increase of the generated interference.
- α: is the broadcasted cell-specific path loss compensation factor for FPC. The basics of the OLPC is to compensate for a fraction α of the distance dependent path-loss and slow variations, determining the basic operating point. The path loss compensation factor variation would bring the system into a trade-off between total UL capacity and cell-edge data rate.
- L (dB): is the DL path-loss estimated by the UE. This estimation is done based on the DL RSRP.
- Δ_{TF}: is a UE specific parameter that allows a finer tuning of transmission power considering the transport format that is allocated to the user. Without loss of generality, UEs do not consider any additional offset in this dissertation.

- Δ_i: is an optional closed loop correction that can be accumulative or absolute and it is signaled by the eNB. Since the focus of this work is to analyse the performance of the system under OLPC conditions this parameter is just set to zero.

From the previous paragraphs it is clear that P_0 and α are not only the most important parameters, but also those with major impact in the system performance. Both must be adjusted at a time, setting an optimal combination to assure an interference operating point in the scenario to achieve optimal system performance.

3.2.2 Concept of Fractional Power Control

From equation 3.1 it is inferred that the PC formula determines the transmitted power per radio resource block, given its dependency with the allocated bandwidth M; this implies that the power transmitted across the allocated bandwidth is constant, which is the same to say that the PSD, expressed in equation 3.2, is constant. It is important to remark that along this dissertation, and unless the opposite is indicated, the PSD is measured as the power per PRB and not per Hz. This simplifies notation and allows skipping a factor 12×15 throughout all equations (from 12 subcarrier per PRB with 15 kHz separation).

$$\delta = P_0 + \alpha \cdot L. \tag{3.2}$$

Note that the PSD is linearly dependent with P_0, while the dependence on α varies jointly with the UE measured PL.

Impact of α

The fractional path-loss compensation α regulates the percentage of correction the UE must conduct when transmitting. When α tends to unity, the user compensates all the path-loss, behaving as a traditional full compensation scheme. Figure 3.1(a) shows the resulting fractional path-loss, or UE compensation, with respect to the distance for different configurations of α; as seen, when the path-loss factor is reduced, corrections to be performed at high distances are virtually much lower than with higher values of α. As a result, when α tends to zero, UEs placed at the cell-edge and those placed closer to the eNB transmit with closer PSD values, as shown in figure 3.1(b), where the slope for $\alpha = 0.8$ is noticeable higher than for $\alpha = 0.4$.

Concluding, the main objective of the FPC is to reduce the level of interference generated by the cell-edge at the expense of lowering the target SINR of the most interfering UEs. While low values of α compromises the overall cell fairness, by equating the transmit power in the cell, high values provide a more fair solution in terms of SINR. Figure 3.2(a) shows the UE SINR cumulative distribution function (cdf) for two different configurations of FPC.

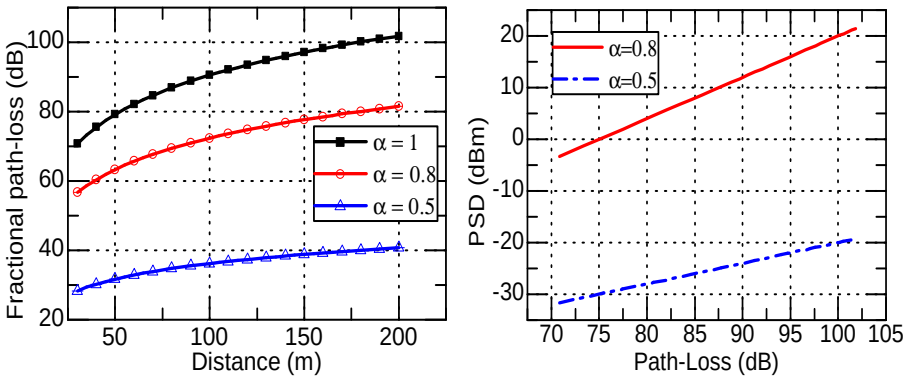

(a) Fractional path-loss, $P_0 = -60\,dBm$ (b) Transmitted power in one resource block, $P_0 = -60\,dBm$

Figure 3.1: Impact of α in the UE transmitted power

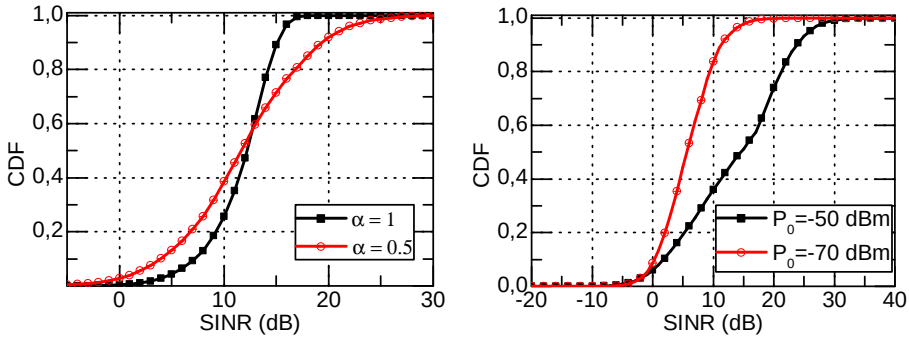

(a) SINR performance vs α, $P_0 = -50\,dBm$ (b) SINR performance vs P_0. $\alpha = 0.6$

Figure 3.2: Power control SINR performance

Impact of P_0

While a change in α impacts the fairness and maintains the average values, a change in P_0 horizontally shifts the curve of the SINR not altering as much the fairness distribution, as shown in figure 3.2(b). P_0 is equal to all UEs in the cell, therefore a rise in it leads to an overall increase of power; it behaves as an offset to the transmitted power. It is worth noticing that an increase in P_0 does not imply an improvement of the SINR in the same level because it impacts on the interference generated as well.

Table 3.1: Power control evaluation: Synthetic scenario

Parameter	Value
Pixel size	5 m
Area	168 x 168 pixels
Transmitters	14 sites (Tri-sectorial antennas)
Propagation model	L = 35,5+37,6log(d); d = distance in meters
Shadow fading	Log-normal, 8 dB standard deviation

3.3 System Performance of FPC

The analysis hitherto done concludes that each possible combination of FPC parameters define an operational point and a consequently performance. The objective is now to define the operating point on which cell performance and fairness are accordingly compromised in two different scenarios: a synthetic macro-case deployment, and a realistic urban deployment. Note that, at this stage, the adjustment does not consider the use of aggregated carriers.

3.3.1 OLPC Optimal Performance in Macro-Case Scenario

Scenario highlights

The synthetic scenario system model comprises 13 tri-sectorial cells equally distributed along 3 km^2 with an ISD of 500 m. Other system aspects are listed in Table 3.1. Specific information about the synthetic scenario is provided in appendix A.

Performance Evaluation

Several configurations of α and P_0 are simulated and the performance evaluation is done in terms of BLER, interference generated, UE throughput distribution and transmit power. In particular, the interference is measured with the Interference over Thermal (IoT) metric, calculated as:

$$IoT = \frac{I + \sigma_n^2}{\sigma_n^2} \tag{3.3}$$

where, I is the aggregate interference power perceived in one radio resource and σ_n^2 is the additive white Gaussian noise power in the same bandwidth.

Figure 3.3 depicts the cdf of the IoT and SINR for the configurations that provided lower BLER performance. Solutions with very low α, such as $\alpha = 0.4$ and $\alpha = 0.5$ generate less interference because UEs in the cell edge are transmitting with low power levels, as shown in figure 3.3(a). On the other hand, when P_0 is configured

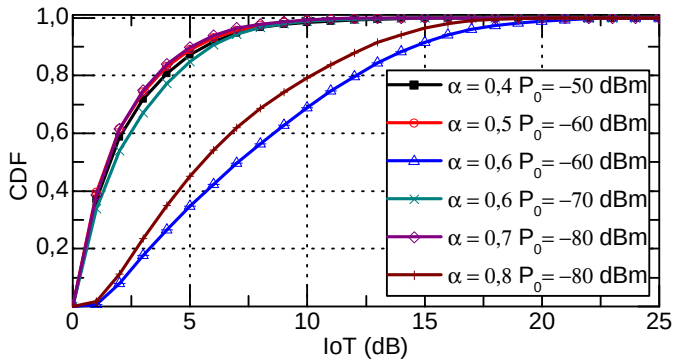

(a) IoT measured per UE and PRB

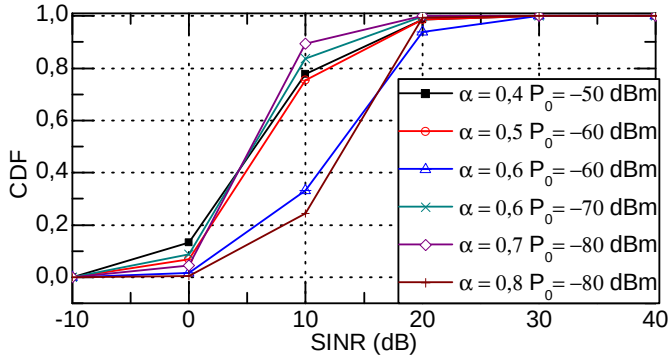

(b) SINR performance measured in the PUSCH channel

Figure 3.3: Synthetic case: Different FPC parameters configuration, IoT and SINR

low together with a moderate value of path-loss compensation, the resulting transmit power in the cell-edge is also reduced, therefore interferences are contained; it can be noted in the same figure that the IoT distributions for configurations $\alpha = 0.5$; $P_0 = -60\,\text{dBm}$ and $\alpha = 0.7$, $P_0 = -80\,\text{dBm}$ closely resemble. As shown in figure 3.3(b), this is done at the expense of reducing the SINR level in the cell.

The system aims at keeping IoT levels below 16 dB in all the scenario, this way a correct functioning of the eNB is assured. In this sense, the solutions, which are more aggressive in the interference generation, are still below this IoT margin. Figure 3.4 compares these two solutions in terms of UE throughput, figure 3.4(a), and transmit power, figure 3.4(b). Average throughput is higher for a lower path-loss compensation solution, however, there is a throughput loss in the lower part of the cdf. It is noticed that in the configuration with $\alpha = 0.8$ there is a tendency of having a higher number of UEs transmitting at maximum power levels. These UEs are mainly located in the cell edge and, given the higher demands in terms of path-loss, are more likely to transmit near the maximum allowed power. This situation is going

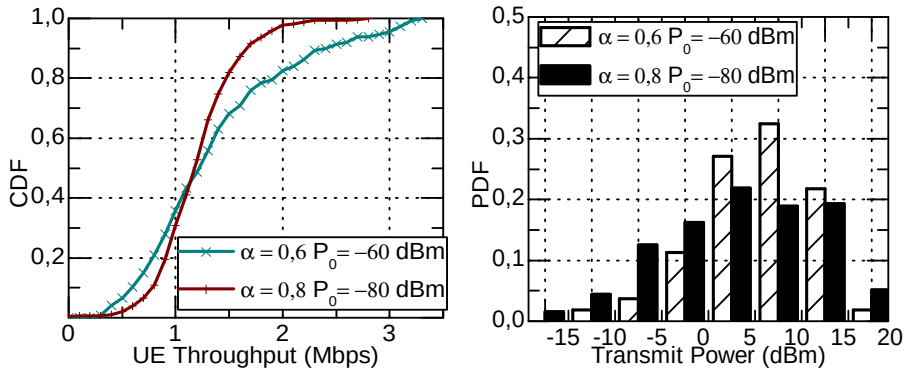

(a) UE Throughput distribution

(b) UE Transmit power distribution

Figure 3.4: Synthetic case: FPC parameters configuration, throughput and transmit power

to be further aggravated with the use of CA, where the UE allocated bandwidth is increased. Therefore, if cell edge UEs must compensate a higher part of their path-loss they are going to be deprived of CA, essentially because of power scarcity. The lower throughput observed in 3.4(a) for $\alpha = 0.6$ can be compensated further on with the use of aggregated carriers, since there are less power limited UEs.

3.3.2 OLPC Optimal Performance in Realistic Deployments

Scenario highlights

The FPC is studied under a realistic scenario obtained from the MORANS initiative developed during the European COST Action 273 [86] and whose aim was the definition of scenarios with different levels of realism, so that researchers were able to test and compare RRM algorithms, at the planning and system level, with a more realistic distribution of the base stations. The propagation model considered in this system model is the COST 231-Walfisch-Ikegami [87]. The scenario comprises a dense urban area composed by a fraction of the city of Vienna. In particular, the following inputs are provided by the MORANS scenario:

- Area of simulation: Universal Transverse Mercator (UTM)-30 coordinates of the selected area.
- Building information: Represents the height at a given pixel. This information is used to compute the streets direction and it also is an input to the propagation model that realistically considers these buildings as a source of diffraction.
- Site and transmitter information: physical location, height and patterns.

Table 3.2: Power control evaluation: Realistic scenario

Parameter	Value
Pixel size	5 m
UTM upper left coordinates	600500 m X 5340500 m Y
Area	500 x 500 pixels
Transmitters	16 sites (Trisectorial antennas)
Propagation model	COST 231-Walfisch–Ikegami
Indoor losses	15 dB

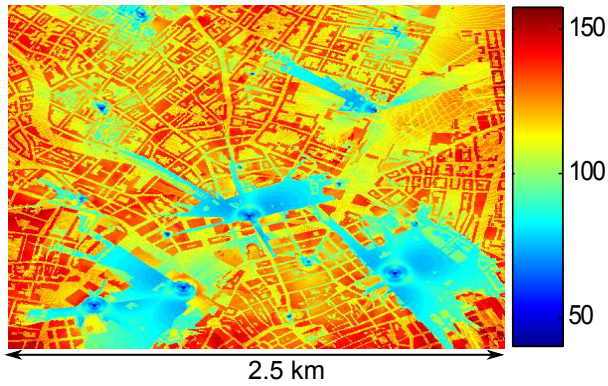

Figure 3.5: Realistic scenario path-loss (dB)

The system model parameters are summarized in Table 3.2. Figure 3.5 shows a plot of the selected area in terms of the path-loss, where it is seen that the realistic environment presents many sources of losses. The areas with no line of sight are the most attenuated ones, as signals are shadowed by the buildings nearby; also indoor communications are severely affected by the large attenuations. This leads to user transmission power limits, as they may have to compensate for a larger path-loss.

Performance Evaluation

The FPC configuration performance is done in terms of call drops, IoT, SINR, UE throughput distribution and PSD. The percentage of call drops is defined as the UEs that access the scheduler but never succeed in their transmissions. It is recalled that cell selection is done based on the DL RSRP and the UL transmissions rely on the UE power to overcome the large path-losses, as for example the case of indoors. Figure 3.6(a) depicts the IoT of the configurations that provided lower call drops. All the FPC settings result in quite similar performance and the interference generated does not have a big impact despite the difference in transmit power, given the increased path-loss distribution of the scenario. The SINR measured at the PUSCH, shown in figure 3.6(b), shows that high values of α improves the lower

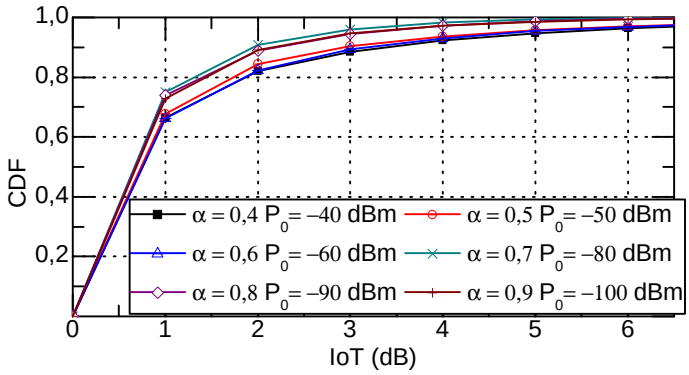

(a) IoT measured per UE and PRB

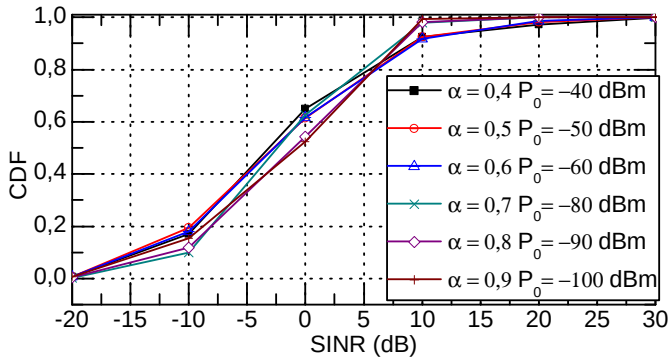

(b) SINR performance measured in the PUSCH channel

Figure 3.6: Realistic case: Different FPC parameters configuration

region of the distribution, and the median SINR is improved by nearly 3 dB in the case of $\alpha = 0.7$ and $\alpha = 0.8$; however, this is at the expense of lowering the higher part of the distribution.

Figure 3.7 shows the performance of the FPC configurations in terms of the UE throughput distribution, where it is stressed at first sight the increased diversity among the different settings. Thus conclusions can be drawn more effectively that with the previous IoT and SINR analysis. Low values of P_0 result in less average data rate even though the lower part of the distribution is slightly improved. This is mainly attributable to the resulting transmit PSD, whose distribution is shown in figure 3.8. Configurations with low values of P_0 result in lower PSD in such a way that spectral efficiency cannot be maximized. Based on the throughput results, it is suggested the use of $P_0 = -40$ dBm and $\alpha = 0.4$. It sets a good compromise between transmit power and UE achieved throughput. As a conclusion, UEs under such large path-loss are less likely to transmit in aggregated carriers and there is an increased need for addressing CC selection procedures not to jeopardize power limited UEs.

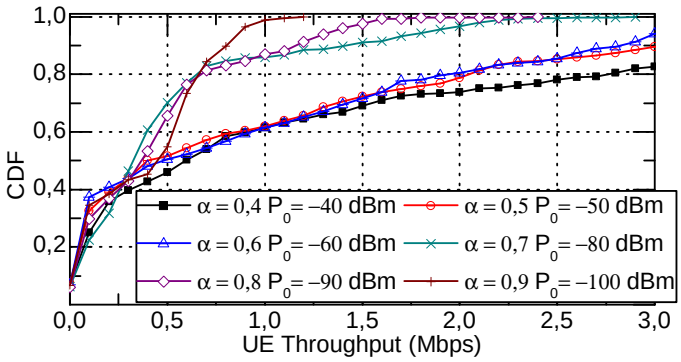

Figure 3.7: Realistic case: UE Throughput distribution

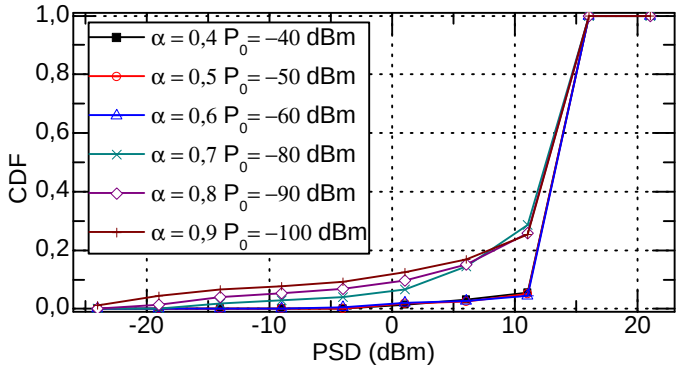

Figure 3.8: Realistic case: UE Transmit PSD distribution

3.3.3 Conclusions

The OLPC is dependent on the path-loss each user estimates, so the environment is a key issue when investigating the performance at the system level. Both scenarios present different limits, in such a way that the versatility presented by the algorithm allows finding suitable configurations for each specific case. As the system is brought into a trade-off between fairness and interferences when applying the FPC, the performance evaluated for one environment may not work for another with different assumptions. In realistic networks the position and configuration of sites leads to different path-loss distributions and different sensitivity to the interference among cells in the deployment, therefore, in realistic networks an interesting approach would be to separately configure the OLPC parameters, in a cell by cell manner, though this would be out of the scope of this dissertation.

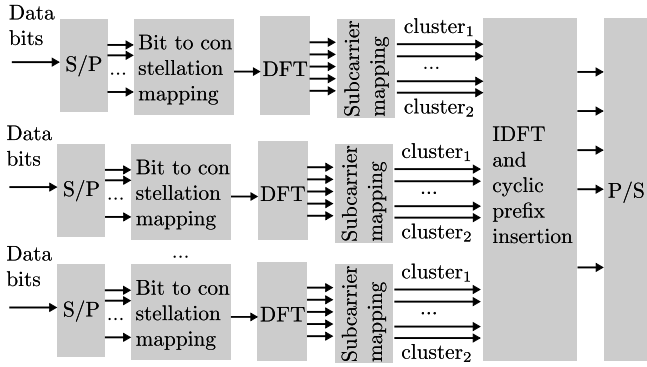

Figure 3.9: NxDFT-D-OFDM signal generation

3.4 Power Considerations with CA

LTE-A has been provided with specific rules to control the UE power to contain interferences and improve the overall performance. Results shown so far do not consider the use of spectrum aggregation, which is indeed challenging from a UE power availability point of view. If UEs suffer from high losses, increasing their allocated bandwidth may not be beneficial, even with the use of fractional path-loss compensations. Moreover, allowing CA and non-contiguous resource allocation in the UL implies changes in the existing access technology; a new access scheme must be provided that supports sparse allocations in an efficient manner.

3.4.1 Multi-cluster Transmission in CA

In previous releases, SC-FDMA was selected to be the multiple access technique adequate for the UL. By allocating UEs a set of contiguous sub-carriers, signals achieved very low PAPR compared to the OFDMA solution. This is a good option as it facilitates the use of efficient PAs in the devices. However, the contiguous allocation impairs scheduling flexibility and reduces frequency diversity. To adapt the UL to the CA capabilities, the 3GPP has agreed to use N x DFT-S-OFDM and to allow non-contiguous resource allocations in each CC, clustered DFT-S-OFDM is used. Separated pieces of spectrum known as *clusters* are allocated to users, with the inconvenience of increasing the PAPR [88, 89]. Nevertheless, this solution provides less PAPR than pure OFDM and it constitutes a good compromise between SC-FDMA and OFDM [90]. With this, radio resources can be allocated with more flexibility, which yields to more frequency diversity gain, and, at the same time, provides compatibility with previous releases of LTE [91]. So, each CC is independently DFT spread, and each transport block is built of non consecutive clusters of PRBs, figure 3.9 shows the new signal generation schematic. In the context of LTE-A the maximum number of allocable clusters is two per CC, and the number of PRBs per cluster depends on the system bandwidth [19].

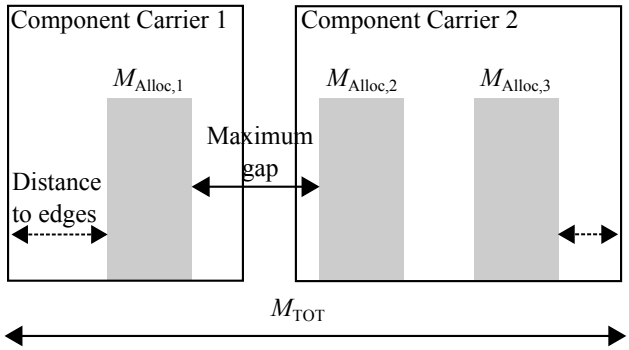

Figure 3.10: Variables of the aggregated signal that affect in the PAPR

The PAs used in radio transmitters have non-linear characteristics, which cause significant distortion in the signals whose instantaneous power fluctuations come too close to saturation level. The use of simultaneous transmissions influences the PAPR and generates increased out of band emissions caused by intermodulation products, which essentially impairs the compliance of the spectrum mask. This drives the need for MPR which depends on the signal generation, as seen in figure 3.10, where variables that impact the PAPR of the signal are shown.

Several authors have worked on obtaining an accurate characterization of the MPR given the spectrum configuration of CA. Authors in [92] concluded that a single metric can be used to determine the required MPR when two CCs are aggregated. This metric is the ratio between the total allocated bandwidth and the entire available bandwidth. Moreover, authors in [93] present an extension of the previous study with further simulations and propose a more accurate estimation of the MPR to be applied. Given these studies, the 3GPP included a MPR mask equation for multi cluster transmission in both multi-CC and single-CC transmission. For intra-band contiguous CA the formula agreed is:

$$\pi_A^{\text{CA}} = \begin{cases} 8.2 & \text{if } 0 < A < 0.025, \\ 9.2 - 40 \cdot A & \text{if } 0.025 \leq A < 0.05, \\ 8 - 16 \cdot A & \text{if } 0.05 \leq A < 0.25, \\ 4.83 - 3.33 \cdot A & \text{if } 0.25 \leq A < 0.4, \\ 3.83 - 0.83 \cdot A & \text{if } 0.4 \leq A \leq 1. \end{cases} \tag{3.4}$$

For single carrier transmissions the MPR for multi clustered allocations is given by:

$$\pi_A^{\text{SC}} = \begin{cases} 8 - 10.12 \cdot A & \text{if } 0 < A \leq 0.33, \\ 5.67 - 3.07 \cdot A & \text{if } 0.33 < A \leq 0.77, \\ 3.31 & \text{if } 0.77 < A \leq 1. \end{cases} \tag{3.5}$$

In both equations, $A = M_{\text{Alloc}}/M_{\text{Tot}}$ is the ratio between the allocated PRBs and total system bandwidth. In the case of CA, the system bandwidth corresponds to

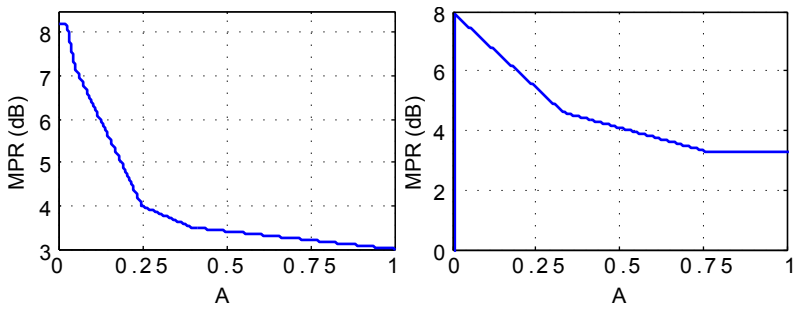

(a) MPR mask for CA (b) MPR mask for single-CC

Figure 3.11: MPR mask for the two non-contiguous cases

the aggregated one. This mask applies the maximum reduction of power for narrow allocated bandwidths, which confirms what was concluded in [94]. Figure 3.11 shows a graphical representation of the MPR to be applied in both cases.

3.4.2 Constrains on Resource Allocation

Given equation 3.1, increasing the transmission bandwidth M_{Alloc} may not benefit all UEs, as the total transmitted power depends on the allocated bandwidth. This is particularly true for cell edge UEs, which are much more likely to transmit at maximum power levels. Power per PRB is constant regardless the number of radio resources allocated, as shown in equation 3.2; but, once P_{max} is reached, the PSD drops as the allocated bandwidth grows. With the inclusion of non contiguous resource allocation, the maximum power is reduced and the PSD of power limited UEs can be severely affected. The total transmitted power in the PUSCH of a CA system is defined as:

$$P_{\text{PUSCH}}^{\text{CA}} = \min(P_{\text{max}}^{\text{MC}} - \pi_A^{\text{CA}}, 10 \log P'), \tag{3.6}$$

where P' is the final sum of the N aggregated CCs:

$$P' = \sum_{i \in N} P_{0_i} M_{\text{Alloc}_i} \alpha_i L_i. \tag{3.7}$$

Equation 3.1 is used to determine the transmission power on each CC, named CC specific power control. The need for specific power setting arises as there might be aggregation scenarios with potentially different propagation or interference conditions. This means that different OLPC parameters can be selected, and that a UE can transmit using different power levels and PSDs on the multiple CCs. If the total transmission power on all CCs exceeds the maximum UE power capabilities, the UE must decide how to reduce it and determine this power reduction for each CC [95].

If the eNB does not know how close the UE is of its maximum transmit power, it can allocate resources for which the UE can not respond efficiently regarding the lack of power. PHRs indicate how much transmission power is left for a UE with respect to the power being used by the current transmission. In Release 10 the CC specific maximum power limit is included in the PHR [30, 96]. Both PHR and CSI provide the eNB with sufficient information to perform a more efficient allocations. As explained in chapter 2, the CSI in the UL is obtained through SRSs, whose power is also adjusted with the same OLPC algorithm (Equation 3.1), where M_{Alloc} corresponds to the SRS bandwidth allocated, M_{SRS}. Sounding and data may have different allocated bandwidths, but the PSD δ measured at the PRB level is kept constant as long as power levels are below $P_{\max} - \pi_A$.

$$\delta = \min(P_{\max} - \pi_A - 10 \log M_{\text{Alloc}}, P_0 + \alpha \cdot L). \tag{3.8}$$

Thus, if bandwidth allocations increase and UEs achieve maximum power levels, apart from impairing the spectral efficiency because of a reduced PSD, it implies that $\delta_{\text{SRS}} \neq \delta_{\text{PUSCH}}$ and the CSI brought by the SRS can be significantly different from the PUSCH. This constitutes one of the causes of misalignment between the sounded information and the actual channel quality which potentially reduces the reliability of the CSI procedure. Several open challenges appear in this regard which are addressed in the following chapters.

Chapter 4

RRM with CA: Scheduling and CC Selection

4.1 Introduction

The LTE-A FPC mechanism introduced in chapter 3 plays an important role in maintaining the required SINR while reducing inter-cell interferences. In the case of multi-cluster transmissions, in single or multi-CC allocations, further considerations must be done in the UE power management. The counterpart of intra-band contiguous CA is that the same PA is used for all the aggregated CCs. The resulting NxDFT-S-OFDM signal has an increased PAPR, which limits the PA efficiency, thus power de-rating becomes essential to assure a working point that ensures linear operation. The MPR impacts directly the CA performance, since large bandwidth allocations require an increased power availability. Based on this, it is necessary to develop RRM procedures that consider power constraints opportunistically, and allow for non-contiguous transmissions in cases where a net throughput gain can be obtained.

This chapter introduces two novel RRM schemes whose main objective is the maximization of the UE throughput. First, a JCS strategy that considers MPR information opportunistically in the scheduling decisions is proposed. Initially, all users are assumed to be appropriate for CA transmission, no RRC operations for CC selection are carried out. To evaluate if a non contiguous resource allocation is suitable, their throughput is estimated. This is done based on the information from past SRSs received by the eNB from the UE. The MPR to be eventually applied depends on several parameters such as the number of CCs and assigned bandwidth; the scheduler will compute the best combination, so that its final allocation decision maximizes the UE throughput. Second, in the context of ICS, a CC selection strategy is proposed with a two-fold novelty. First, in the same line as in the first proposal, the CA eligibility takes into account MPR required for multi-CC transmissions. Second, an acceptance margin is introduced so that UEs are not directly rejected

if they are power limited. Each CC will schedule independently resources with the mechanism introduced in the first part of the chapter. In this manner, UEs not eligible for CA can still transmit in separated clusters, and can benefit from the frequency diversity gain brought by it.

The chapter is organized as follows: the next section recalls the main challenges of the UL resource allocation with CA regarding power settings and MPR. The system model is described in section 4.3, and the novel schemes are presented and evaluated in sections 4.4 and 4.5. Section 4.6 derives a detailed comparison between both CA and single carrier transmissions considering the main LTE-A trade-off among energy efficiency, UE average throughput and fairness. Finally, the chapter is closed summarizing the main concluding remarks in section 4.7.

4.2 Problem Formulation

In the past chapter, the most important UE power setting considerations were addressed and topics like MPR and misalignment caused by differences in PSD where introduced. In this regard, several challenges open up to include CA in the UL transmissions while not impairing the performance in the power limited cases. In the literature review done in section 2.3, it was seen that works considering CA in the UL typically neglect non-contiguous allocations in the cell edge, where UEs are treated as pre-Release 10 devices. This simple solution, at first glimpse may avoid some constraints in the resource allocation process, however, it deprives these UEs from the gains brought by transmitting in aggregated carriers, and outcomes in a less fair global performance. Moreover, the inclusion of hard conditions to classify UEs may well alter the performance in the different environments. In this sense, it is required to provide the scheduling and CC selection processes with sufficient intelligence to perform spectral efficient allocations in any situation. The most important limitations recognised so far when adopting CA in the UL are:

- Increased bandwidth allocations may reduce the UE PSD.
- Non-contiguous resource allocation, in one or multiple CCs, needs MPR to accomplish the LTE spectrum emission mask, which leads to a potentially further PSD reduction, thus worsening the link budget even more.
- Imperfect CSI brought, in part, by the misalignment between SRSs transmit power and data transmit power.

Based on this, the main novelties presented in this chapter can be summarized as follows:

- Individual assessment of throughput improvements or deteriorations brought by non-contiguous resource allocations in the form of:

1. A cross-CC resource scheduler in charge of deciding the eligibility of UEs for both single or multi CC transmissions which is designed to maximize the UE data rate.
2. A CC selection process that considers power limitations when deciding and also accounts for the frequency selective gain brought by non-contiguous allocations.

- Introduction of reference signals, in the form of SRSs, to perform realistic CSI acquisition and support the assessment.
- Study of the feasibility of CA in terms of the LTE-A trade-off: energy efficiency, UE average throughput and fairness.

4.3 System Model

Consider a macro cell network with a set of $\mathcal{J}$ eNBs, each one has a total number $\mathcal{I}$ of associated users. Each eNB employs $\mathcal{L}$ CCs in the same frequency band with the exact same bandwidth. Each CC is comprised of $\mathcal{R}$ PRBs which are allocated to users each TTI. Frequency selective scheduling is possible in the UL with the use SRSs, which are transmitted periodically or occasionally, depending on the UE needs. UEs at the cell edge typically transmit hopped SRSs to have more reliable measurements due to power limitations. The standard allows transmitting simultaneous SRS in different CCs, however power scaling may be necessary; to avoid this, SRSs of different CCs are alternated in along the TTIs. The eNB allocates a set of M_{SRS} contiguous PRBs to be sounded and obtain a CSI measurement. The signal received per PRB r at the eNB side in its lth CC and one RTT later is denoted as $S_{l,r}^{\mathrm{UL}}(i,j)$. For the sake of simplicity subindex l has been omitted in all equations

$$S_r^{\mathrm{UL}}(i,j) = P_{\mathrm{SRS}} h_r(i,j)\, d(i,j)^{-\alpha}\, 10^{\frac{\chi}{10}}, \tag{4.1}$$

where P_{SRS} is the transmitted power from equation 3.1; $h_r(i,j)$ is the Rayleigh fading at PRB level; $d(i,j)$ is the distance from user i to the eNB j and α is the path loss exponent; χ is a Normal random variable with zero mean and standard deviation σ.

With this, the eNB can estimate the user's i CSI at PRB r in carrier l as:

$$\gamma_r^{\mathrm{SRS}}(i,j) = \frac{S_r^{\mathrm{UL}}(i,j)}{I_r(i,j) + \sigma_n^2}, \tag{4.2}$$

where σ_n^2 was defined in chapter 3 and I_r is the total aggregate inter-cell interference perceived in PRB r which is modeled as:

$$I_r(i,j) = \sum_{n \in N} P_{\mathrm{SRS},n} h_r(i,j)\, d(i,j)\, d(n,j)^{-\alpha}\, 10^{\frac{\chi}{10}}, \tag{4.3}$$

where N is the set of interfering UL users associated to the neighbouring cells.

Following this sounding process along the entire $\mathcal{R}$ lets to obtain a single value of $\gamma_r^{\mathrm{SRS}}(i,j)$ for every PRB. This information is used by the scheduling entity to perform spectrally efficient decisions and also for the link adaptation to assign the most appropriate MCS.

The scheduler's main task is to allocate M_{PUSCH} in order to maximize throughput while maintaining a proportional fairness in the coverage area. Based on the average $\overline{\gamma^{\mathrm{SRS}}(i,j)}$ over the allocated PRBs, the eNB signals the UL scheduling grant.

The received PUSCH signal one RTT later from the allocation is:

$$S^{\mathrm{UL}}(i,j) = P_{\mathrm{PUSCH}} h(i,j)\, d(i,j)^{-\alpha}\, 10^{\frac{\chi}{10}}, \tag{4.4}$$

where P_{PUSCH} is obtained from the OLPC algorithm with the corresponding MPR reduction in case of multi cluster allocation (equations 3.4 and 3.5). The resulting SINR is:

$$\gamma^{\mathrm{PUSCH}}(i,j) = \frac{S^{\mathrm{UL}}(i,j)}{\overline{I(i,j)} + \sigma^2}, \tag{4.5}$$

where $\overline{I(i,j)}$ is the average interference perceived in all M_{PUSCH}. From equations 4.2 and 4.5 it is inferred that a difference in both may arise if the UE power required exceeds the maximum power levels. This misalignment is mainly due to $\delta_{\mathrm{SRS}} \neq \delta_{\mathrm{PUSCH}}$, and it is quantified as ΔP:

$$\Delta P = P_{\mathrm{SRS}} - P_{\max} + \pi_A + 10 \log \frac{M_{\mathrm{PUSCH}}}{M_{\mathrm{SRS}}}. \tag{4.6}$$

4.4 Non-Contiguous Resource Scheduling: A Joint Carrier Scheduling Case

In terms of UE power availability, not all of them are valid candidates for adopting CA or multi cluster transmission, their throughput could be reduced when compared to the localized allocation. However, non contiguous resource allocation brings an intrinsic frequency diversity gain that, in some cases, could well overcome the extra losses brought by the MPR. Following this thought, each UE should be independently assessed to verify whether a CA transmission would imply a net gain in throughput. Otherwise, Release 8 conditions (use of SC-FDMA) ought to be maintained to not impair their QoS.

The proposal is to extend the scheduling information so that resource allocation algorithms account for MPR information along with PHRs from the user and anticipate possible SINR imbalances between information from SRS and SINR in the eventual scheduled PUSCH resources. Schedulers with this feature should compute the loss in SINR affected by the power reduction and derive if this implies a change in the chosen MCS. Existing sounded signals are used to predict if the gain brought by the allocation of separated clusters can overcome the loss in transmitted power.

No extra signalling is required for this new operation.

4.4.1 Multi-cluster Scheduler for Joint Resource Allocation

Our general allocation model is a HARQ aware scheduler based on PF decisions that has been added the capability of allocating separated clusters of both CCs. The scheduler is divided in two parts as presented in [97]. First a time domain (TD) scheduler followed by a frequency domain (FD) one. The new operation features are included in Algorithm 1 which is explained in detail in the following paragraphs.

The TD scheduler is in charge of sorting users following a PF policy and generating the final reduced set of UL users allowed to be served in the current TTI. The procedure is HARQ aware and so the subset of users $\mathcal{H}$ with pending re-transmissions is included in the group. Then, the scheduler completes the list following the prioritization metric τ computed for every user i that sent a scheduling request ($0 < i < I$):

$$\tau(i) = \frac{R_{\mathrm{b}}^{\mathrm{G}}(i)}{\overline{R_{\mathrm{b}}}(i)}, \tag{4.7}$$

where $R_{\mathrm{b}}^{\mathrm{G}}(i)$ is the bitrate to be granted for the current service of i and $\overline{R_{\mathrm{b}}}(i)$ is its past average throughput.

From the final sorted list, a subset of users is chosen to be served in the current TTI.

$$\mathcal{U} = \{u_1, u_2, \ldots, u_{|\mathcal{U}|} : \tau(u_j) \geqslant \tau(u_{j+1}) \forall j\}$$

The system bandwidth is divided into C clusters of M_{cluster} PRBs each one, therefore the size of $\mathcal{U}$ is given by:

$$|\mathcal{U}| = \max\left(\frac{M_{\mathrm{Tot}}}{2M_{\mathrm{cluster}}} - |\mathcal{H}|, 0\right) = \max\left(\frac{C}{2} - |\mathcal{H}|, 0\right). \tag{4.8}$$

The FD scheduler allocates PRBs to UEs in $\mathcal{U}$ aiming at maximizing the spectral efficiency. On the other hand, synchronous non-adaptive HARQ is considered, and so re-transmissions re-use the same allocation bandwidth and MCS. Therefore signaling is reduced since there is no need for new UL allocation grants. For each user $i \in \mathcal{U}$, the scheduler gets the sounded SINR at the PRB level $\gamma_{i,l,r}^{\mathrm{SRS}}$. Hence, it selects the MCS which maximizes the throughput. This is done under the constraint that the estimated BLER is smaller or equal than the target BLER at first transmission. The expected throughput in that PRB $R_{\mathrm{b}}^{\mathrm{PRB}}(i,j)$ is estimated from the MCS. Finally, a score $s(i,c)$ per cluster c is computed as its average estimated throughput:

$$s(i,c) = \frac{1}{|\mathcal{P}_c|} \sum_{j \in \mathcal{P}_c} R_{\mathrm{b}}^{\mathrm{PRB}}(i,j), \tag{4.9}$$

where $\mathcal{P}_c$ denotes the set of PRBs in cluster c and $|\mathcal{P}_c|$ is its corresponding cardinality. Here, all clusters have the same size: $|\mathcal{P}_c| = M_{\mathrm{cluster}}$. The result is a matrix $\mathbf{S} \in$

Algorithm 1 MPR aware scheduler

procedure TD SCHEDULER($\mathcal{H}$)
  for all $i \in \mathcal{H}$ **do** re-use allocated PRBs and MCS
  for $i \leftarrow 1, I$ **do**
    if $i \notin \mathcal{H}$ **then** $\tau(i) \leftarrow R_{\mathrm{b}}^{\mathrm{G}}(i)/\overline{R_{\mathrm{b}}}(i)$
    else $\tau(i) \leftarrow 0$
  $\mathcal{U} \leftarrow \{u_1, u_2, \ldots, u_{|\mathcal{U}|} : \tau(u_j) \geq \tau(u_{j+1}) \forall j\}$
procedure FD SCHEDULER($\mathcal{U}, M_{\mathrm{Tot}}, M_{\mathrm{cluster}}, M_{\mathrm{SRS}}$)
  $C \leftarrow M_{\mathrm{Tot}}/M_{\mathrm{cluster}}$
  for all $i \in \mathcal{U}$ **do**
    for $j \leftarrow 1, M_{\mathrm{Tot}}$ **do**
      $\mathrm{MCS} \leftarrow f_1(\gamma_{\mathrm{SRS}}^{\mathrm{PRB}}(i,j), \mathrm{BLER})$
      $R_{\mathrm{b}}^{\mathrm{PRB}}(i,j) \leftarrow f_2(\mathrm{MCS})$
    Generate i-th row of score matrix **S**:
    for $c \leftarrow 1, C$ **do**
      $s(i,c) \leftarrow 1/|\mathcal{P}_c| \sum_{j \in \mathcal{P}_c} R_{\mathrm{b}}^{\mathrm{PRB}}(i,j)$
  for all $i \in \mathcal{U}$ **do**
    Find pair of best clusters:
    $\mathcal{B}_i \leftarrow \arg\max_c(s(i,c))$
    if $|\mathcal{B}_i| > 2$ **then**
      $b_1 \leftarrow \min_c \left(\sum_{\forall u \in \mathcal{U}} s(u,c)\right), c \in \mathcal{B}_i$
      $b_2 \leftarrow \min_c \left(\sum_{\forall u \in \mathcal{U}} s(u,c)\right), c \in \mathcal{B}_i - \{b_1\}$
  $\gamma(i) \leftarrow$ Effective SINR in allocated bandwidth
  if b_1 and b_2 contiguous **then** Localized treatment:
    $\mathrm{MCS} \leftarrow f_1(\gamma(i), \mathrm{BLER})$
    $R_{\mathrm{b}}(i) \leftarrow f_2(\mathrm{MCS})$
  else Multi-cluster treatment:
    if $P_{\mathrm{TX}} > P_{\max} - \pi_{\mathrm{A}}$ **then**
      $\Delta P \leftarrow P_{\mathrm{SRS}} - P_{\max} + \pi_A + 10 \log \frac{2M_{\mathrm{cluster}}}{M_{\mathrm{SRS}}}$
      $\gamma(i) \leftarrow \gamma(i) - \Delta P$
    $\mathrm{MCS} \leftarrow f_1(\gamma(i), \mathrm{BLER})$
    $R_{\mathrm{b}}(i) \leftarrow f_2(\mathrm{MCS})$
    Comparison with localized treatment:
    $b \leftarrow$ Enlarge b_1 with contiguous cluster
    if $b =$ void **then** $b \leftarrow$ Enlarge b_2
    if $b =$ void **then** Allocate just one cluster
    $\gamma'(i) \leftarrow$ Effective SINR in contiguous bandwidth
    $\mathrm{MCS}' \leftarrow f_1(\gamma'(i), \mathrm{BLER})$
    $R'_{\mathrm{b}}(i) \leftarrow f_2(\mathrm{MCS}')$
    if $R'_{\mathrm{b}}(i) > R_{\mathrm{b}}(i)$ **then** Localized allocation
    else Multi-cluster allocation

$\mathbb{R}_{+}^{|\mathcal{U}|\times C}$ containing all cluster scores for every user $i \in \mathcal{U}$, ordered following the TD criteria:

$$\mathbf{S} = \begin{array}{c} \\ \tau(u_j) \geqslant \tau(u_{j+1}) \\ \downarrow \end{array} \begin{array}{c} \begin{array}{cccc} \text{cluster}_1 & \text{cluster}_2 & \dots & \text{cluster}_C \end{array} \\ \left(\begin{array}{cccc} s(u_1,1) & s(u_1,2) & \dots & s(u_1,C) \\ s(u_2,1) & s(u_2,2) & \dots & s(u_2,C) \\ \vdots & \vdots & \ddots & \vdots \\ s(u_{|\mathcal{U}|},1) & s(u_{|\mathcal{U}|},2) & \dots & s(u_{|\mathcal{U}|},C) \end{array} \right) \end{array}. \tag{4.10}$$

For each user in the sorted list, the FD stage will search the set of clusters of both CCs with the highest score $\mathcal{B}_i$. In case more than two clusters share the best value, the scheduler selects those having the lowest accumulated score and so having worse performance in the remaining users.

$$b_1(i) = \min_c \left(\sum_{\forall u \in \mathcal{U}} s(u,c) \right), c \in \mathcal{B}_i, \tag{4.11}$$

$$b_2(i) = \min_c \left(\sum_{\forall u \in \mathcal{U}} s(u,c) \right), c \in \mathcal{B}_i - \{b_1(i)\}. \tag{4.12}$$

Next, the scheduler estimates whether power de-rating is going to be applied by the UE and the corresponding impact on its final throughput. This is done by computing the transmission power to be used by the UE. Since SRSs use the same OLPC algorithm as data, the eNB just requires to know P_{SRS}. Even though this information is not directly reported, the UE can indicate its current power headroom at the MAC layer. Then, as the eNB knows the UE power class (and so its maximum power), the actual power estimation is done. Note that SRS and data might have different allocated bandwidths, but the PSD measured at the PRB level δ_{SRS} and δ_{PUSCH} is kept as long as power levels are below $P_{\max} - \pi_A$. Otherwise, the scheduler computes the user MPR from equation 3.4 or equation 3.5, depending on the allocated configuration, and updates the PSD by subtracting the difference ΔP from equation 4.6. Given the estimation of transmission power and interference plus noise power (addition at subcarrier level in the allocated clusters), the effective $\gamma_{i,l}^{\text{PUSCH}}$ is obtained and used for link adaptation. The corresponding throughput is compared against a contiguous allocation. The configuration resulting in a higher throughput is the allocated one.

4.4.2 Results

Benchmarks

With the aim of analysing the performance of the previous approach under diverse transmission conditions the number of allocated PRBs is varied, and two different scenarios tested: an interference limited (ISD 500 m) and a noise limited scenario (ISD 1732 m). Table 4.1 provides information about the simulation assumptions,

Table 4.1: JCR scheduler: Simulation scenario assumptions

Parameter	Value
Bandwidth	2 x 80 PRBs
SRS BW	16 PRBs
Number of UEs served	10
Number of UEs connected	30
PRBs allocated (ISD 500 m)	2 clusters of 8, 10, 20 PRBs x CC
PRBs allocated (ISD 1732 m)	2 clusters of 4 PRBs x CC
Simulation time	40 kTTI

further information about the simulation conditions are given in appendix A. The performance of the proposed JCS process is tested and compared against several benchmark scenarios:

- Cont: Contiguous SC-FDMA allocation.
- MC: Multi-cluster MPR agnostic allocation. All UEs make use of two separated clusters and CA transmission.
- MC-Th: Threshold algorithm presented in [21] and applied for CA joint scheduling. In this case, the average value of MPR is set to 6 dB.
- MC-MPR: The actual proposal, multi-cluster MPR aware allocation.

Algorithm analysis

To evaluate the algorithm performance, results are first analyzed in the interference limited scenario with a constant cluster size of 8 PRBs. Figure 4.1 shows the cdf of the average user throughput. Transmitting in more than one cluster of PRBs improves the system performance. It can be seen that in all three MC solutions the throughput is increased with respect to the contiguous allocation policy. This gain is brought by the extra frequency diversity, since the scheduler enjoys more flexibility to choose the best spectrum areas. Table 4.6 summarizes the average and cell edge throughput and the resulting BLER obtained at the first attempt for all four cases.

The proposed algorithm lets increase both the average and the cell edge throughput. The MC-MPR algorithm brings the system into a hybrid solution, in which information about UE's power availability is smartly used by the scheduler to allocate clusters in a contiguous or separated manner. The increase in average throughput is higher than 11% with respect to the case in which all UEs transmit in separated clusters (MC scheduler), and more than 16% in the 5th percentile worst throughput. If power limited UEs transmit in separated clusters their maximum transmitted power is reduced (affected by the MPR), which has a direct impact on the PSD.

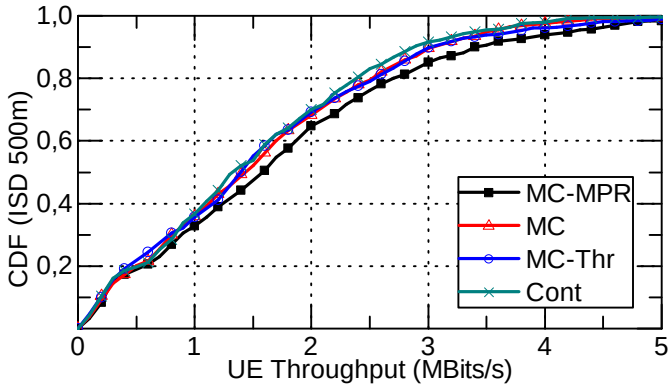

Figure 4.1: JCS scheduling: Average UE Throughput

Table 4.2: Throughput values for Cluster size = 8 PRBs

Throughput	MC-MPR	MC	MC-Thr	Cont
Average (Mbits/s)	1.78	1.60	1.61	1.54
Cell-edge (kbps)	141	121	105	108
BLER (%)	29.24	31.54	29.27	33

The improvement seen in the MC-MPR scheduler is because it allows for localized transmissions in power limited cases. Hence, UEs do not require power de-rating and their link budget is not impaired, thus there is no reduction of PSD. Improvements are also noticeable with respect to the threshold-based scheduler that selects CA users based on their attenuation to the eNB. In this case the average rate increase is similar to the previous strategy, around 11%; however cell edge throughput increases 34%. MC-Thr solution treats all cell edge UEs equal as they are classified given their attenuation with respect to the serving eNB. For lower bandwidth allocations not all UEs in the cell edge are power limited and the gains brought by non-contiguous allocation can improve the 5th percentile worst throughput as well. Besides, even in power limited situations with its consequent PSD reduction the gain brought by frequency diversity overcomes this loss.

As seen in table 4.2 the solution that provides the lowest BLER at the first attempt is MC-MPR. By definition, the increase in BLER is essentially because the average $\overline{\gamma_i^{\mathrm{SRS}}}$ differs from the received $\overline{\gamma_i^{\mathrm{PUSCH}}}$; figure 4.2(a) shows the difference between both SINR metrics. Apart from the strong interference (and so SINR) variability the UL experiences, applying MPR and reducing the PSD also creates differences between both SINRs. When comparing the BLER improvement in all CA scheduling strategies, the highest improvement is with respect to MC strategy which does never consider ΔP (if any) in the MCS allocation process. There is no gain with respect to MC-Thr because in this case, cell edge UEs who may have

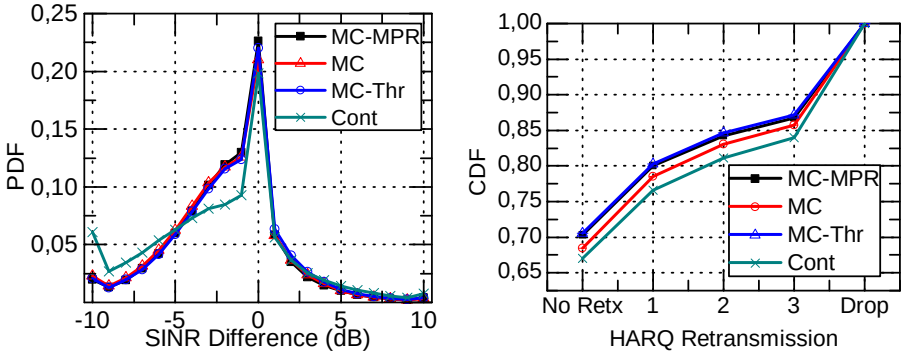

(a) pdf of SINR error

(b) cdf of the HARQ process

Figure 4.2: JCS scheduling: SINR misalignment and HARQ process distributions

$\Delta P \neq 0$ are banned from multi cluster transmission, and therefore there is no misalignment between γ_{SRS} and γ_{PUSCH} caused by this. As explained in section 4.3, the total equivalent γ_{SRS} is calculated as the average of individual $\gamma_{\text{SRS}}^{\text{PRB}}$. For a given coherence band, the channel variation over a lower number of consecutive PRBs tends to be flatter than in a larger allocations. Thus, although scheduling decisions are opportunistic, large localized allocations are more likely to be affected by deep fadings. For this reason the probability of having short term fadings in the allocated region is higher because the correlation among the different PRBs is lower when both are fairly distant. For this reason there is a higher improvement of the BLER with respect to the contiguous bandwidth allocation strategy. Occasional allocation of contiguous resources is allowed in MC-MPR and MC-Thr schedulers, however, in both cases the probability of this event to occur is low. Figure 4.2(b) shows the CDF of the HARQ process. When the SINR difference is high there is an increased probability of having retransmissions, and also of having lost packets. High number of retransmissions increases the delay, and therefore reduces the UE throughput.

Cluster size impact

An increase in M_{Alloc} implies a higher P_{TX} which may also decrease the PSD. Based on this, for an increase in bandwidth the probability of transmitting in separated clusters must be reduced in order to always keep the best performance. Figure 4.3 shows two metrics that are very much related one to another. First, the probability of transmitting in separated clusters and second the average transmitted power, both versus the cluster size. The threshold based strategy does not consider the allocated bandwidth, therefore as the cluster size increases, the probability of non contiguous allocation remains equal. The optimal selection of CA users is not only related to the path-loss (L) but also to M_{Alloc} because both control the total P_{TX}. Tables 4.3 and 4.4 show the results for increased bandwidth configurations. There is still improvement in throughput for cluster size to 10 PRBs, but this improvement is

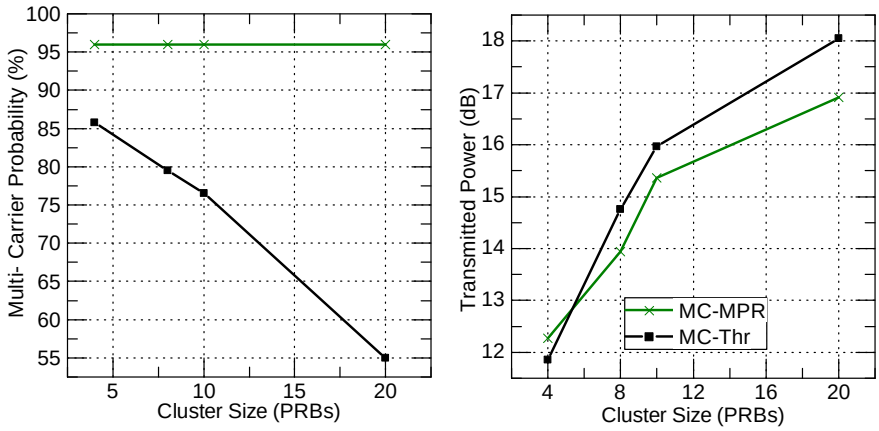

Figure 4.3: JCS scheduler: Probability of transmitting in separated clusters vs power

Table 4.3: Throughput values for Cluster size = 10 PRBs

Throughput	MC-MPR	MC	MC-Thr	Cont
Average (MBits/s)	2	1.9	1.88	1.7
Cell-edge (kbps)	131	121	127	102
BLER (%)	28	28.6	28	31

not as significant as it was with 8 PRBs and it is much lower in the case of 20 PRBs. As M_{Alloc} grows, the gain brought by multi-clustered transmissions reduces with respect to contiguous ones. This is because the increase in UE power demands to transmit such a high bandwidth overcomes the multi-clustering gain seen in lower bandwidth configurations.

Performance under large ISDs

In a noise limited scenario, with ISD = 1732 m, $\overline{P_{\text{TX}}}$ increases owing to the higher path-losses. In this sense, the cluster size must be reduced to assure that a low

Table 4.4: Throughput values for Cluster size = 20 PRBs

Throughput	MC-MPR	MC	MC-Thr	Cont
Average (MBits/s)	2.86	2.85	2.85	2.7
Cell-edge (kbps)	131	123	120	137
BLER (%)	27	27	27	28

Table 4.5: Probability of transmitting in separated clusters vs transmitted power for Cluster size = 4 PRBs

	MC-MPR	**MC-Thr**
P(CA)(%)	75	65
$\overline{P_{\mathbf{TX}}}$**(dBm)**	17	17.8

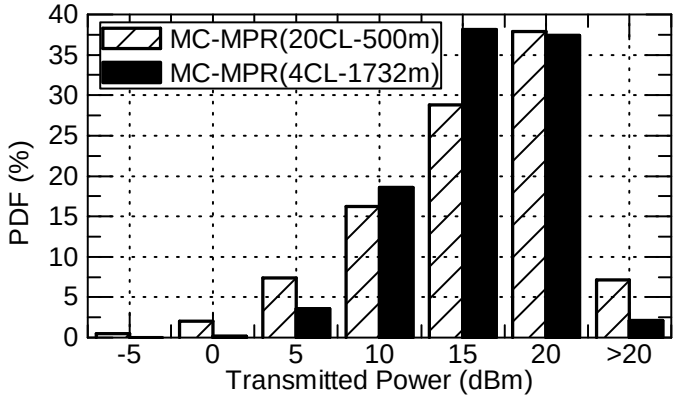

Figure 4.4: JCS scheduler: pdf of transmit power. Comparison between interference and noise limited scenarios

number of UEs transmit under maximum power conditions. In the last section it was seen that the probability of transmitting in separated clusters is closely related to the average transmitted power. In a large ISD condition, this probability versus the transmitted power is shown in table 4.5. The $\overline{P_{\mathrm{TX}}}$ under noise limited conditions is close to the one in the interference limited scenario with a cluster size of 20 PRBs, near 17 dBm. When comparing the probability of transmitting in separated clusters of both scenarios, the noise limited has an increase of 20% with respect the interference limited one. This is because both transmission power probability density function (pdf) are fairly different as shown in figure 4.4. Although average power values are similar, the probability of having one user transmitting at maximum power levels is still larger for the interference limited scenario with higher transmission bandwidth. Therefore the result is that in large ISDs the algorithm is able to successfully allocate more UEs in separated clusters. As the path-loss to the eNB increases with higher ISDs, the MC-Thr algorithm decreases the probability of transmitting in separated clusters with respect to the lower ISD case. However, as seen in table 4.5 there is still a 10% difference when comparing it to the proposed algorithm.

Table 4.6 summarizes the throughput results. The increase in distance to the serving cell results in an overall throughput reduction, when compared to the low ISD performance. Throughput gains when L grows are similar to those with increased bandwidth. The improvement of MPR wise decisions in opportunistic scheduling can

Table 4.6: Throughput values for Cluster size = 4 PRBs

Throughput	MC-MPR	MC	MC-Thr	Cont
Average (kbits/s)	472	463	423	409
Cell-edge (kbits/s)	61	45	66	53
BLER (%)	34	36	34	35

still be noticed with a lower percentage of gain. It is worth mentioning how much the cell edge performance is impaired given forced multi-clustered transmissions, there is a 35% difference in the cell edge with respect to the MC strategy. However, it is still beneficial to allow opportunistic non-contiguous allocations under high path-loss circumstances, given that cell-edge gains are still appreciated.

4.4.3 Concluding

Adding the MPR information and assessing the UE capability of transmitting in separated clusters of resources lets the system improve the overall performance. It has been shown that the cell edge and average UE capacity are enhanced when considering the gains of CA transmission individually. MPR wise decisions reduce the misalignment between the CSI obtained through the SRSs and the SINR in the shared channel which yields to an improved BLER and a the corresponding reduction in retransmissions and discarded packets. However, the SINR error experienced in all the strategies is very high and further improvements are needed to reduce the SINR misalignment. The potential gains of multi-cluster transmission are shown to depend on the power increases because of (a) larger bandwidth allocations and (b) the increase in path-loss due to larger ISD. In the first case, the proposed JCS is the only solution that reacts and adjusts the use of clustered transmissions to the new power conditions, while the probability of transmitting in a non-localized manner remains constant in the MC-Thr case. The performance under large ISDs is still improved, allowing opportunistic non-contiguous transmissions in the cell edge when the allocation is profitable.

4.5 A New UL CC selection Strategy

The JCS strategy needs to manage a wide range of resources and evaluate each UE independently to obtain the maximum gains. By adding to the system smart CC selection process and performing ICS, the number of operations the scheduler has to do can be reduced, since non-contiguous allocations must be evaluated only in those UEs that are not eligible for CA transmission.

This section proposes considering UE power constraints to decide whether it is capable of making the most of CA. This decision is made by the eNB at the

RRC level once the UE has indicated its CA capabilities which are essentially the possibility of transmitting over several carriers, supported band combinations and bandwidth classes [7]. Apart from this, the eNB also takes into account the UE available power, that can be derived by comparing the PHRs and the UE power class. In this sense, this CC selection should be checkable accounting for the UE mobility; this mechanism works at a higher time scale than the scheduler and decisions are taken in a longer-term.

4.5.1 Algorithm description

UEs can be configured by the CC selection process to transmit in more than one CC based on its power capabilities. So, this procedure must be done ensuring a throughput increase. Since non-contiguous resource scheduling is allowed in LTE-A in one CC, several scheduling options arise when dealing with CA and ICS:

- CA user: UEs that are capable of transmitting over aggregated carriers and having two clusters in each CC. The number of allocated PRBs for this case is denoted by $M_{\text{Alloc}} = M^{\text{CA}}_{\text{PUSCH}}$. This option provides the widest bandwidth and the highest frequency diversity. It is also the one requiring an increased transmission power and so the less likely for UEs with power limitations.

- SC user: UEs that cannot hold the large aggregated bandwidth are allocated resources in one CC, $M_{\text{Alloc}} = M^{\text{SC}}_{\text{PUSCH}} = M^{\text{CA}}_{\text{PUSCH}}/n$ (n, number of CCs). Nevertheless, SC UEs can yet transmit in two separated clusters if this provides a net throughput gain when compared to a two contiguous cluster allocation (single cluster treatment without MPR). The scheduler introduced in section 4.4 is applied to them. MPR information for single CC transmission expressed in equation 3.5 is considered in opportunistic scheduling decisions.

Note that the MPR to be applied just depends on M_{Alloc}. For this reason a UE transmitting in two CCs but being allocated contiguous clusters in each one is not an interesting option. This would require the same MPR than the described CA user but frequency diversity would be reduced.

Let's consider a power limited UE that, under CA conditions, needs a transmission power $P^{\text{CA}}_{\text{TX}}$ that is higher than the maximum allowable: $P^{\text{CA}}_{\text{TX}} > P_{\max} - \pi^{\text{CA}}_{A}$. Given that that non-contiguous resource allocation brings an intrinsic scheduling gain, the final decision can be softened by quantifying whether there is a throughput degradation if the UE stays as a CA one. Indeed an acceptance margin that catches the existence of throughput gain is derived. Since MPR implies a SINR reduction of $\Delta S = P^{\text{CA}}_{\text{TX}} - (P_{\max} - \pi^{\text{CA}}_{A})$, the MCS under CA conditions MCS_{CA} would be equal or worse than the one chosen if the UE was classified as single carrier MCS_{SC}.

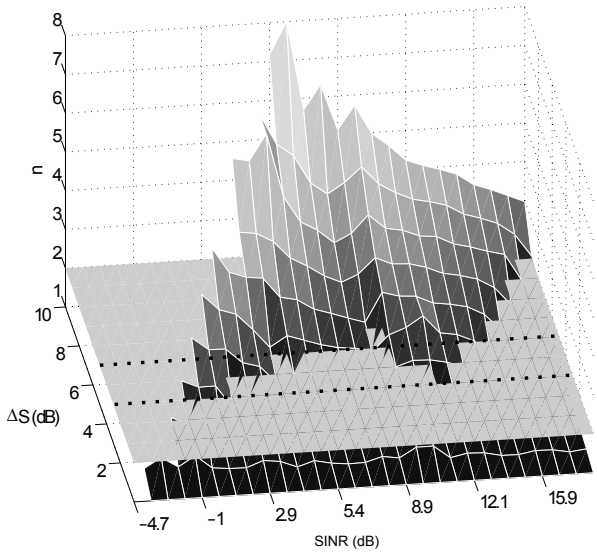

Figure 4.5: Evolution of n for different values of acceptance margin and minimum SINR required for MCS

Therefore a throughput variation ΔT appears when comparing both cases:

$$\begin{aligned}\Delta T &= \frac{1}{\mathrm{TTI}}\left(\mathrm{b}(\mathrm{MCS_{CA}})\cdot M^{\mathrm{CA}}_{\mathrm{PUSCH}} - \mathrm{b}(\mathrm{MCS_{SC}})\cdot M^{\mathrm{SC}}_{\mathrm{PUSCH}}\right)\\ &= \frac{M^{\mathrm{SC}}_{\mathrm{PUSCH}}}{\mathrm{TTI}}\left(n\cdot \mathrm{b}(\mathrm{MCS_{CA}}) - \mathrm{b}(\mathrm{MCS_{SC}})\right). \end{aligned} \tag{4.13}$$

Being $\mathrm{b}(\mathrm{MCS_X})$ the number of bits transmitted by $\mathrm{MCS_X}$. Remaining in CA would represent a throughput gain if $\Delta T > 0$ which is equivalent to:

$$n > \frac{\mathrm{b}(\mathrm{MCS_{SC}})}{\mathrm{b}(\mathrm{MCS_{CA}})}. \tag{4.14}$$

Graphical representations of a particular study case are provided in figure 4.5 in order to complement the explanation. Let's assume the case $n = 2$, SC users would be allocated half the bandwidth of a CA one. For that specific case, Figure 4.5 represents the evolution of n for different values of ΔS and the SINR required at each MCS to target a BLER of 10% in the first transmission attempt. The link to system level abstraction has been done as in [98]. Note that the surface has missing values for certain combinations of low SINRs and ΔS. Those are the cases in which not even the first MCS would be able to meet the target BLER under CA conditions and so the UE would be classified as SC.

An horizontal plane at $n = 2$ is also plotted for the sake of clarity. Thus, all combinations of (SINR, ΔS) that fall below the plane represent cases in which the

UE should remain as a CA one. The cut between the surface and the horizontal plane represents the maximum ΔS allowable in each case. The UEs classification is not performed at the RRM time scale, therefore a unique value is desired to be used when evaluating CA candidates. From the figure it can be obtained that for $n = 2$, candidate values for the maximum allowable power variation $\Delta S_{\max}$ would be in the range between 3 and 5 dB, as indicated by the dotted lines. Most of the frontier falls between those two values. A more risky value, 5 dB, is a valid option since CA offers more frequency diversity than SC and so it is expected that in average the allocated MCS would be higher, thus allowing a slightly higher $\Delta S_{\max}$ than the average frontier on Figure 4.5.

Even though users have no available power to accomplish the condition, ΔS is an acceptance margin value that assures that CA transmissions will increase the average throughput. So, the final condition that a UE must accomplish to be a CA candidate is expressed as follows:

$$P_{\text{TX}}^{\text{CA}} + \Delta S_{\text{MAX}} \leq P_{\text{MAX-CA}} \tag{4.15}$$

This condition is set to classify UEs as CA and SC. Note that UEs could be re-evaluated periodically to account for their mobility within the cell. Nevertheless the time scale for re-selections would be in the order of seconds.

4.5.2 Performance Evaluation

Benchmarks

The CC selection strategy proposed in this section is tested and compared against other benchmark strategies:

- Strategy 1: Proposed solution, CC selection with acceptance margin. SC UEs can also benefit of multi-cluster allocation.
- Strategy 2: Threshold based CC selection following [21]. SC users cannot benefit of multi-cluster transmission.
- Strategy 3: No tolerance or MPR information in CC selection. Selection criteria is based on the power availability considering the UE class maximum power [19].
- Strategy 4: No CA transmission, both CCs are used for load balancing.

The simulated scenario is detailed in appendix A, however, specific simulation assumptions are listed in table 4.7.

Numerical Results

Analysis starts by evaluating the impact of each CC selection algorithm on the user average and cell edge data rate performance, figure 4.6 compares all strategies.

Table 4.7: CC selection: Simulation scenario assumptions

Parameter	Value
Bandwidth	2 x 80 PRBs
SRS BW	16 PRBs
Number of UEs served	10
Number of UEs connected	30
PRBs allocated	2 clusters of 4 PRBs x CC
Simulation time	40 kTTI

Graphics represent four metrics: the average and 5th percentile worst UE throughput, the average transmitted power per UE and the fairness indicator Jain's Index. This last metric measures the variability of throughput to obtain fairness. If UE power class is considered but not the MPR to be applied (Strategy 3), many UEs get to transmit in both CCs. The main drawback of this strategy is that the cell edge can be severely punished: the result is a 40% loss towards Strategy 1 with no relevant variation in the average throughput. In fact, Strategy 3 is not accurate when deciding which UEs are power limited, the cell edge performance deterioration is because power limited UEs are stressing their power resources with a consequent decrease in their performance. On the other hand, when a moderate value of path-loss threshold is considered in Strategy 2 (110 dB), nearly 8% of users are deprived of bandwidth extension, being considered power limited. This leads to an average throughput decrease of slightly more than 5% compared to Strategy 1, cell edge is however not maximized as results for Strategy 1 are nearly 3% higher. These results verify that the proposed solution considers UEs based on the performance gains and the ones that benefit of aggregated transmissions are never jeopardized. Also, cell edge throughput is enhanced given that Strategy 1 allows multi-cluster to non-CA UEs. As a consequence, fairness is also higher in the proposed scheme, with more than 9% improvement on the Jain's index. While all values of average transmitted power are close, Strategy 3 has the lowest one. The scheduling procedure followed by Strategy 3 is to always allocate separate clusters. Given this, no user in the scenario is able to transmit at the maximum power level determined by its power class.

If a low number of UEs is selected for CA there is an impact in the average cell throughput. Figure 4.7 compares the performance of Strategy 1 with Strategy 4, where no CA is considered, Strategy 2 with a very conservative value of threshold, 100 dB, and finally, Strategy 1 with the minimum acceptance margin, 3 dB. Strategy 1 more than doubles the average UE throughput when compared to the non-CA strategy, because of the increase in bandwidth allocations. When only contiguous allocations in one CC are carried out, there is a more fair and homogeneous performance around the cell area, as reflected with the Jain's index value. Given this, the cell edge throughput in Strategy 4 is 7% higher than Strategy 1. Strategy 2 with 100 dB threshold deprives more than 30% of the UEs in the scenario of CA, because the algorithm considers them power limited. This lets the cell edge increase

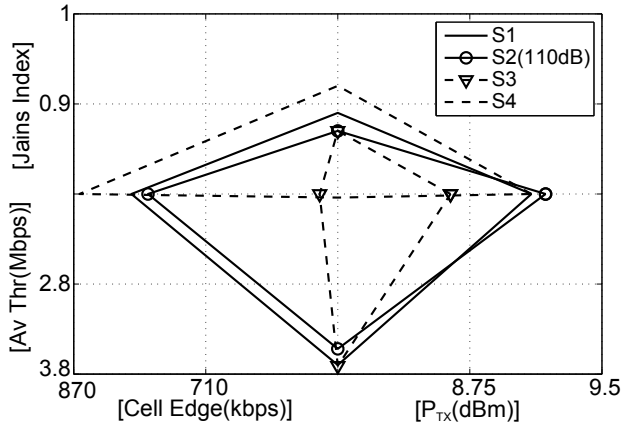

Figure 4.6: CC selection: Performance comparison of all strategies with reference values: Strategy 1 5 dB acceptance margin, Strategy 2 110 dB threshold

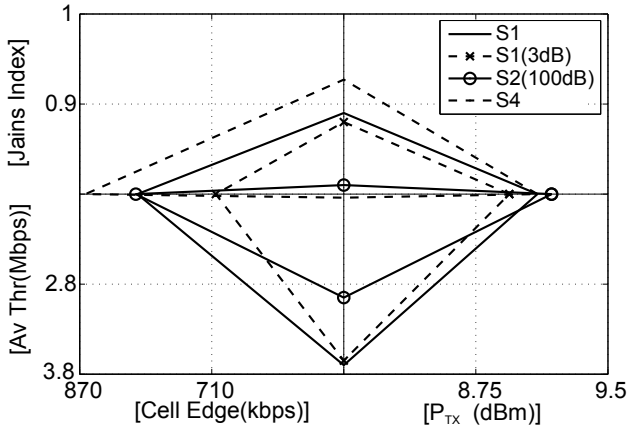

Figure 4.7: CC Selection: Performance comparison for low permissive configurations, Strategy 1 with acceptance margin of 5 and 3 dB, Strategy 2 with 100 dB threshold

with respect to the previous 110 dB threshold case, but the average throughput significantly decreases towards Strategy 1. Also, Strategy 2 threshold lets the average UE throughput increase with respect to Strategy 4 but fairness decreases. This comparison reflects the need for compromising cell edge performance maximization towards average cell performance maximization. Strategy 1 is also compared to itself by changing the acceptance margin to a more conservative value, where less UEs are considered as CA compliant. Cell edge throughput decreases nearly 14% with respect to the 5 dB solution, and the only improvement seen is in the transmitted power, which is slightly reduced. Strategy 1, allowing a 5 dB tolerance gives the best performance as it controls the BLER and allows to increase throughput to users that are transmitting at maximum power levels, while never jeopardizing their

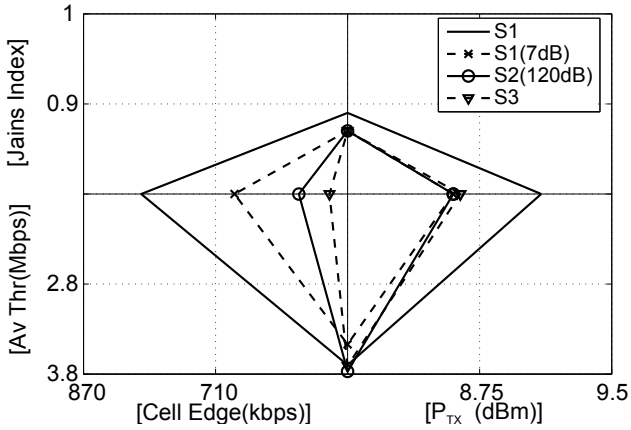

Figure 4.8: CC Selection: Performance comparison for high permissive configurations, Strategy 1 with acceptance margin of 5 and 7 dB, Strategy 2 with 100 dB threshold value

performance.

Following the analysis on the variation of the path-loss threshold, figure 4.8 introduces a new case, now increasing the 110 dB reference. In particular, the less prohibitive value of 120 dB is analysed which relaxes the access to CA. Also Strategy 1 is tested for an acceptance margin of 7 dB. Recalling Figure 4.5 most MCSs were not able to tolerate such margin when $n = 2$. Nevertheless, the margin just indicates the maximum value and so just part of the UEs will be incorrectly led as CA. From the figure it can be seen that for both cases, if the CA condition is relaxed, cell-edge throughput decreases and just a marginal increase in the average throughput is obtained. In Strategy 1 with 7 dB margin, the average throughput just increases 1% and there is a loss of almost 17% in the 5th percentile throughput, with respect to the 5 dB case. The algorithms let to worsen the cell edge performance by allowing more CA transmissions, and hence extending bandwidth to power limited UEs. Strategy 2 with threshold 120 dB does even worse, with more than 30% loss in the cell edge with respect to Strategy 1 with 5 dB of margin. Under these circumstances both permissive cases allow 99% of UEs to transmit over the aggregated carriers. In Strategy 1 with 5 dB tolerance value, 98% of users access to CA transmission resulting in nearly the same average throughput and high improvements in the cell edge. Nevertheless, still applying CA in all UEs provides the worst cell-edge performance.

4.5.3 Concluding

Results show that providing a simple acceptance margin to the CC selection process can enhance the system performance compared to hard conditions such as path-loss thresholds or maximum power availability. The proposed technique lets improve the cell edge throughput while maintains the average throughput with respect to other

strategies which allow high number of CA transmissions.

4.6 CA against Single-CC: A Tradeoff Study

So far, two novel RRM procedures have been analysed in terms of system performance. However, all these complex requirements in terms of transmit power for CA can potentially increase energy consumption in the UE. Battery life-time is a very important issue and green efficient communications in the UL must be pursued; besides, UL RRM solutions must assure that there is a strong relationship between the required and the available energy. Given this, a trade off arises in LTE-A among energy efficiency, UE average throughput and fairness. The UE energy consumption can be reduced by optimizing the hardware and the resource allocation. The selection of single-CC or CA based on the UE power availability can lead to more energy efficient communications. On the other hand, the PA is the component with the highest energy consumption in the UE. Even when no data is transmitted the PA consumes DC power for holding its operating point [99]. Hardware energy consumption can be reduced by applying Discontinuous Transmission and Reception (DTX) [30] which enables energy saving sleep modes.

One approach to reduce energy consumption in the UE side is to design the bandwidth allocation mechanism to assure that data is transmitted in the most efficient way. Work in [100] investigates the power consumed by a UE based on the scheduler allocation. Conclusions summarize that it is more energy efficient to allocate a high number PRBs with lower order MCS even though it leads to a higher transmission power. The reason is that the transmission time is shorter for a user with many PRBs. The two proposed procedures have a direct impact on the efficient use of the available energy. These two procedures allocate bandwidth in a smart manner, with the aim of being more efficient from the energy point of view without worsening the spectral efficiency.

4.6.1 Performance Evaluation

Benchmarks

To evaluate the impact that resource allocation has on the tradeoff among energy efficiency, average throughput and fairness different allocation scenarios are simulated. First of all, single-CC transmissions are evaluated where all UEs transmit in one CC and the MPR scheduler decides whether multi-clustering is suitable or not, with the algorithm presented in 4.4. Here, two sizes of clusters are evaluated. In the CA scenario, two cluster sizes are considered for single carrier UEs that are considered CA not compliant:

- Scenario A: All UEs are allocated the same bandwidth. So cluster size is doubled for single carrier UEs.

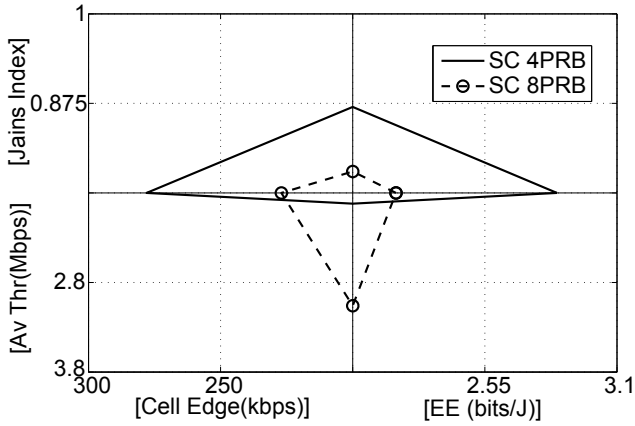

Figure 4.9: EE Study: Performance comparison of SC scenarios.

- Scenario B: It maintains the same cluster size, so single carrier UEs have a reduced bandwidth with respect to CA users, the same scenario perviously analysed in section 4.5.

Simulation assumptions largely follow the ones in table 4.7.

Numerical Results

The first item to be analyzed is the cluster size in single-CC transmissions. Figure 4.9 shows the UE average and cell edge throughput together with the energy efficiency and Jain's index for two cluster sizes: 4 and 8 PRBs. Both cluster sizes solve the tradeoff in different ways. In general, the average throughput maximization is done at the expense of the other metrics. If the cluster size is doubled, more users will transmit at maximum power levels; also, larger bandwidths turn the scheduler less flexible when allocating the best scored resources. However, users with limited power headroom are jeopardized. Nearly 20% of throughput in the cell edge is lost because of the increase in the allocated bandwidth. This increase in average UE throughput leads to the conclusion that UEs must be sharply defined between power limited and non-power limited when conducting high bandwidth allocations. If the cluster size is reduced, and hence, less PRBs are allocated, energy efficiency improves 23% because more bits are sent per PRB given that the PSD is higher; as widely explained along this chapter, shorter allocations avoid further power limitations. Finally, given the values of throughput it is clear that the scenario with reduced cluster size offers the best fairness.

Next, CA environment is introduced where two different CA scenarios are tested. First, Scenario A, in which all UEs are allocated the same bandwidth, 16 PRBs regardless if they are considered as CA compliant or not, categorized as single carrier UE. Single carrier UEs can transmit contiguous PRBs and therefore avoid MPR,

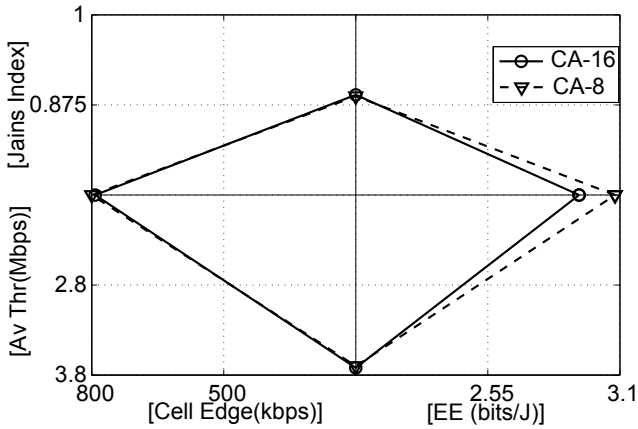

Figure 4.10: EE Study: Performance comparison of CA scenarios. Scenario A 16 PRBs allocated, and Scenario B 8 PRBs allocated.

if that implies an improvement in throughput. Second, Scenario B, in which single carrier UEs are allocated 2 clusters and CA UEs are allocated 2 clusters per CC, with the same cluster size 4 PRBs. Results are shown in figure 4.10. Again values of average and cell edge throughput are shown together with the fairness Jain's index and the energy efficient metric. In this case, both scenarios lead to nearly the same average and 5th percentile worst UE throughput, and therefore the same fairness index. In this case, limiting the cell edge bandwidth ends up to be more energy efficient, nearly 5%. This means that, again, power limited users are more likely to reduce their transmitted bandwidth with the aim of improving the energy consumption.

A fair comparison cannot be conducted between the single-CC and CA transmissions because in the latter the bandwidth is double. One possible solution would be to represent the spectral efficiency in bits/Hz however, having a wider available band also allows a more flexible operation of the scheduler, a poorer CSI at the PRB level, and so on. For that reason a new comparison is performed in which the CA bandwidth is halved (10 MHz per CC). The performance of CA changes, as shown in figure 4.11. When the system bandwidth is reduced less users are allocated per TTI, given the lower bandwidth availability. For this reason, it is more efficient to allocate a larger number of resources, as the overall transmission time is shorter and less power is required from the UE side. Pure single-CC and CA transmissions are also compared in figure 4.11, in this case both cases have access to the same system bandwidth. In this comparison, CA results to be more energy efficient than single-CC communications. Also, cell edge throughput is increased given the higher scheduling flexibility and frequency diversity. To sum up, the CA solution is good not only as a throughput enhancement strategy but it is also a good option to solve the LTE tradeoff of energy efficiency, average throughput and fairness.

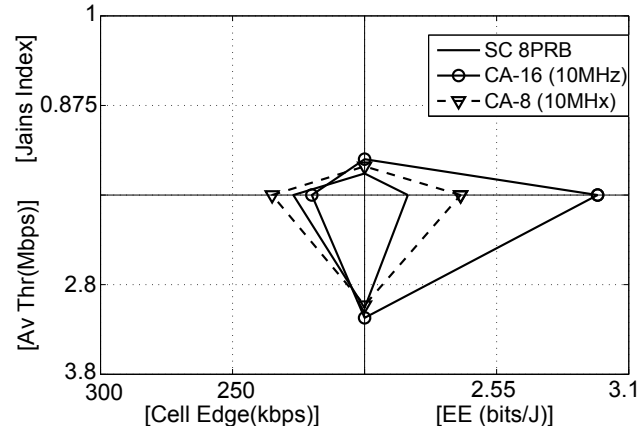

Figure 4.11: EE study: Performance comparison of CA scenarios with 10 MHz per CC. CA with all users having 16 PRBs allocated, and CA with SC users having 8 PRBs allocated; and SC with cluster size = 8 PRBs

4.7 Concluding Remarks

This chapter has addressed the topic of resource scheduling and CC selection with CA. Multiple challenges have opened up to efficiently include CA in the UL, among the many limitations the UL encounters, transmission in wider bandwidths represents an extra effort for UEs in power terms. Power limited UEs become a challenging target: they should not be directly banned from CA transmission because a more homogeneous distribution of throughput and spectral efficiency along the cell area is desired, but on the other hand, increased bandwidth allocations may impair their performance. In this sense, the prior art proposes to evaluate the path-loss as a CA selection scheme. However, there is much more than path-loss to power setting considerations, for instance, bandwidth allocations also impact the performance.

In this regard, this chapter has presented two novel solutions that tackle one of the main UL problems: power availability versus spectral efficiency. A novel scheduling algorithm has been proposed in which the effect of power de-rating is taken into account. Each UE scheduling case is independently assessed, and the gain or loss brought by multi-cluster allocations is quantified. To support this assessment, the estimated user channel information obtained via SRS is employed. No new signalling operations are required to run this algorithm. Both, 5th and 50th percentile UE throughput are improved in the different study cases. For low ISD scenarios with short bandwidth allocations, non-contiguous transmissions are still preferred against classic UL localized carrier mapping. In general, when UEs are not power limited they can easily improve their spectral efficiencies by transmitting in separated pieces of spectrum. Conversely, under high power demands, contiguous allocations provide the best throughput performance. Based on this, the proposed scheduling solution, MC-MPR, analyses each UE independently, coming up with the solution that maximizes their performance. In this sense, the solution adapts

itself to different power requests, resulting in enhanced scheduling decisions.

Finally, an original CC selection condition has been devised that goes one step beyond the existing techniques by considering throughput improvements even at maximum power levels. The algorithm considers the MPR to be applied by a CA transmission and introduces an acceptance margin that captures the throughput gain or loss. This way it prevents wrongly rejecting a subset of power limited UEs as CA capable. Power limited users can also benefit from CA if their excess in power is not higher than the proposed acceptance margin. This parameter is accurately calculated based on the link level minimum SINR to allocate MCSs. This solution allows for large improvements in the cell edge while not deteriorating the average UE throughput.

With the aim of comparing the feasibility of CA from an energy efficient point of view, a study is driven where singe-CC communications are compared against CA ones in terms of throughput, energy efficiency and fairness. The reduction in PSD conducted by high bandwidth allocations in power limited UEs result in a lower energy efficiency, less bits are sent per PRB and connections must take longer. Therefore, decisions based on power availability are crucial to allow the energy efficiency maximize. Adding the CA RRM procedures the capability of assessing power limitations makes CA more efficient by adding the flexibility of separating UEs into groups: the ones that can extend bandwidth, and the ones that do not.

To sum up, the main conclusions highlighted from this RRM study are:

1. CA improves the average system performance by allowing the simultaneous transmission across multiple CCs.

2. The improvements brought in terms of fairness and cell edge throughput depend very much on the strategies conducted in the cell edge, where UEs are more likely to be power limited. If decisions on multi-carrier transmissions are taken with specific knowledge of the UE power constraints, then CA can perform outstanding improvements in the cell edge. Therefore, the cell edge shall not be excluded from CA but encouraged through smart scheduling decisions.

3. CA constitutes not only an improved solution in terms of average and cell edge throughput but is also a desired solution in terms of energy efficiency. As long as bandwidth allocations provide the minimum PSD loss, wider transmissions allow to finish communications faster and reduce the UE connection time.

4. SRSs are crucial for the correct functioning of both algorithms as they provide all the information for the channel estimation. Therefore, the SRSs allocation is an important parameter that must be fine tuned in order to obtain the best performance out of them.

Chapter 5

Uplink CSI Improvements

5.1 Introduction

In the last chapter, it was verified that CA is an important feature that allows operators to provide increased energy efficiency and UE data rate by using larger operational bandwidths without the need for having a contiguous, large piece of spectrum. However, conclusions agreed that accurate CSI is key to capitalize the improvements in the RRM. In the UL, obtaining up-to-date CSI relies on the UEs that send reference signals throughout the available bandwidth. This procedure is quite challenging when considering the ever increasing bandwidth demands and the introduction of CA. Information from many radio resource blocks becomes outdated and unreliable for scheduling operations. Besides, interference values are more variant in the UL than in the DL given the constant changes of the position of the interferers and their transmission power.

This chapter proposes two methods to deal with the imperfect CSI in the UL. First, the introduction of a polynomial extrapolation method to obtain a prediction horizon that allows extending the reliability of the channel quality evaluation along time. The mechanism succeeds with moderate interference, situation that can be provided by IC strategies or under low to medium load levels. Second, an integration of ICIC with CSI reporting is proposed to reduce the delays in sounding provoked by increased available bandwidths; two well-known ICIC techniques are introduced in the sounding process, SFR and FFR.

Section 5.2 goes through the main constraints the CSI encounters in the UL stressing out the motivations to include novel strategies that deal with this problem. Section 5.3 reviews the systems and methods that are suitable to address this problem and sections 5.5 and 5.6 present the proposed schemes based on prediction and ICIC techniques, respectively. Finally, this chapter ends listing the main conclusions.

5.2 Imperfect CSI in the UL

To achieve a good link adaptation and allow opportunistic frequency domain scheduling in the UL, the eNB needs to evaluate the UE channel response. With this aim, the device sends SRSs, which can occupy the entire system bandwidth (wideband SRS) or just a small piece that hopes along the entire band. Wideband SRS provide poor channel information in the cell edge, where UEs are often power limited and suffer from increased interference. According to the explanation devoted to SRSs in section 2.4, hopped SRSs provide the system with a more reliable CSI in power limited cases, but needs an increased time delay to sound the entire system bandwidth. This problem is more critical with the use of CA, where the total available bandwidth increases and the UE has to sound a larger piece of spectrum.

A second problem with UL CSI is the intrinsic rapid variations of the interference levels. This is not only owed to short term fading, but also because of scheduling decisions. With every TTI, allocated resources are updated and so the sources of interference in each PRB change. This implies fast SINR variation and reduces the sounding reliability, eventually generating errors in the LA and reducing the UE throughput. For this reason, using mechanisms for interference variability contention can yield to lower CSI errors.

This section describes the motivation for including accurate CSI acquisition methods and goes through the main challenges opened to accomplish this in the UL in a CA context.

5.2.1 Motivation

The number of users sharing the available bandwidth as well as the sounding bandwidth B_{SRS} impact the delay in the channel measurement. Table 5.1 shows the time delay T_{sound}, in milliseconds, experienced between two consecutive sounding measurements in one frequency resource block. This time delay varies depending on the number of users connected to the eNB and the piece of bandwidth being sounded each TTI, B_{SRS}. Delays shown also account for the use of two CCs (20 MHz each) which are not simultaneously sounded. Each carrier is sounded separately on different transmission intervals, to avoid further power reductions inflicted by non-contiguous transmission in the UL. The main problem of having increased delays in the channel measurement is the lack of up to date information in the scheduling decisions and link adaptation. Figure 5.1 shows two different examples of channel state measurement with the use of SRS. The first figure, 5.1(a), has a time delay between two samples of 10 ms and the second one, figure 5.1(b), has a time delay of 30 ms. A lower time delay can capture enhanced channel information in terms of instantaneous deep fadings.

One limiting aspect of the UL channel measurement is its intrinsic interference variability, which impacts the CQI by constantly altering the aggregate interference level experienced. According to the scheduling decisions, interferer UEs may change from one transmission time to another, and the impact on the SINR depends

Table 5.1: Time delay in milliseconds between two consecutive SRS measurements (T_{sound}). Two CC of 20 MHz each.

Number of UEs	$B_{\mathbf{SRS}}$					
	4	**8**	**16**	**20**	**40**	**80**
8	40	20	10	8	4	2
24	40	20	10	8	4	4
40	40	20	10	8	8	6
72	40	20	10	16	12	8

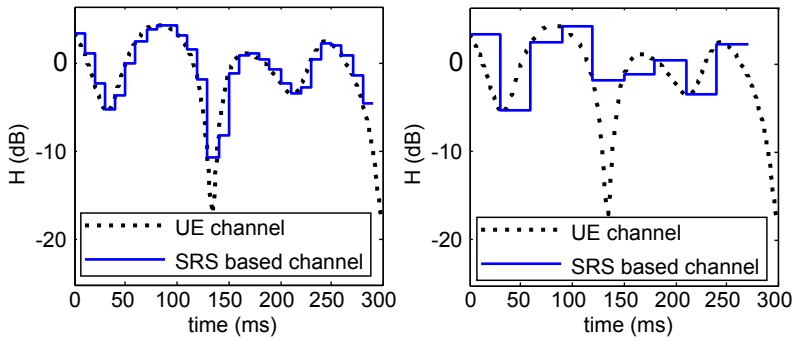

(a) UE Channel measured by SRS with time delay of 10 ms

(b) UE Channel measured by SRS with time delay of 30 ms

Figure 5.1: Channel measurement for two different T_{sound}

on the larger or lesser the pool of candidates is: the former generates increased interference variability compared to the latter. Figure 5.2 shows the SINR measured over the PUSCH for two different schedulers: RR and PF. In this simulation case, in the RR scheduler allocations in all eNBs are perfectly synchronized, therefore the interference is seen as a constant and generates less time-varying SINR fluctuations. However, this type of scheduling decisions do not account for fairness or throughput maximization. In this regard, the PF scheduler provides more changeable allocations which influences the interference variability.

Another variable that impacts the interference variability is the number of UEs having active connections: the higher the number of UEs, the more variable the interference becomes. The probability of having always the same interferer source is lower as the number of connections increase. Figure 5.3 shows the evolution of the SINR over time for two different eNB occupancies. When the cell occupation is low, the interference variation over time results in a less changeable SINR, while increasing the load in the cell leads to increased variations of the SINR.

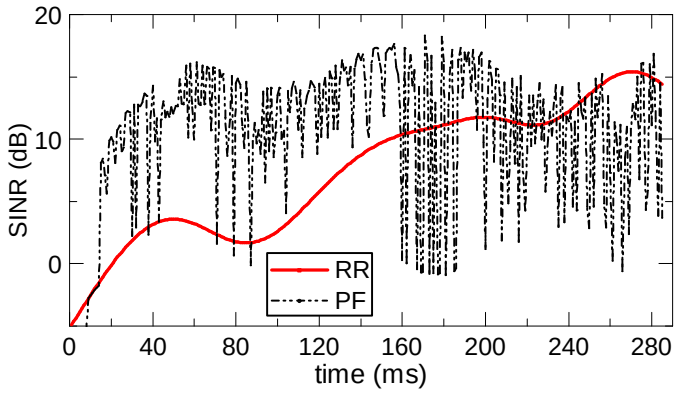

Figure 5.2: SINR evolution for RR and PF schedulers.

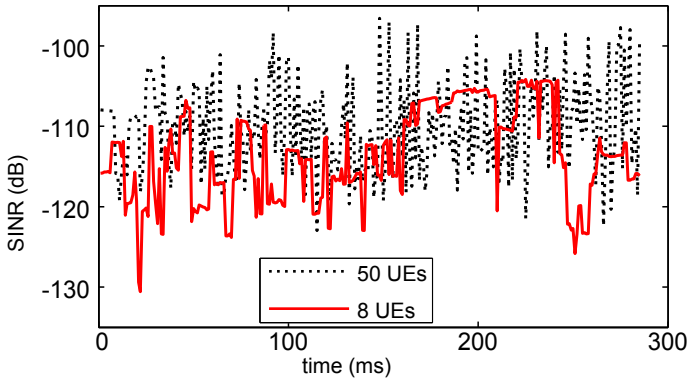

Figure 5.3: SINR evolution for two cell occupancies

5.2.2 Open Challenges

The previous section addressed the main UL limitations when pursuing a neat CSI, and it is observed that the interference fluctuation and the absence of accurate CQI can seriously damage the performance of promising opportunistic scheduling algorithms. Therefore, there is a clear need for designing original solutions that can successfully provide a better performance of the RRM algorithms.

In the UL, the scheduler decides the allocation based on the last SRS received, and aims at maximizing the cell performance with ideally opportunistic scheduling decisions. The eNB must also decide which MCS is suitable based on the UE channel conditions. In conditions of low time-varying SINR, a decision that generates a moderate BLER can be done based on the past SRS, which is also the case in low SRS reporting intervals. In UL interference limited scenarios or in cases where the time between measurements is high, SINR information provided by the last SRS transmission can be easily outdated. From one TTI to another the SINR may vary

more than 10 dB which makes the past SRS almost immediately obsolete. Thus, accurate CQI at the eNB can highly improve both scheduling and link adaptation.

In this context, the principal open challenge to cope with the ever-changing SINR conditions can be defined as: the design of strategies that facilitate the CSI acquisition, while considering realistic UL interference and reference signals delays. To that end, different techniques are studied and proposed. The main contributions of this chapter can be summarized as follows:

- Introduction of a prediction technique in the CSI acquisition process that considers: realistic interference generation and SRS delays caused by hopping along the entire band, and worsened by the RTT.
- Introduction of an IC strategy to support predictions in interference limited conditions. The cancellation is quantified an evaluated under different interference conditions.
- SRS management with classic ICIC strategies, SFR and FFR, that allow to reduce the sounding delay.

5.3 CSI Acquisition Improvement

This section is devoted to study the available methods to improve the CSI accuracy. Several strategies can be adopted separately or together to improve the system performance. Prediction schemes are evaluated to improve the SINR knowledge at the receiver end. Also, interference management techniques, such as cancellation and coordination strategies, are studied to complement predictions or to address the problem by reducing the SRS delay.

5.3.1 Prediction Methods

In chapter 2 the most significant strategies proposed by the research community to improve link adaptation were reviewed. According to this survey, the most appealed strategy is the signal prediction, which essentially calculates the next sample by modelling the desired signal in different ways. This dissertation has studied three well known prediction filters and one mathematical piece-wise polynomial interpolation method. All of them are described in the following sections.

Wiener based prediction filters

The Wiener prediction method is an optimal linear filter that minimizes the Minimum Square Error (MSE) between the desired and the filter output signal. The fundamental task is to design an impulse response $h(t)$ that provides an output $y(t+1)$ that closely resembles the desired signal $d(t)$, in this case, the output $y(t+1)$

corresponds to the predicted CQI t_p TTIs later. This time gap is referred to as the prediction horizon. Given the SRS discrete nature, the input data is in the form of a vector containing n data points, $\mathbf{x}_n$. Therefore the analysis is done for the discrete case where $t = n$. The error to be minimized is expressed as:

$$\begin{aligned}\xi &= \mathbb{E}\left[|d(n) - y(n+1)|^2\right] \\ &= \mathbb{E}\left[|d(n) - \mathbf{h}^{\mathrm{T}}\mathbf{x}_n||d(n) - \mathbf{x}_n^{\mathrm{T}}\mathbf{h}|\right] \\ &= \mathbb{E}\left[|d(n)^2|\right] + \mathbf{h}^{\mathrm{T}}\mathbb{E}\left[|\mathbf{x}_n\mathbf{x}_n^{\mathrm{T}}|\right]\mathbf{h} - \mathbf{h}^{\mathrm{T}}\mathbb{E}\left[|\mathbf{x}_n d(n)|\right] - \mathbb{E}\left[|\mathbf{x}_n^{\mathrm{T}} d(n)|\right]\mathbf{h}. \end{aligned} \tag{5.1}$$

Given the expansion of the error ξ in equation 5.1 the expression can be simplified to:

$$\xi(\mathbf{h}) = P_{\mathrm{d}} + \mathbf{h}^{\mathrm{T}}\mathbf{R}\mathbf{h} - \mathbf{h}^{\mathrm{T}}\mathbf{p} - \mathbf{p}^{\mathrm{T}}\mathbf{h}, \tag{5.2}$$

where,

- $P_{\mathrm{d}} = \mathbb{E}\left[|d(n)^2|\right]$ is the reference signal power,
- $\mathbf{R} = \mathbb{E}\left[|\mathbf{x}_n\mathbf{x}_n^{\mathrm{T}}|\right]$ is the data auto correlation matrix, and
- $\mathbf{p} = \mathbb{E}\left[|\mathbf{x}_n d(n)|\right]$ is a cross correlation vector between the data and the desired signal.

With this, the optimal Wiener filter coefficients can be calculated as:

$$\begin{aligned}\tfrac{\mathrm{d}}{\mathrm{d}\mathbf{h}}\left(\xi(\mathbf{h})\right) &= 0, \\ \mathbf{h} &= \mathbf{R}^{-1}\mathbf{p}. \end{aligned} \tag{5.3}$$

To obtain the optimal prediction filter that minimizes the MSE it is required to compute $\mathbf{R}$ and $\mathbf{p}$. These variables are essentially second order statistics of the SINR and the channel itself.

LMS prediction filters

The LMS algorithm is the most extensively used adaptive linear prediction filter. The filter coefficients are periodically re-adjusted to predict the signal to be. It consists of two components, the first component is the filter impulse response and the second component is the coefficient update mechanism. The filter output $y(n+1)$ can be expressed as:

$$y(n+1) = \mathbf{x}_n\mathbf{w}_n^{\mathrm{T}}, \tag{5.4}$$

where $\mathbf{w}_n$ represents the filter coefficient weight vector for an n^{th} order filter. The filter coefficients are adapted whenever $d(n)$ is available and the error can be updated; this adaptation process is repeated until the error function ξ is zero:

$$\mathbf{w}_{n+1} = \mathbf{w}_n + \mu\xi\mathbf{x}_n, \tag{5.5}$$

where μ is the step size and controls the rate of coefficient convergence. The error function ξ_n to be minimized must be chosen. If MSE error is selected, as in the

Wiener case, the resulting coefficients depend on the statistics of $x(n)$ and $d(n)$. Therefore other error functions are desirable, as for example $\xi(n) = d(n) - x(n)$.

Kalman prediction filters

The Kalman filter is an optimal autoregressive method used to estimate signals by minimizing the error covariance. In fact, the method tries to estimate the state $\mathbf{x}_{n+1}$ of a discrete time controlled process governed by the linear stochastic equations:

$$\mathbf{x}_{n+1} = \mathbf{A}\mathbf{x}_{n-1} + \mathbf{B}\mathbf{u}_n + \mathbf{w}_{n-1}, \tag{5.6}$$

$$\mathbf{z}_n = \mathbf{H}\mathbf{x}_{n+1} + \mathbf{v}_n. \tag{5.7}$$

Where,

- $\mathbf{x}_{n+1}$ is the estimated signal value,
- $\mathbf{A}$ is the transition matrix that relates the state at the instant $n-1$,
- $\mathbf{x}_{n-1}$ is the previous value of the signal to be estimated,
- $\mathbf{B}\mathbf{u}_n$ is the control signal, which most typically is set to zero,
- $\mathbf{H}$ is known as the measurement matrix, which is most typically the identity matrix,
- $\mathbf{v}_n$ and $\mathbf{w}_n$ are the measurement and process noises, respectively.

Essentially, what the Kalman model comes to say is that each sample $\mathbf{x}_{n+1}$ is a linear combination of its own previous value plus a control signal and a process noise; and any measurement value $\mathbf{z}_n$ is a linear combination of the signal value and the measurement noise. Therefore, the estimation of the mean and standard deviation of the noise functions is required. The Kalman method has two different set of equations: the time update, which is the prediction itself, and the measurement update, which is the correction. The time update equations can be expressed as:

$$\hat{\mathbf{x}}_{n+1} = \mathbf{A}\hat{\mathbf{x}}_{n-1} + \mathbf{B}\mathbf{u}_n, \tag{5.8}$$

$$\mathbf{P}_n = \mathbf{A}\mathbf{P}_{n-1}\mathbf{A}^{\mathrm{T}} + \mathbf{Q}. \tag{5.9}$$

The measurement update equations can be expressed as:

$$\mathbf{K}_n = \mathbf{P}_n\mathbf{H}^{\mathrm{T}}\left(\mathbf{H}\mathbf{P}_n\mathbf{H}^{\mathrm{T}} + \mathbf{R}\right)^{-1}, \tag{5.10}$$

$$\hat{\mathbf{x}}_{n+1} = \hat{\mathbf{x}}_{n+1} + \mathbf{K}_n\left(\mathbf{z}_n - \mathbf{H}\hat{\mathbf{x}}_{n+1}\right), \tag{5.11}$$

$$\mathbf{P}_n = \left(\mathbf{I} - \mathbf{K}_n\mathbf{H}\right)\mathbf{P}_n. \tag{5.12}$$

Where: $\hat{\mathbf{x}}_{n+1}$ represents the estimate of $\mathbf{x}$ at time $n+1$ (instant of next sample arrival), $\mathbf{K}_n$ is the Kalman gain, $\mathbf{P}_n$ is the error covariance matrix, and $\mathbf{R}$ and $\mathbf{Q}$ are the measurement and process noise covariance matrices. The method does first

a rough estimate of $\hat{\mathbf{x}}_{n+1}$ which then corrects in the measurement update correction state.

The variances of the process and measurement noise, $\mathbf{R}$ and $\mathbf{Q}$, must be estimated as an input for the time and measurement update equations 5.9 and 5.12. Some works mentioned in the literature review use the same second order statistics as in the Wiener filter to model the process and measurement errors [43]. Other works considering interferences [44], estimate the variance of the measurement and error noise based on both, the interference measurements in a time window and the error characteristics of the interference at the receiver, respectively.

SINR prediction based cubic splines

A spline is a numeric function that is piece-wise defined by several polynomial functions, in the particular case of cubic splines, degree three polynomials. The spline can be used for prediction by extrapolating the last polynomial function, and obtaining a future value of the curve, which was, in this case, built upon the past SINR samples. In this sense, the use of splines constitutes a much different approach compared to the previous strategies, this mathematical method does not filter the signal, and it can approximate functions with less computational complexity, as shown in [101]. The cubic spline extrapolation method avoids complex error calculations, as in the Wiener case where the obtention of second order statistics are mandatory; also, since prediction is not in a discrete form as in the previous cases, the curve provides broader information about its behaviour in the future. The fundamental idea behind this is getting a set of smooth curves through a number of predefined data points, in this case the SINR measured from previously received SRS. So given a past observation time in the interval $[a, b] = \{a = x_0 < x_1 < \cdots < x_m = b\}$, the SINR prediction function $\mathcal{S}(x)$ is a third order spline and satisfies the form:

$$\mathcal{S}(x) = \begin{cases} s_1(x) & \text{if } x_0 \leq x < x_1, \\ s_2(x) & \text{if } x_1 \leq x < x_2, \\ \vdots & \\ s_m(x) & \text{if } x_{m-1} \leq x < x_m. \end{cases} \tag{5.13}$$

where each $s_i(x)$ is a third order polynomial defined by:

$$s_i(x) = a_i(x - x_i)^3 + b_i(x - x_i)^2 + c_i(x - x_i) + d_i. \tag{5.14}$$

To calculate the unknown coefficients of the spline function $4 \cdot m$ equations are required. They can be posed considering that:

- $\mathcal{S}(x)$ must be contiguous on its entire interval, $s_i(x_i) = s_{i+1}(x_i)$. This means that each polynomial goes through two consecutive data points, obtaining $2 \cdot m$ equations.
- To make $\mathcal{S}(x)$ smooth across the intervals its first and second derivative $S'(x)$

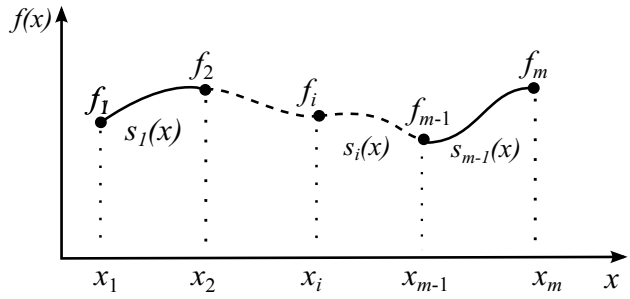

Figure 5.4: Piecewise polynomial interpolation of data points.

$S''(x)$ are also contiguous. This results in $2 \cdot (m-1)$ equations.

- Finally, the boundary conditions provide the two missing equations. In this case a natural spline is assumed, $\mathcal{S}''(x_0) = 0$, $\mathcal{S}''(x_m) = 0$.

Figure 5.4 depicts the explained mathematical method.

Selection of realistic prediction method

The Wiener filter, or any linear prediction method that is based on the MSE minimization, require a previous knowledge of the SINR and channel statistics. In general, fading channels can be studied and the second order statistics can be derived, however, doing this while considering interferences is a much more difficult task in the UL, where the variability follows no statistical rule. The same rationale applies for the Kalman filter, where the variances of the process and measurement noise must be estimated as an input.

The LMS adaptive filter has the advantage of not necessarily depending on the first or second order statistics, however it is mandatory to have a constant separation between samples and also with the predicted sample. In a realistic UL system the CSI can be measured in a more or less constant fashion, however, it depends on the eNB sounding bandwidth parameters, C_{SRS} and B_{SRS}, the number of users connected, the number of multiplexed UEs, the type of sounding enabled for each UE (periodic or aperiodic) and the sounding periodicity assigned to each UE, if necessary. Assuming that periodic CQI samples are available at the eNB, an LMS filter was implemented to obtain the next CQI value. No gains were observed when using predictions compared to the baseline situation, the SRS based CSI acquisition. The prediction horizon set was T_{sound}, meaning that the next CQI to arrive was being predicted. The only cases in which the LMS solution provided acceptable results where for very low values of SRS delay ($T_{\mathrm{sound}} \simeq 2\,\mathrm{ms}$) and neglecting interferences. In addition to this, the discrete nature of the LMS filter made impossible to predict the CQI in those TTIs that were not a multiple of T_{sound}, for example when predicting the CQI at the next reception time 1 RTT later. It is

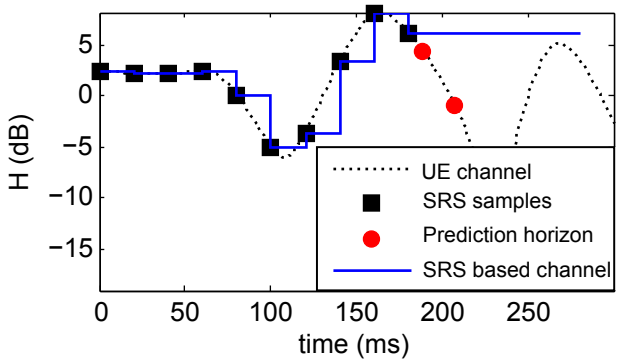

Figure 5.5: Continuous time formulation of the prediction

not possible to predict values in between two consecutive samples with the use of LMS, unless an interpolating algorithm is used to complement the solution.

Indeed, the suitability of the resources may be assessed by the scheduler at any time; therefore, the main challenge of the selected prediction method is to provide the most accurate SINR at the time of reception $t_p = t + 1RTT$, where t is the scheduling instant. In particular, the time span, with respect to the reception of last sample, where predictions may be taken goes from $t_p = 1RTT$, concurring with a SRS reception instant, to $t_p = T_{\text{sound}} - 1 + 1\,\text{RTT}$, corresponding to the prediction one time instant before the arrival of the next SRS, figure 5.5 shows a graphical example of this. This implies a need for mechanisms that provide predictions in a contiguous time.

From the previous paragraphs, cubic splines appear to be an interesting and promising solution that suits well the constraints of the problem, in particular:

1. The difficulty to estimate error measurements correctly in the uplink, given the rapid SINR variability.
2. It is a continuous time formulation itself, without the need for additional interpolators.

5.4 Interference Cancellation and Coordination

Other methods that can be introduced to help the scheduling decisions are based on interference management. As seen in section 5.2, one of the most limiting aspects in the UL is the random interference generated, whose variability depend on a number of factors, such as allocation policies and the number of UEs having active connections. In this regard, it is expected that if interference management is carried out in the UL this may help to improve the CSI.

Interference Cancellation: The basic concept of this strategy is that the

interference power can be reduced by decoding and subsequently subtracting the interference signals [102]. Although IC techniques are suitable for DL and UL, these are particularly attractive for the UL, since all the processing is done in the eNB side. Two main types of IC receivers can be found in the literature: first, multi-user receivers that are able to decode and subtract multi-user signals, from the received one, according to descending power [103]; second, spatial suppression, which uses multiple antennas to detect and suppress the interference [49].

Inter-Cell Interference Coordination: This is a very broadly discussed topic in the literature, and probably the most spread technique used for interference management. The fundamental idea is to coordinate the transmission of the different cells to reduce the interference generated, or at least its impact. Countless techniques have been devised in the literature that intend to maximize the spectral efficiency by not dramatically increasing the reuse, while containing the impact of the transmissions. The frequency reuse is a key factor when designing mobile networks, since unitary reuse is desired, but it is not beneficial for all UEs in the cell. In this regard, UEs are classified based on their interference vulnerability and smaller parts of the spectrum are disposed for their exclusive use. With this, UEs experiencing or generating high levels of interference will transmit in smaller and dedicated parts of the available bandwidth, and if this is coordinated among a set of eNBs, interference generation can reduce significantly.

5.5 Method for SINR Prediction

Given the previous paragraphs, this section presents the proposed prediction method to improve the imperfect CSI as well as the performance evaluation and results discussion.

5.5.1 Cubic Spline Extrapolation

Cubic splines provide a continuous solution, where the future sample can be calculated at any time, figure 5.6 shows how the spline correctly matches an Extended Pedestrian B (EPB) channel model beyond one RTT of 8 ms. This qualitative analysis shows a superior channel evaluation than just keeping constant the last SRS information (SRS based channel on the plot). Note however, that interference is not present yet. The squares indicate the reporting points or times in which the eNB receives an SRS from the UE, with a reporting interval of 10 ms in this example. It is remarkable that no matter how often SRS are received, if the user is allocated that resource, it will be being used one RTT later in the best case, so at least that prediction horizon should be aimed.

The presence of interference yields a much noisier evolution of SRSs, so the resulting spline is expected to have sharper variations. Figure 5.7 shows an example of prediction in case of a channel affected by interference from users in neighbouring cells. It is evident how the presence of large interference variations from one TTI to

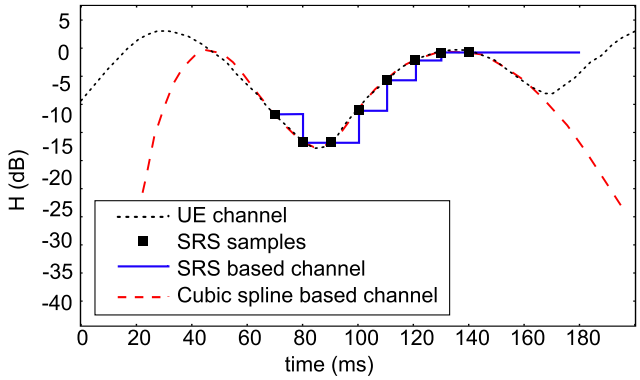

Figure 5.6: UE channel prediction based on piecewise polynomial extrapolation.

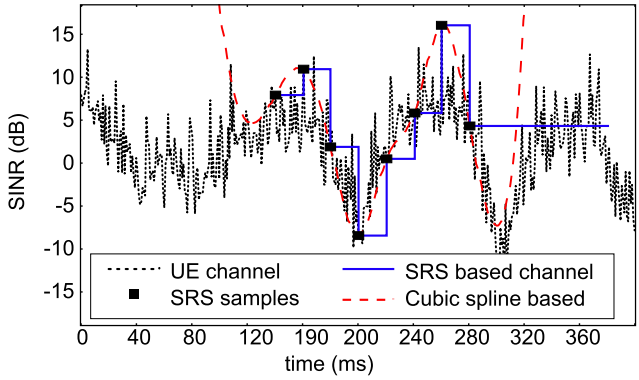

Figure 5.7: UE channel prediction based on piecewise polynomial interpolation, effect of low SINR.

the next may imply that the spline is not able to follow the channel and so wrong scheduling decisions can be taken about the quality and suitability of particular PRBs. Moreover, in some cases the first derivative at the last SRS reporting point can be very high and so the duration of the reliable prediction horizon is dramatically reduced. Hence, it is necessary to introduce a divergence detection mechanism. The spline is considered to diverge when a more than 10 dB variation occur in less than one RTT, this simplistic heuristic is enough to filter out those cases. Then the last prediction that was considered as reliable is kept fix until a new SRS update.

5.5.2 Performance Evaluation

To evaluate the prediction method under the realistic UL conditions system level simulations are carried out. The selected method, cubic splines, is compared to a linear extrapolation method, in which the last two SRS samples are used to calculate the future sample, and to the baseline scenario, where the scheduler just uses the

Table 5.2: Channel prediction: Simulation scenario assumptions

Parameter	Value
Bandwidth	2 x 80 PRBs
B_{SRS}	16 PRBs, 8 PRBs, 4 PRBs
T_{sound}	10 ms, 20 ms, 40 ms
Number of UEs served	10 and 15
Number of UEs connected	10 and 30
PRBs allocated	2 clusters of 2 PRBs x CC
Simulation time	10 kTTI

SINR at the last SRS for the allocation and link adaptation.

Simulation conditions

Simulations are carried out in the synthetic layout described in appendix A. With the aim of testing the proposed strategy under different interference situations three scenarios are studied:

- A low Resource Utilization (RU) scenario where 10 UEs have an active connection to each cell and 50% of the resources are actively used.
- Higher number of UEs, 30 have an active connection with 50% of the resources being actively used.
- High number of active connections 30 UEs and 75% RU.

The allocated resources per UE remain constant on each studied scenario and the RU varies depending on the number of UEs that are allowed to access the scheduler. There is a fixed number of UEs allocated by the frequency domain scheduler at each TTI [104]. Specific simulation conditions are given in table 5.2.

Results and discussion

The performance of the CSI acquisition methods are evaluated with the pdf of the SINR error, or misalignment. This error is measured as the difference between the SINR measured in the PUSCH transmission and the sounded or predicted signal used for scheduling and link adaptation. Let recall that the prediction instant, or prediction horizon, can go from one RTT, in the case when the SRS has just been received in the current TTI, or $T_{\text{sound}} - 1 + 1$ RTT in the worst case. Figure 5.8 shows the performance of the prediction methods when no interferences are considered; in this case, the number of connections and the RU are irrelevant given that only the Signal to Noise Ratio (SNR) is measured, the sounding bandwidth is 16 PRBs.

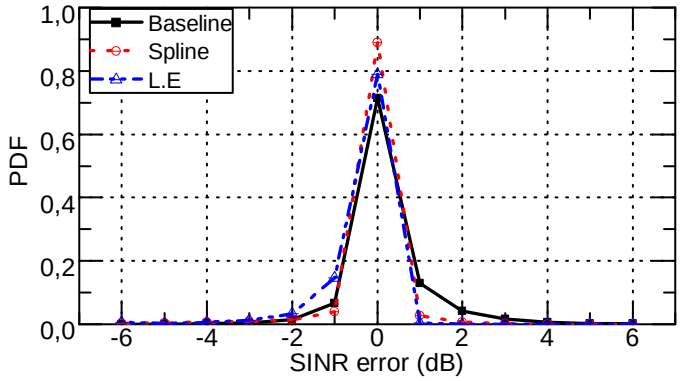

Figure 5.8: pdf of SNR error measurement.

There is almost 20% of improvement in the null error probability with the use of splines, and also errors between -2 dB and 2 dB are reduced. This shows that there is a wide room for improvement with the use of cubic splines, that outperform also the linear extrapolation case.

As explained in section 5.3.1, the piece-wise polynomial method needs SINR points measured from the SRS to interpolate and construct the whole curve. The number of past SRSs used for this purpose has an impact in the extrapolation result, figure 5.9 shows the curve construction with different number of sampling points. The minimum number of points to construct a curve is three, and as the number increases, more polynomials are considered which leads to different curve constructions. However, there is a maximum point in which by adding more polynomials no difference is recognised. In the figure the spline construction achieves a state of no further change when more than 8 SRS samples are considered.

When the interferences are considered in the CSI acquisition process, the picture is very different, as seen in figure 5.10 which shows the pdf of the SINR error for the three interference scenarios simulated. Interference variations lead to strong errors in the channel measurement; in all the scenarios evaluated the probability of error zero never surpasses 35% for the baseline case, and predictions perform clearly worse. Under such conditions it is not possible to improve the CSI, because not even the SRSs are providing sufficient information to correctly reconstruct the SINR curve. The interference variability is the main limitation of the channel estimation based on prediction or sounding.

With the aim of improving the SRS information, and also to support predictions and obtain higher probability of null error, IC strategies are introduced. The initial study done with the SNR shows that the prediction method is able to improve CSI, however, the complete removal of interferences is complex and no IC receiver is capable of doing this, such an assumption would not be realistic. Therefore, an intermediate scenario shall be encountered where the IC can provide significant improvements to the SINR prediction and the CSI acquisition itself. Figure 5.11 shows

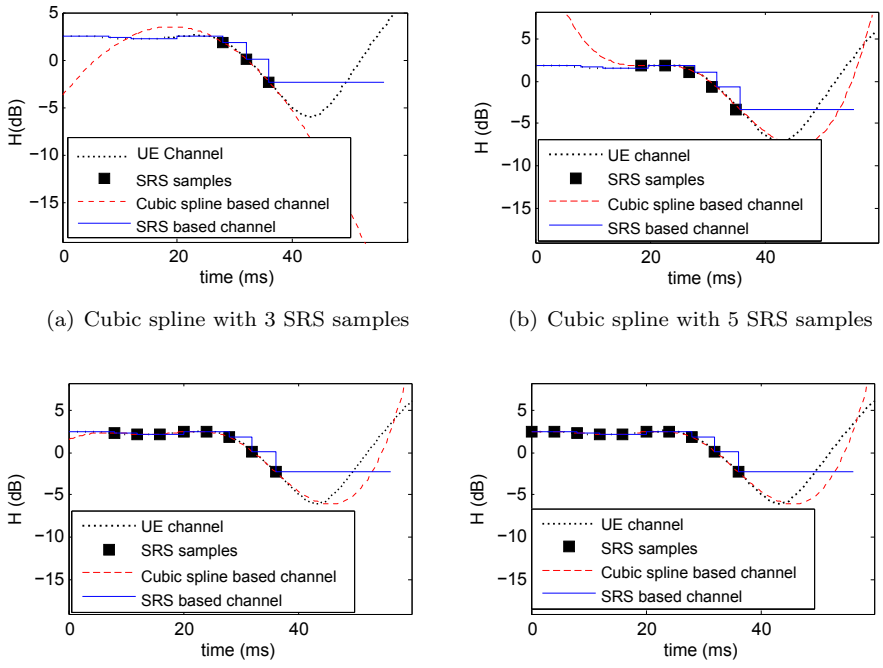

(a) Cubic spline with 3 SRS samples

(b) Cubic spline with 5 SRS samples

(c) Cubic spline with 8 SRS samples

(d) Cubic spline with 10 SRS samples

Figure 5.9: Cubic spline construction with different number of SRS samples

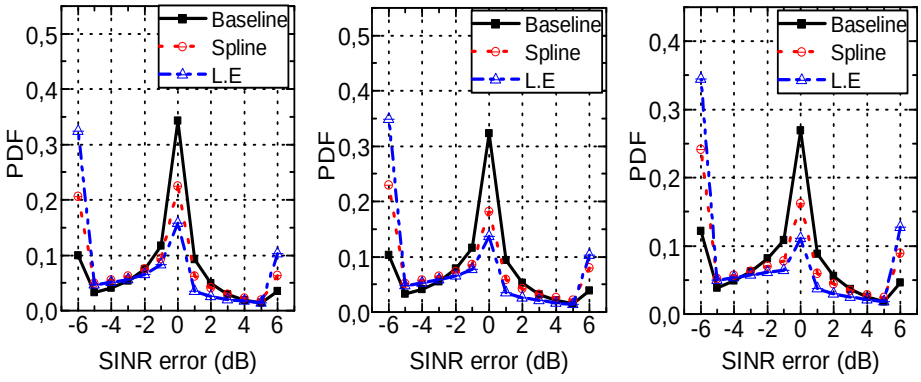

(a) 10 UEs and RU=50%

(b) 30 UEs and RU=50%

(c) 30 UEs and RU=75%

Figure 5.10: SINR error distribution for the different evaluated scenarios in normal interference conditions

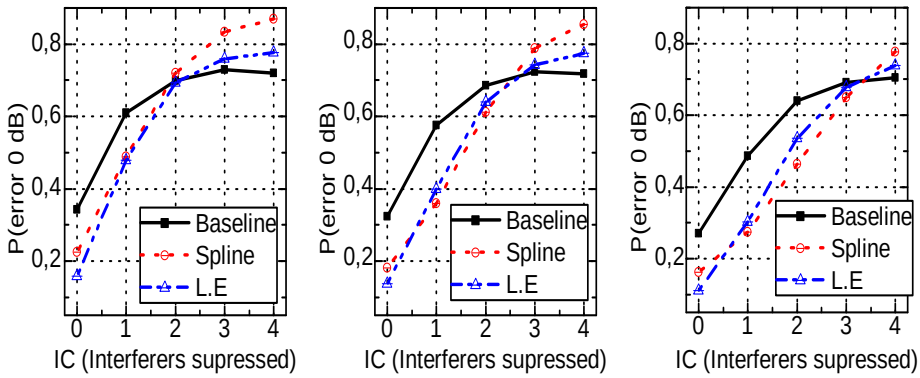

(a) 10 UEs and RU=50% (b) 30 UEs and RU=50% (c) 30 UEs and RU=75%

Figure 5.11: Probability of null SINR error versus the number of sources of interference cancelled

the percentage of null SINR error under different IC conditions. The interference cancelled is expressed in terms of interference sources; information about the amount of dBs cancelled is not provided since the most dominant interference source affecting to the different UEs may have tenths of dBs of difference, hence, no absolute value of dBs level can be provided. Each interference scenario has a different minimum cancellation threshold. For instance, in the low load case if two sources are cancelled the cubic spline offers a 2% improvement over the baseline case, and this improvement boosts as the number of cancelled interferences grows. The linear extrapolation method provides poorer performance compared to the polynomial solution, however it also offers some improvements as the interference variability is reduced. When the number of connections increase and the RU is kept at 50%, three cancelled sources are necessary to provide improvement with the spline method, and when the RU increases to 75% four sources are needed to be cancelled. This performance is expected, since the number of UEs connected and the RU affect directly to the interference generation and variability. However, it is interesting to note, that in all the interference scenarios studied, for a number of cancellations higher than two the baseline scenario does not offer much improvement and arrives to a saturation point, while in the prediction case the improvement continues to grow. Apart from the interference impact, it is recognised that the baseline case presents an upper bound limit in its performance, which cannot be further improved by removing sources of interference. Note that the divergence control mechanism added to the spline prediction method helps not to increase huge errors in the SINR prediction, and not to grow it more than the one already provided by the SRS.

This upper bound limit the SRS has is very much related to the sounding delay, as shown in figure 5.12 which depicts the probability of having a null error for different sounding periodicities, no interferences are considered. If T_{sound} is low, there is higher room for improvement, but when T_{sound} increases the performance deteriorates, and

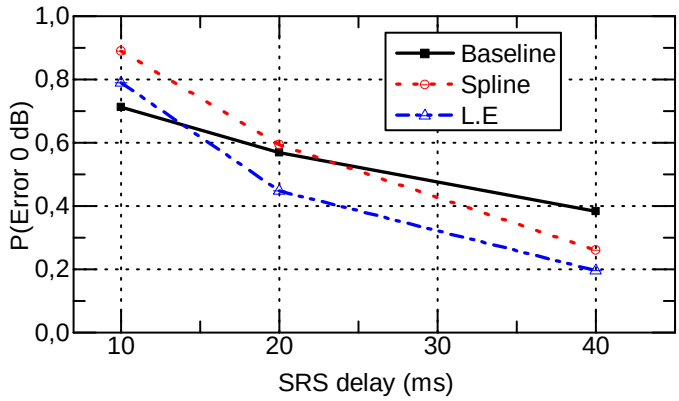

Figure 5.12: Probability of null SINR error versus the SRS delay

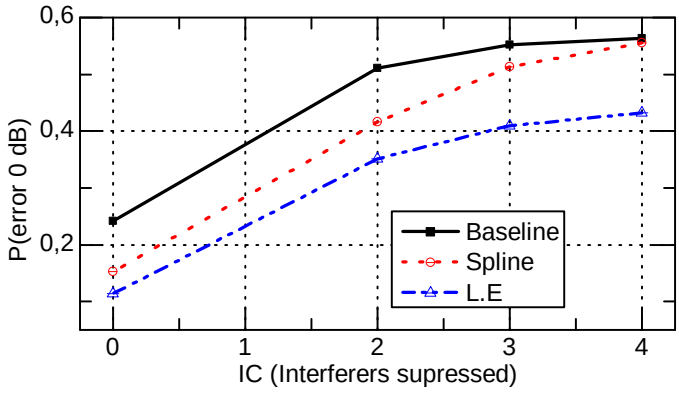

Figure 5.13: Probability of null SINR error versus the number of sources of interference cancelled with higher delay

in the worst case, there is not even an improvement margin. It is then expected that in such conditions the introduction of IC strategies result in a different performance than the one discussed before. Figure 5.13 shows the percentage of null error for different number of interferences suppressed, in this case only the worst case scenario in terms of interferences is evaluated, 30 UEs having active connections and 75% of RU. When the SRSs samples are more separated in time, the cubic spline offers less improvement, and with the same number of interferences suppressed it is unable of surpassing the baseline performance. As shown in the previous figure 5.12, even in cases where no interferences are considered, if the delay increases up to 40 ms the spline is never able to exceed the baseline performance. Nevertheless, it is worth mentioning that the baseline upper limit performance, in the absence of interference, for the smallest sounding bandwidth (i.e. 40 ms reporting interval) resembles the performance obtained under harsh interferences, which leads to the conclusion that a strong delay in measurement is as detrimental as high interference variability.

5.6 Method for SRS Delay Reduction

The results shown so far have addressed the imperfect CSI issue by trying to anticipate what will happen at the precise moment of reception; but hitherto, the issue of the delay has yet not been corrected. From the experience gained in the past sections, and the examples given at the beginning of this chapter, one of the main handicaps of sounding is the large delay in high bandwidth settings. Thus, it is necessary to reduce the SRS delay T_{sound} to achieve improvements in the channel measurements. This section proposes to introduce classic, traditional ICIC techniques, widely used in wireless communications, to reduce the sounding bandwidth in the cell edge, and with it, the transmission bandwidth. This solution aims at reducing the time delay between two samples and improving the overall performance. First, an introduction to the sounding procedure with the use of SFR and FFR is provided followed by the performance evaluation.

5.6.1 SFR and FFR ICIC methods

ICIC techniques allow to control the generated interference in the network by coordinating the transmissions in the shared channel. Two well known ICIC techniques are SFR and FFR, where a small part of the spectrum is reserved for the exclusive use of UEs placed in the cell edge. According to this, it is proposed to apply ICIC in the sounding procedure of cell edge UEs with a two fold aim: first, to reduce the delay in CSI measurement and second, to tackle the interference issue. By reducing the sounding region, and the available bandwidth, the delay T_{sound} is naturally reduced; also, concentrating a group of users in one region of the spectrum reduces the interference variability.

The main idea of ICIC is that the entire bandwidth is divided into different parts, as shown in figure 5.14. Each eNB attached to the same site reserves a different part of the spectrum for its own cell edge exploitation. Cell centre UEs of all eNBs share the rest of the band; channel conditions of these UEs are not critical owing to the shorter distance to the cell. FFR largely follows the SFR scheme, however, the cell edge part is not shared among the sectors. One piece of band is divided into three parts, and each eNB has exclusive access to one of those spectrum pieces. Less band is accessible by cell edge UEs in the FFR strategy, however it is less interfered than in SFR given the frequency reuse 3 that is enjoyed at the edge.

The main task of the SRSs is to provide the eNB with sufficient information to enable the most accurate frequency domain scheduling and also low error link adaptation. If sounding is carried out in a smaller part of each CC, then data transmissions must be allocated in those sounding regions, to assure that link adaptation is done correctly and perform a spectrally efficient transmission. The procedure of the ICIC-based SRS allocation and the system model are explained in the following lines.

Each user, regardless if it is cell edge or not, is assigned a user block ub and a cyclic shift n_m (where $m \in M$ and M is the number of multiplexed UEs) to carry out

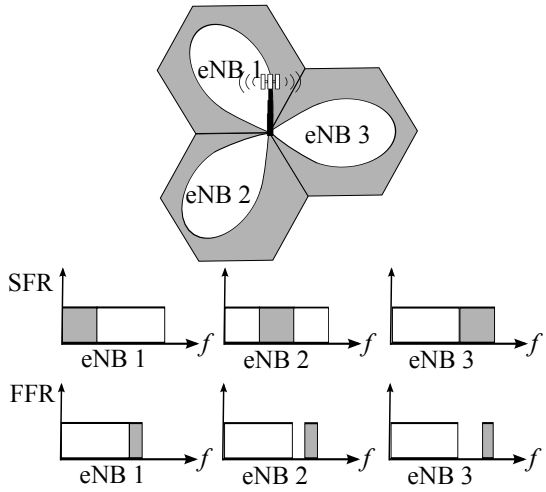

Figure 5.14: ICIC techniques SFR and FFR

the SRS FDM and CDM multiplexing explained in section 2.4.1. All UEs with the same ub share the same allocation, therefore different cyclic shifts n_m are assigned. The scheduler in charge of sounding resources allocates groups of successive PRBs to each user block; in one allocation process it distributes the total bandwidth along all the user blocks. UEs considered to be cell edge are only eligible for transmitting in the ICIC reserved area, and the remainder of the users may be allocated the rest of the band. The signal received per resource block r at the eNB side in its lth CC and one RTT later is calculated following equation 4.1, subsequently the eNB estimates user's i CSI at PRB r in carrier l using equation 4.2. Note that only users sharing cyclic shifts and user blocks are considered to interfere each other. The sounding process eventually lets to obtain a single value of $\gamma_r^{\mathrm{SRS}}(i,j)$ for every PRB. eNBs have pre-allocated ICIC sounding regions on each CC, so that cell edge UEs with enough power capabilities can still benefit from CA and frequency diversity gain. Users do not sound both CCs simultaneously, and the sounding bandwidth M_{SRS} is the same for all UEs and all CCs.

5.6.2 Performance Evaluation

To evaluate the performance gains of introducing ICIC in the sounding process, the two methods, SFR and FFR are tested by means of system level simulation. Different number of UEs with active connections and different RU values are studied and compared with the aim of introducing different interference patterns in the scenario of evaluation.

Table 5.3: ICIC: Simulation scenario assumptions

Parameter	Value
Bandwidth	2 x 72 PRBs
FFR Bandwidth	2 x 8 PRBs
SFR Bandwidth	2 x 24 PRBs
SRS BW	8 PRBs
Number of UEs served	6 and 9
Number of UEs connected	10 and 30
PRBs allocated	2 clusters of 3 PRBs x CC
Simulation time	10 kTTI

Simulation conditions

The proposed method is evaluated in the synthetic scenario described in appendix A. A study under different interference conditions is performed by varying the number of UEs in the scenario as well as the RU in the cell. In particular, the following cases are analysed:

- FFR and SFR:
  1. Low number of UEs and low RU: Each cell has 10 UEs with active connections and 50% of the resources are being actively used.
  2. Low number of UEs and high RU: Same conditions than before with 75% of RU.
  3. High number of UEs and low RU: Each cell has 30 UEs with active connections, 50% of RU.
  4. High number of UEs and high RU: Same conditions than before with 75% of RU.
- Baseline: No ICIC is considered when allocating sounding or PUSCH resources. The same cases are simulated for the baseline scenario as well.

Specific simulation conditions are given in table 5.3. Note that the allocated bandwidth is kept constant regardless the scenario, and the RU depends on the number of UEs that access the scheduler.

Results and discussion

Figures 5.15(a), 5.15(b) and 5.15(c) show the sounded SINR obtained from the SRSs with respect to the SINR measured in the PUSCH at the time of reception; the same cell edge user in one resource block is tested with and without ICIC in the low

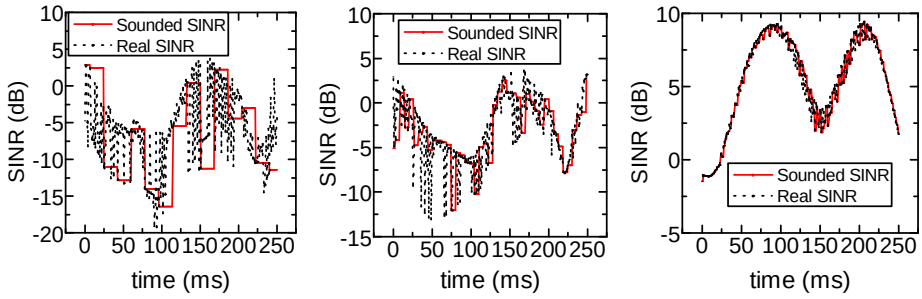

(a) Baseline scenario (b) SFR scenario (c) FFR scenario

Figure 5.15: Comparison of sounding information versus PUSCH SINR

loaded scenario. Both SFR and FFR allow a much faster update of SRS information than the baseline solution, obtaining more accurate measurements of the channel. In fact, CSI measurements with FFR, which updates faster than SFR, appears to be more noisy-like and follows almost perfectly the SINR in the PUSCH. Thus, the more the sounding area is reduced, the lower T_{sound} becomes, and the actual SINR can be better followed.

The CSI provided by the SRSs with the baseline SRS allocation process differs very much from the actual SINR experienced by the cell edge UE. The information gathered in this case may be useful for frequency domain scheduling, since broadly, general information about deep fadings can be derived and compared among the different PRBs. However, information about the instantaneous interference generated is never provided and instant measurements may vary 10 dB. On the contrary, by including ICIC in the sounding allocation process the SINR variations and channel fadings are better captured and the SINR information is far more accurate. Another advantage of the ICIC method is that cell edge interference is less changeable because allocations are less variable among users; and on the other hand, a cell edge UE is never interfered by other cell edge UE in near cells. This is worth of note in the recently discussed figures, where the real SINR in figure 5.15(a) is more variable than the real SINR experienced in figures 5.15(b) and 5.15(c). The variability of the aggregate interference changes which is owed to the reduction in the number of users transmitting in the ICIC reserved area. In SFR, only a fraction of UEs are allocated sounding resources in the reserved portion of the spectrum; FFR has even less interference variability, given the lack of interferers in the neighbouring sectors. In the baseline scenario all UEs are allocated sounding resources along the whole CC bandwidth, which lets the scheduler cover all the available spectrum thus leading to a wider range of possible interferers, the PF scheduling decisions will determine them on each TTI.

This improvement in the interference perception and the reduction of the delay yields a more accurate CSI in some of the simulated scenarios as shown in figures 5.16 and 5.17, where the pdf of the SINR error is represented. The SINR error

is measured as the difference between the SRS information used in the allocation instant, and the SINR measured in the PUSCH. In all the scenarios evaluated SFR strategy provides the highest probability of null error in the CSI measurement, especially in those cases where the number of connections are low, figures 5.16(a) and 5.16(b). The FFR scheme allows a low number of cell edge UEs in the ICIC band, given the reduced bandwidth availability and the allocated bandwidth length (two clusters of 3 PRBs); for all the scenarios the maximum number of ICIC UEs that are allowed to access the scheduler is one. Scenarios with low number of connections offer a reduced interference variability, which yields to a better appreciation of the delay reduction, in both ICIC and non-ICIC UEs. When the number of UEs connected to the eNB increases, the picture is quite different. Enhancements brought by both ICIC techniques are reduced with respect to the previous case, and FFR performs closer to the baseline solution. When the active connections increase, there is a higher variability of the generated interference, and the delay improvements are less prominent in the error calculation. In particular, comparing the FFR with the SFR solutions, the SFR still provides an increase of the null error probability, while FFR no; FFR limited bandwidth for the cell edge allows only one UE in the ICIC region on each scheduling interval, while in the SFR case up to four may be allocated. Cell edge UEs are the ones that benefit most from the delay reduction and interference coordination, and in the case of FFR the occurrences of these set of UEs are less frequent. Nevertheless, both ICIC solutions still provide lower probability of increased errors, especially between -5 dB and -1 dB.

The RU alteration does not impact significantly the results tendency nor the absolute values in both 30 UE scenarios, however, it does impact the probabilities in the 10 UE case, though tendency is maintained. The RU affects the interference ideally in the number of interference sources, the lower the RU is, the less the probability of having an interference source from the neighbouring eNBs. This may generate higher or lower values of aggregate interference. In a low variant SINR scenario, as the one with 10 active connections, the constant change of number of interference sources has an increased influence, since constitutes a cause of variability to the interference absolute value. Indeed, this effect is also present in the high variant interference scenario (30 connections), but it is less dominant, since there is another cause of interference variability: the increased number of connections.

Refining the CSI acquisition is the first step for improving the overall system performance. When the SRS information is more accurate the BLER reduces, which leads to less retransmissions and a possible improvement of the cell throughput. Figures 5.18 and 5.19 depict the BLER experienced by the UE at the first transmission attempt. Note that the BLER measurement is taken at a different time scale than the SINR error measurement. The BLER at first attempt is computed once the UE finishes its connection (i.e. when the buffer is empty), and the SINR error is calculated each TTI. In this sense, when the scheduler is more competitive to access, RU=50%, the cell edge UEs have less probability of being scheduled, especially in the FFR case, regardless the cell occupancy. Therefore, when accounting for the BLER obtained in connections that have successfully finished, the FFR solution performs closer to the baseline solution. However, this does not happen in the case of SFR, where more cell edge UEs are allowed to access the scheduler, obtaining more

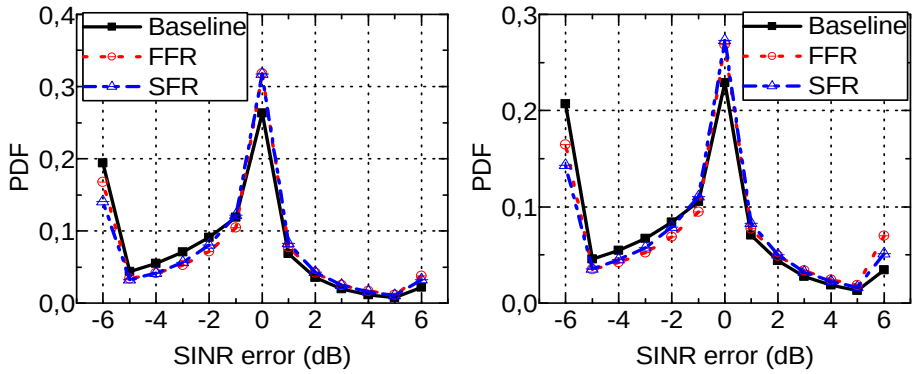

(a) SINR error: 10 UEs, RU=50%

(b) SINR error: 10 UEs, RU=75%

Figure 5.16: SINR error for low number of connections

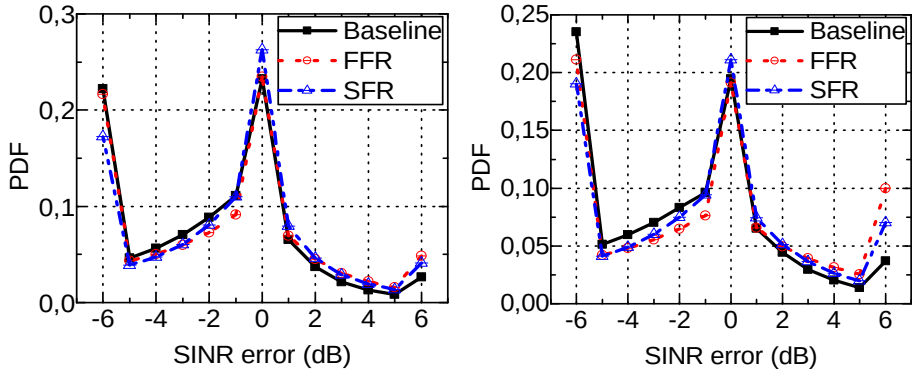

(a) SINR error: 30 UEs, RU=50%

(b) SINR error: 30 UEs, RU=75%

Figure 5.17: SINR error for high number of connections

frequent allocations. Conversely, when the scheduler is less competitive increasing the RU, and with it the number of UEs that are allowed to access the scheduler, cell edge UEs in the FFR case may be scheduled more often, resulting in more successful cell edge connections, which is reflected in the BLER calculation.

The ICIC available bandwidth makes the performance of the FFR solution very much sensitive to the number of cell edge UEs, or UEs in the ICIC region. If a large number of UEs is allowed to enter the ICIC band, less UEs are being scheduled in the remainder piece of bandwidth, generating very little interference to other cell centre UEs. On the other hand, this situation generates large queues to access the scheduler in the ICIC band, and the experienced throughput in the cell edge is therefore seriously impaired. This situation is very unlikely to happen in a real

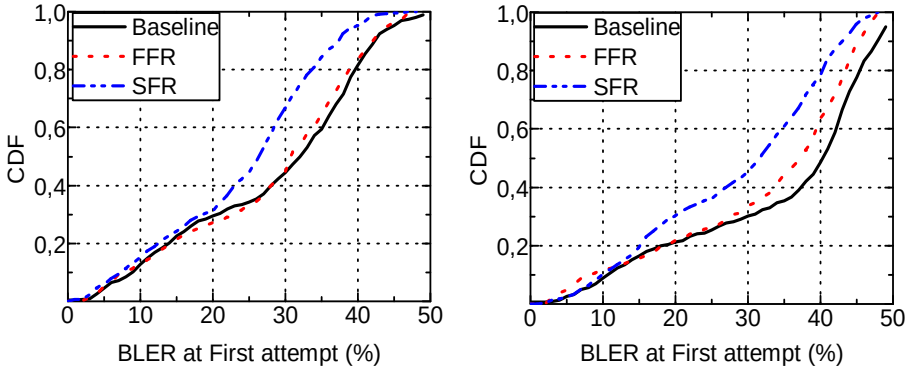

(a) BLER with 10 active connections (b) BLER with 30 active connections

Figure 5.18: cdf of UE BLER for the RU=50% scenarios

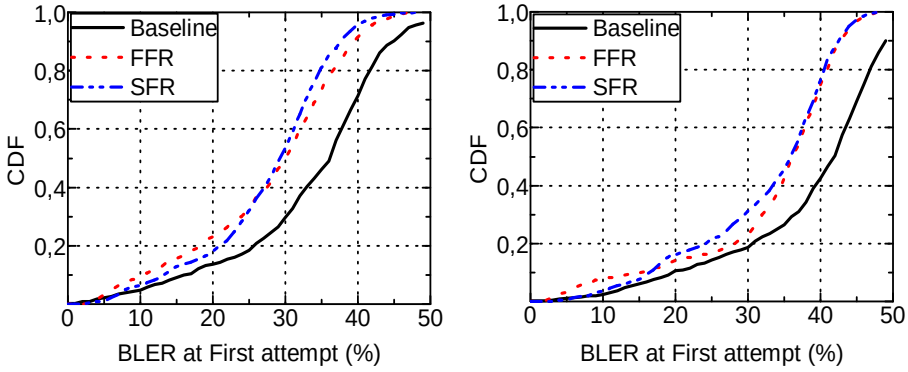

(a) BLER with 10 active connections (b) BLER with 30 active connections

Figure 5.19: cdf of UE BLER for the RU=75% scenarios

communications system, for such reason, a reduced number of UEs in the ICIC area is preferred. This compromise is less probable in the SFR scenario, where a larger number of cell edge UEs may access the scheduler on each allocation interval. Constraining the number of UEs in the ICIC band in the simulation setting of the FFR, results in having different path-loss distributions in all three scenarios, SFR, FFR and baseline. For such reason, comparisons in terms of throughput are not fair, and only the SFR and baseline strategies are being analyzed in these terms. Nonetheless, note that the SFR solution has always outperformed the FFR in terms of BLER and error results. Hence, figures 5.20 and 5.21 show the throughput improvements in terms of throughput obtained in the SFR scenario compared to the baseline strategy. The error improvements and the BLER reduction are consequently

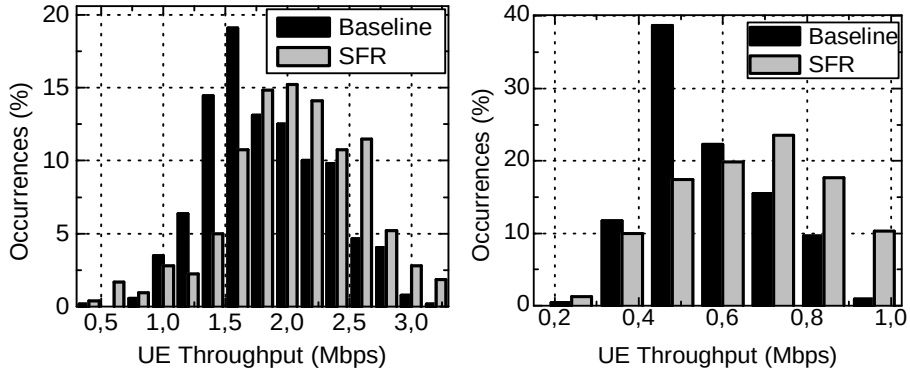

(a) UE Throughput with 10 active connections (b) UE Throughput with 30 active connections

Figure 5.20: Histogram of UE throughput for low RU

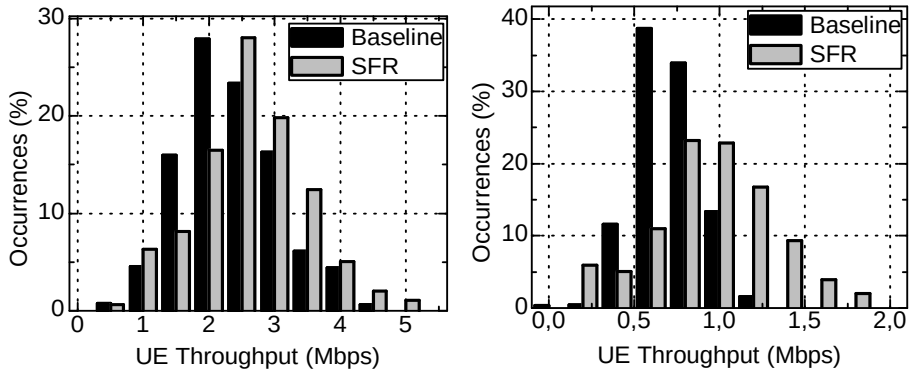

(a) UE Throughput with 10 active connections (b) UE Throughput with 30 active connections

Figure 5.21: Histogram of UE throughput for high RU

reflected in a higher bit-rate, which is mainly derived from the delay and interference variability reduction.

Shortening the SRS periodicity results in more accurate estimations of the future SINR, reducing BLER, and, as long as the frequency selective gain brought by the scheduling flexibility is not neglected, improvements in cell throughput can be materialized. Employing CA still provides the system with an increased bandwidth, which, in the case of SFR, lets UEs benefit from frequency diversity gain while restricting the sounding channels. There is no further signalling or implementation changes required to support this functionality, since the allocation of sounding resources is done in the eNB at a RRC level and signalled to the UE.

5.7 Conclusions

This chapter has addressed one of the main problems that the UL of LTE-A may encounter when pursuing good spectral efficiency and low BLER transmissions. Imperfect CSI acquisition and knowledge impairs the correct performance of other auspicious RRM algorithms, because it entails increased errors and retransmissions. The UL channel presents two main challenges to improve the CQI accuracy, first, the ever-changing interference that results from variable scheduling decisions, and second, the delay in channel reporting. In LTE-A the UE sends SRSs every sub-frame to provide a complete knowledge of the SINR across the entire available band, and this information is useful to support frequency domain scheduling decisions and accurate link adaptation. Thus, increased time-variations of the SINR values and large delay between two consecutive measurement reports can be detrimental for the correct UE performance. With the aim of improving the SINR knowledge, this dissertation has proposed the use of two strategies, which have been evaluated under different interference situations and compared against the baseline and other benchmark solutions. Both proposals and the main conclusions are detailed in the following:

1. A cubic spline extrapolation method that allows extending the SINR knowledge between the reception of two SRSs.
    - The proposed solution has shown a wide room for improvement of the SINR misalignment, when delays are kept below 20 ms and in absence of interference.
    - The CSI acquisition can be severely damaged in high interference variability conditions, therefore, this would be a feasible solution only if a certain level of IC is performed. The level of IC has been accordingly quantified, and the proposed solution presents almost a linear improvement with respect to the level of interference cancelled, while in the baseline scenario it has been recognised an upper limit inflicted by the SRS delay.
    - Predictions built with high delay SRSs result in poorer improvements even in the absence of interference. In fact, results show that high values of delays outcome in similar performance results as in harsh interference conditions, for all three cases: the baseline and the two prediction methods. Delay reduction is mandatory to obtain a correct UE performance. However, the delay in sounding depends essentially in the number of UEs connected to the cell and the number of UEs being multiplexed, and it is worsened by the increase in available bandwidth. In this sense, in overly charged cells it is mandatory to provide a mechanism that allow to reduce the sounding delay, while assuring that all the connected UEs are allowed to sound.
2. Linked with the conclusions drawn in the previous proposal, two ICIC methods are integrated the sounding process. This strategy is proposed mainly to reduce the available bandwidth in the cell edge, with its consequent decrease in delay; also, coordinating the allocations among the different eNBs lowers the interference variability in the cell edge.

- The decrease in SRS reporting interval provides a more accurate CQI, since the SINR in the PUSCH is better represented by the sounding signals.
- A reduction in the interference variability mainly in the cell edge is observed, especially in the FFR case, which enjoys a higher reuse in the ICIC band.
- In low charged eNBs, the delay reduction appreciation is higher, owing to the reduced interference variability. This results in a higher improvement of the SINR misalignment. When cells have more UEs with active connections, the SINR error reduction is lower, and the FFR strategy performs closer to the baseline than to the SFR strategy, which still provides improvements.
- In the case of FFR, this bandwidth reduction impairs the scheduling flexibility and no gains can be achieved. Thus, an intermediate scenario, such as SFR is desirable.

Chapter 6

Further improvements in UL performance with CA: Towards 5G

6.1 Introduction

The strategies hitherto proposed have focused on improving the spectral efficiency and the UE throughput performance from a scheduling and resource management point of view. Adding intelligence into the MAC and RRC layers has shown significant improvements in terms of data rate and fairness. However, the non-constant QoE of UEs along the cell area motivates to increase the number of serving eNBs by adding cells of shorter coverage, bringing the network closer to the UE. This change in the deployment allows to further improve the network capacity by enabling better load balancing among the cells and eliminating coverage holes. However, this new paradigm of system design brings with it significant open challenges to assure a correct operation such as: backhaul improvement, mobility and interference management, cell association and UL/DL relationship.

Essentially, HetNets consist of several cells with different DL coverage sizes as a result of strong disparities in the eNBs transmit power. Given this, the cell offering the optimal RSRP-based association in the DL may not be the optimal in the UL, where the closest cell is the one allowing the maximum received power; this is known as the UL/DL imbalance problem. The literature has proposed solutions based on biasing which increase the SCell DL coverage making it similar to the UL one (recall sections 2.1 and 2.5 for definitions); UEs in the expanded range area are associated to the SCell in both UL and DL. In this situation, the UL of UEs is fairly improved, while the DL is suboptimal associated, since the maximum received power is still provided by the MCell. Whereas expanding the range of low power nodes partially compensates UL interference issues, DL interference is increased at the new SCell

edge. For this reason, eICIC mechanisms have been investigated. These techniques are mostly variations of the same idea: frame muting and coordinated scheduling. Indeed, the 3GPP introduced the possibility of using ABS since LTE-A Release 10.

Eventually, the range expansion technique is limited to moderate offset values and the adjustment is not trivial for very heterogeneous coverage footprints as it will occur in ultra dense deployments. Besides, current research work assumes slow updates (scale of seconds) for interference coordination [105, 106]. The reasons are an increased RTT (due to X2 signaling delays) but more importantly, the need to guarantee the system stability. In light of this, other authors propose the complete decoupling of both UL and DL to ensure an optimal association in both links.

This chapter addresses the UL/DL imbalance problem in an inter-band CA environment, where separated frequency carriers are aggregated and generate different coverage footprints. The UL/DL imbalance problem impacts the performance of UL CA for reasons that stem directly from the power availability. Aiming at maximizing spectral efficiency in both UL and DL, a decoupling strategy is considered with two association rules. The first, is a fully flexible policy that allows UEs to decouple the UL CCs separately, based on the minimum path-loss; the second, decouples both carriers based on the coverage of one CC only. The study is carried out through mathematical analysis with the use of a stochastic geometry model, and both, numerical results and system level simulations are provided to validate the association rules.

Section 6.2 describes the motivation to include DUDe in a carrier aggregated system and stresses the main contributions presented in this chapter. Thereupon section 6.3 explains the system model based on stochastic geometry and the analytical derivations related to the association probabilities, capacity and outage are presented. Section 6.4 discusses the numerical results based on the mathematical derivation and section 6.5 describes the realistic performance evaluation with the system level simulation results. The chapter is concluded in section 6.6.

6.2 System Design for DUDe with CA

In MCell-only network deployments, cell selection criterion is mainly influenced by the cell transmitting power, essentially the reference signal strength and quality received. In a HetNet context, conducting this type of cell selection or association outcomes in some system problems:

1. Overly charged MCells and under used SCells. This leads to suboptimal data rates and poor fairness in the whole HetNet; UEs placed under the MCell coverage are less likely to be scheduled, while SCell UEs have higher opportunities to transmit. Also, higher interference variability may be observed owing to the increased cell load in the macro tier.

2. UL and DL imbalance. In particular, macro cell edge UEs are receiving higher DL reference signal power from the macro, while being positioned nearer to

the SCell, which outcomes in a very poor UL connection though an optimal DL one.

3. Degraded CA performance in the UL given the increased number of power limited UEs.

These problems can be solved by splitting the UL and DL (DUDe) and associating each link with the best serving cell according to the maximum received power. Better UL load balancing is provided and UEs are optimally connected to the UL serving cell in terms of received power.

DUDe is under the umbrella of the *dual connectivity* concept, defined in [67] as one of the 3GPP study items for the SCell enhancements. In this type of connectivity, one UE receives from, or transmits to, more than one cell, and with the use of CA other system design besides single carrier DUDe can be considered. For instance, inter-node radio resource aggregation is a potential solution for improving cell edge throughput, which is particularly suitable for inter-band CA co-channel deployments, where the coverage region of both CCs are different, or for dedicated HetNet deployments. Given the scarce spectrum resources and the objective of maximum spectral efficiency, the dedicated deployment is less likely in real communication systems, and a full reuse of all the frequency bands is recommended to maximize capacity. With the aim of improving the UE performance with dual connectivity, a HetNet deployed in such conditions must pursue the following design goals:

- Homogenize both the QoE of all UEs, and the UL and DL data rates, allowing more flexible connections among cells.
- Control the generated interference not to impair the spectral efficiency brought by the association flexibility.

To this end, this chapter proposes the inclusion of DUDe in multi-carrier HetNets. An extension of the decoupled concept is studied, where each carrier can be associated independently based on the received power. The main novelties presented in this chapter can be summarized as:

- Recognition and study of all the possible combinations of association cases. In particular three association rules are compared:
    1. **PCD: Per Carrier DUDe.** This is a full flexibility association rule in which each UL carrier associates independently to the eNB which receives the highest signal power. Note that to have different UL carriers connected to different cells, particular propagation conditions must be considered in the different tiers. The SCell and the MCell do not share the same radio frequency propagation, for this reason one UE may be receiving a higher power from the SCell in a lower frequency CC whereas the MCell receives the highest power in the highest frequency CC, as shown in figure 6.1(a).

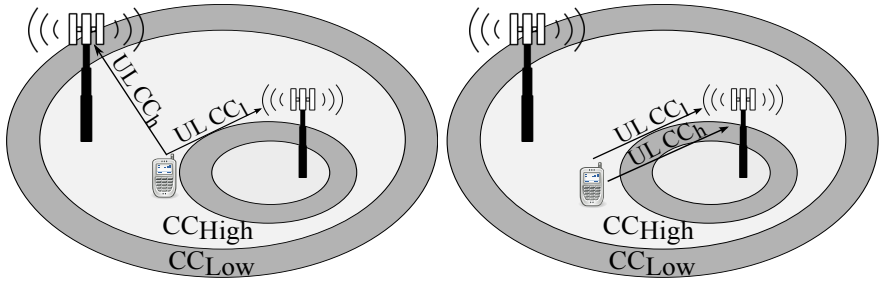

(a) Per-carrier UL/DL decoupling (b) Both carriers UL/DL decoupling

Figure 6.1: Decoupled associations studied

2. **BCD: Both Carriers DUDe.** A second case in which both carriers are decoupled together considering the lowest frequency received power, shown in figure 6.1(b).
3. **DLRP: DL Received Power.** The classical association policy.

- Stochastic geometry modeling of a multi-tier co-channel HetNet with inter-band CA. Derivation of performance metrics such as, association probability, distance distribution derivation for association rules, spectral efficiency analysis and outage calculations.
- Evaluation of gains brought by decoupled connections with respect to DLRP associations.
- UL interference analysis for both PCD and BCD cases. Conclusions are drawn regarding both decoupling policies based on the mathematical analysis and performance results.

6.3 System Model: Stochastic Geometry Analysis

This section provides the modeling and analysis of a decoupled inter-band CA HetNet using stochastic geometry [107]. Spatial stochastic process, such as PPP (recall section 1.2), has been widely used in literature to model the eNB locations and to derive many different performance metrics [108]. Some DL examples are: coverage and rate analysed in [109], level of load balancing in [110], outage and association probabilities in biased HetNets in [111], among others. The UL analytical modeling closely follows the DL one, however some changes in the interference modeling shall be considered as shown in [112]. PPP has also been adopted in the CA study for single and multi tier wireless networks in [113].

The derivation of the association probabilities considering inter-site CA are obtained in the following. Also, UL performance metrics such as spectral efficiency

and outage probability are derived for the three different association cases. Note that PCD constitutes the optimal association in terms of path-loss, and BCD and DLRP are considered suboptimal in the association of at least one carrier.

6.3.1 System Model

A two tier heterogeneous cellular network is modelled using independent homogeneous PPP. The location of the cells and devices is denoted as Φ_v, which is a set of points obtained by an independent PPP with an intensity λ_v, where $v = m$ for MCells, $v = s$ for SCells and $v = d$ for devices. The study considers two different frequency CCs not necessarily located on the same band; one low frequency carrier CC_{l} and one high frequency carrier CC_{h}. The same path-loss exponent α_v for all bands is considered, however, different values may be contemplated for each tier.

The transmit power used by MCells, SCells and devices is P_m, P_s and P_d, respectively. The analysis is performed for a typical device located at the origin $x_d = (0, 0)$ and variables $x_m, x_s \in \mathbb{R}^2$ correspond to the two-dimensional coordinates of the MCell and the SCell. Given this, the power received by the typical device in the DL from an eNB located at $x_v \in \Phi_v$ where $v \in S, M$ is denoted as S_v^{DL} and the signal power received at the same eNB in UL is denoted as S_v^{UL}:

$$S_v^{\mathrm{DL}} = P_v h_{x_v} C_{f_i}^{\beta_v} \|x_v\|^{-\alpha_v} \tag{6.1}$$

$$S_v^{\mathrm{UL}} = P_d h_{x_v} C_{f_i}^{\beta_v} \|x_v\|^{-\alpha_v}, \tag{6.2}$$

where h_{x_v} is the Rayleigh fading and is an exponentially distributed random variable with unit mean; $\|x_v\|$ is the distance from x_v to the origin. The frequency dependent path-loss associated to CC i is denoted as C_{f_i}, and β_v is the frequency dependent path-loss exponent associated to each cell type:

$$C_{f_i}^{\beta_v} = \left(\frac{\mu_i}{4\pi}\right)^{\beta_v}, \tag{6.3}$$

where μ_i corresponds to the wavelength of CC_i. For simplicity in the analysis, shadowing is ignored.

The motivation to consider different frequency path-loss exponents on each tier, is to capture the radio propagation changes in both cell types: frequency propagation in SCells is different to that of MCells. While MCells are placed above the landscapes, the SCells are placed within the landscape (i.e. trees, lampposts) and signals to and from them travel through the objects of the landscape. Work detailed in [114] has shown significant difference between MCell and SCell radio propagation, and stresses out that different radio frequency considerations must be taken in network planning and optimization. In addition to this, the 3GPP provides different channel models for each test environment in [115], where different values of β_v are considered in both urban macro and urban micro channel models for the non-line of sight case. Also, different values of α_v are considered, though in this case, the distance dependent path-loss exponents are much closer.

If $N(A)$ is denoted as the number of points that fall in the area A, the distribution of $N(A)$ is two-dimensional Poisson. The probability of having k nodes in A is:

$$P\left[N(A)=k\right]=\frac{1}{k!}\left(\lambda A\right)^{k}\exp\left(-\lambda A\right). \tag{6.4}$$

Let now denote $X_v \equiv \|x_v\|$ as the distance of the closest point from Φ_v to the origin, under these assumptions, the random variable X_v is Rayleigh distributed:

$$\begin{aligned} F_{X_v} &= \Pr\left(X_v \leq x\right) \\ &= 1-\Pr\left(X_v > x\right) \\ &= 1-\Pr\left(\text{No nodes in } \left(A=\pi x^2\right)\right) \\ &= 1-\Pr\left(N(A)=0\right) \\ &= 1-\exp\left(-\lambda A\right). \end{aligned} \tag{6.5}$$

And from here, the pdf and cdf of X_v is given by:

$$f_{X_v}(x) = 2\pi\lambda_v x e^{-\pi\lambda_v x^2}, x \geq 0 \tag{6.6}$$

$$F_{X_v}(x) = 1-e^{-\pi\lambda_v x^2}, x \geq 0. \tag{6.7}$$

The mobile user locations are placed according to the homogeneous PPP Φ_d, with intensity λ_d. Considering the uplink of LTE/LTE-A, intra-cell interference is null and so just inter-cell interferences are present. The model in this work follows the approach in [82]. Assuming a single dominant interference source per eNB, the number of interfering devices equals to the number of eNBs. Given this, only a fraction of all devices will cause any UL interference. Hence, a useful operation of point process can be applied. The *thinning* operation is used to randomly select a fraction of points from the original process with probability p, defined as the probability that a given device transmits: $p=\frac{N_{ms}-1}{Nd}$; where N_{ms} is the average number of eNBs (both MCells and SCells) and N_d is the average number of devices. The result of the thinning process yields a new poisson process denoted as Φ_{I_d} whose intensity is equal to $\lambda_{I_d}=p\lambda_d$.

The SINR of the typical device connected to an eNB located at $x_v \in \Phi_v$ is:

$$\gamma_v^{UL}=\frac{P_d h_{x_v} C_{f_i}^{\beta_v}\left\|x_v\right\|^{-\alpha_v}}{I_{x_v}+\sigma^2}, \tag{6.8}$$

where σ^2 is defined in chapter 3 and the total aggregate interference is expressed as $I_{x_v}=\sum_{x_j\in\Phi_{I_d}} P_d h_{x_j} C_{f_i}^{\beta_j}\left\|x_j\right\|^{-\alpha_j}$. Table 6.1 summarizes the mathematical notation of the system model.

Table 6.1: Mathematical notation

Parameter	Value
Φ_v	PPP process
λ	Intensity
P_v	Transmit power
CC_i	Frequency CC
α_v	Path-loss exponent
x_v	Position
$\|x_v\|$, X_v	Distance
S_v^{DL}	DL Received power
S_v^{UL}	UL Received power
C_{f_i}	Frequency dependent path-loss
β_v	Frequency dependent path-loss exponent
γ_v^{UL}	UL SINR
C_{x_v}	Capacity
σ^2	Noise power
I_{x_v}	Aggregate interference

6.3.2 Association Probability

The DL criteria of association is that the device connects to the eNB from which receives the highest average transmission power, given by 6.9. In the UL the UE associates to the eNB that receives highest average signal power as in 6.10:

$$\mathbb{E}_h\left[S_v^{\mathrm{DL}}\right] = \mathbb{E}_h\left[P_v h_{x_v} C_{f_i}^{\beta_v} \|x_v\|^{-\alpha_v}\right] = P_v C_{f_i}^{\beta_v} \|x_v\|^{-\alpha_v}, \tag{6.9}$$

$$\mathbb{E}_h\left[S_v^{\mathrm{UL}}\right] = \mathbb{E}_h\left[P_d h_{x_v} C_{f_i}^{\beta_v} \|x_v\|^{-\alpha_v}\right] = P_d C_{f_i}^{\beta_v} \|x_v\|^{-\alpha_v}. \tag{6.10}$$

Given this, the device is associated as follows:

$$\text{if } P_m C_{f_i}^{\beta_m} \|x_m\|^{-\alpha_m} > P_s C_{f_i}^{\beta_s} \|x_s\|^{-\alpha_s} \quad \text{to a Mcell in the DL in carrier } i, \tag{6.11}$$

$$\text{if } C_{f_i}^{\beta_m} \|x_m\|^{-\alpha_m} > C_{f_i}^{\beta_s} \|x_s\|^{-\alpha_S} \quad \text{to a Mcell in the UL in carrier } i. \tag{6.12}$$

For the PCD association the different cases identified are explained in the following sections. Note that for the BCD association case, results largely follow the ones presented in the prior art for single carrier DUDe studies [82, 83]. In BCD the received power in one carrier considered to decouple, and the event of decoupling just one CC is not considered.

Case 1: All carriers connected to the Macro eNB

Both the DL and the UL is served by the MCell in CC_{l} and CC_{h}. The joint probability that a device will associate with the MCell in both links and for all carriers is defined by the following events:

$$P_m C_{\mathrm{h}}^{\beta_m} \|x_m\|^{-\alpha_m} > P_s C_{\mathrm{h}}^{\beta_s} \|x_s\|^{-\alpha_s} \cap P_d C_{\mathrm{h}}^{\beta_m} \|x_m\|^{-\alpha_m} > P_d C_{\mathrm{h}}^{\beta_s} \|x_s\|^{-\alpha_s},$$
$$\|x_m\|^{-\alpha_m} > \frac{P_s}{P_m} \frac{C_{\mathrm{h}}^{\beta_s}}{C_{\mathrm{h}}^{\beta_m}} \|x_s\|^{-\alpha_s} \cap \|x_m\|^{-\alpha_m} > \frac{C_{\mathrm{h}}^{\beta_s}}{C_{\mathrm{h}}^{\beta_m}} \|x_s\|^{-\alpha_s}. \quad (6.13)$$

Similarly, for the lowest frequency CC:

$$P_m C_{\mathrm{l}}^{\beta_m} \|x_m\|^{-\alpha_m} > P_s C_{\mathrm{l}}^{\beta_s} \|x_s\|^{-\alpha_s} \cap P_d C_{\mathrm{l}}^{\beta_m} \|x_m\|^{-\alpha_m} > P_d C_{\mathrm{l}}^{\beta_s} \|x_s\|^{-\alpha_s},$$
$$\|x_m\|^{-\alpha_m} > \frac{P_s}{P_m} \frac{C_{\mathrm{l}}^{\beta_s}}{C_{\mathrm{l}}^{\beta_m}} \|x_s\|^{-\alpha_s} \cap \|x_m\|^{-\alpha_m} > \frac{C_{\mathrm{l}}^{\beta_s}}{C_{\mathrm{l}}^{\beta_m}} \|x_s\|^{-\alpha_s}. \quad (6.14)$$

The power of the SCell is significantly smaller that the transmit power of the MCell and hence, P_s/P_m is less than one. So, the events of this case are reduced to:

$$\|x_m\|^{-\alpha_m} > \frac{C_{\mathrm{l}}^{\beta_s}}{C_{\mathrm{l}}^{\beta_m}} \|x_s\|^{-\alpha_s} \cap \|x_m\|^{-\alpha_m} > \frac{C_{\mathrm{h}}^{\beta_s}}{C_{\mathrm{h}}^{\beta_m}} \|x_s\|^{-\alpha_s}. \quad (6.15)$$

Owing to frequency propagation conditions the received signal in the low frequency carrier is higher than the received signal in the high frequency component,

$$P_v C_{\mathrm{h}}^{\beta_v} \|x_v\|^{-\alpha_v} < P_v C_{\mathrm{l}}^{\beta_v} \|x_v\|^{-\alpha_v},$$
$$\|x_v\|^{-\alpha_v} < \frac{C_{\mathrm{l}}^{\beta_v}}{C_{\mathrm{h}}^{\beta_v}} \|x_v\|^{-\alpha_v}. \quad (6.16)$$

Given the expression in 6.16 and assuming $\beta_s > \beta_m$ it is inferred that $\frac{C_{\mathrm{l}}^{\beta_s}}{C_{\mathrm{l}}^{\beta_m}} > \frac{C_{\mathrm{h}}^{\beta_s}}{C_{\mathrm{h}}^{\beta_m}}$. The resulting joint probability reduces to satisfying the UL event of the lowest frequency CC:

$$\begin{aligned}
&\Pr(\text{case 1}) = \Pr\left(\|x_m\|^{-\alpha_m} > \frac{C_{\mathrm{l}}^{\beta_s}}{C_{\mathrm{l}}^{\beta_m}} \|x_s\|^{-\alpha_s}\right) \\
&= \Pr\left(X_s > \left(\frac{C_{\mathrm{l}}^{\beta_s}}{C_{\mathrm{l}}^{\beta_m}}\right)^{1/\alpha_s} X_m^{\alpha_m/\alpha_s}\right) \\
&\overset{(a)}{=} \int_0^\infty \left(1 - F_{X_s}\left(\left(\frac{C_{\mathrm{l}}^{\beta_s}}{C_{\mathrm{l}}^{\beta_m}}\right)^{2/\alpha_s} x_m^{\alpha_m/\alpha_s}\right)\right) f_{X_m}(x_m)\, \mathrm{d}x_m \\
&= \int_0^\infty e^{-\pi\lambda_s \left(\frac{C_{\mathrm{l}}^{\beta_s}}{C_{\mathrm{l}}^{\beta_m}}\right)^{2/\alpha_s} x_m^{2\alpha_m/\alpha_s}} 2\pi\lambda_m x_m e^{-\pi\lambda_m x_m^2}\, \mathrm{d}x_m. \quad (6.17)
\end{aligned}$$

where (a) is obtained by calculating the probability $\Pr(X_1 < X_2)$ where X_1 and X_2 are two random variables, the probability is calculated as:

$$\Pr(X_1 < X_2) = \int_0^\infty \Pr(X_1 < X_2 | X_1 = x) f_1(x) \mathrm{d}x \quad = \int_0^\infty (1 - F_2(x)) \, \mathrm{d}x. \tag{6.18}$$

If $\alpha_m = \alpha_s = \alpha_\mathrm{p}$ then the expression in 6.17 is simplified to:

$$\Pr(\text{case 1}) = \frac{\lambda_m}{\lambda_s \left(\frac{C_1^{\beta_s}}{C_1^{\beta_m}} \right)^{2/\alpha_\mathrm{p}} + \lambda_m}. \tag{6.19}$$

Note that in the above expression the denominator needs to be always positive. Moreover, for the special case in which $\alpha_m = 4$ and $\alpha_s = 2$:

$$\begin{aligned} \Pr(\text{case 1}) &= \int_0^\infty e^{-\pi \lambda_s \frac{C_1^{\beta_s}}{C_1^{\beta_m}} x_m^4} 2\pi \lambda_m x_m e^{-\pi \lambda_m x_m^2} \, \mathrm{d}x_m \\ &\overset{(a)}{=} \int_0^\infty \lambda_m e^{-\sqrt{\pi} \lambda_s \frac{C_1^{\beta_s}}{C_1^{\beta_m}} u^2} e^{-\lambda_m u} \mathrm{d}u \\ &= \lambda_m \sqrt{\frac{\pi}{b}} e^{\lambda_m^2 / 4b} \frac{1}{2} \mathrm{erfc}\left(\frac{\lambda_m / \sqrt{2b}}{\sqrt{2}} \right), \end{aligned} \tag{6.20}$$

where (a) results from the variable change $u^2 = \pi^2 x^2$, $b = \sqrt{\pi} \lambda_s \frac{C_1^{\beta_s}}{C_1^{\beta_m}}$. For other values of α_m and α_s the expression in 6.17 must be solved with numerical integration.

Case 2: DL connected to MCell and UL connected to SCell

This case corresponds to the UL and DL decoupling. When considering CCs with different coverage regions two different decoupling events can occur:

- Case 2.1: The lowest frequency is associated to the SCell in the UL, and the highest frequency remains associated to the MCell for both links, UL and DL. This case is depicted in figure 6.1(a).

- Case 2.2: All DL carriers are connected to the MCell and UL carriers are connected to the SCell, as shown in figure 6.1(b).

Given equation 6.16 and assuming $\beta_s > \beta_m$, for $P_v = P_d$ one UE can have a larger UL received power in the MCell for the highest frequency CC and a larger received power to the SCell for the lowest frequency carrier. **The joint UL/DL association**

probability for case 2.1 is defined by the following events:

$$P_m C_{\mathrm{h}}^{\beta_m} \|x_m\|^{-\alpha_m} > P_s C_{\mathrm{h}}^{\beta_s} \|x_s\|^{-\alpha_s} \cap P_d C_{\mathrm{h}}^{\beta_m} \|x_m\|^{-\alpha_m} > P_d C_{\mathrm{h}}^{\beta_s} \|x_s\|^{-\alpha_s},$$
$$\|x_m\|^{-\alpha_m} > \frac{P_s}{P_m} \frac{C_{\mathrm{h}}^{\beta_s}}{C_{\mathrm{h}}^{\beta_m}} \|x_s\|^{-\alpha_s} \cap \|x_m\|^{-\alpha_m} > \frac{C_{\mathrm{h}}^{\beta_s}}{C_{\mathrm{h}}^{\beta_m}} \|x_s\|^{-\alpha_s}. \quad (6.21)$$

Similarly, in the lowest frequency CC:

$$P_m C_{\mathrm{l}}^{\beta_m} \|x_m\|^{-\alpha_m} > P_s C_{\mathrm{l}}^{\beta_s} \|x_s\|^{-\alpha_s} \cap P_d C_{\mathrm{l}}^{\beta_m} \|x_m\|^{-\alpha_m} < P_d C_{\mathrm{l}}^{\beta_s} \|x_s\|^{-\alpha_s},$$
$$\|x_m\|^{-\alpha_m} > \frac{P_s}{P_m} \frac{C_{\mathrm{l}}^{\beta_s}}{C_{\mathrm{l}}^{\beta_m}} \|x_s\|^{-\alpha_s} \cap \|x_m\|^{-\alpha_m} < \frac{C_{\mathrm{l}}^{\beta_s}}{C_{\mathrm{l}}^{\beta_m}} \|x_s\|^{-\alpha_s}. \quad (6.22)$$

Given that $P_s/P_m < 1$ the events are reduced to:

$$\|x_m\|^{-\alpha_m} > \frac{C_{\mathrm{h}}^{\beta_s}}{C_{\mathrm{h}}^{\beta_m}} \|x_s\|^{-\alpha_s} \cap \frac{P_s}{P_m} \frac{C_{\mathrm{l}}^{\beta_s}}{C_{\mathrm{l}}^{\beta_m}} \|x_s\|^{-\alpha_s} < \|x_m\|^{-\alpha_m} < \frac{C_{\mathrm{l}}^{\beta_s}}{C_{\mathrm{l}}^{\beta_m}} \|x_s\|^{-\alpha_s}. \quad (6.23)$$

Assuming that $P_m >> P_s$:

$$\frac{C_{\mathrm{h}}^{\beta_s}}{C_{\mathrm{h}}^{\beta_m}} > \frac{P_s}{P_m} \frac{C_{\mathrm{l}}^{\beta_s}}{C_{\mathrm{l}}^{\beta_m}}. \quad (6.24)$$

The domain that satisfies both UL and DL conditions for CC_{l} and CC_{h} is:

$$\frac{C_{\mathrm{h}}^{\beta_s}}{C_{\mathrm{h}}^{\beta_m}} \|x_s\|^{-\alpha_s} < \|x_m\|^{-\alpha_m} \leq \frac{C_{\mathrm{l}}^{\beta_s}}{C_{\mathrm{l}}^{\beta_m}} \|x_s\|^{-\alpha_s}. \quad (6.25)$$

Given this, the joint association probability for this case is calculated as:

$$\Pr(\text{case 2.1}) = \Pr\left(\left(\frac{C_{\mathrm{l}}^{\beta_m}}{C_{\mathrm{l}}^{\beta_s}} \right)^{1/\alpha_m} X_s^{\alpha_s/\alpha_m} \leq X_m < \left(\frac{C_{\mathrm{h}}^{\beta_m}}{C_{\mathrm{h}}^{\beta_s}} \right)^{1/\alpha_m} X_s^{\alpha_s/\alpha_m} \right)$$
$$= \int_0^\infty 2\pi\lambda_s x_s e^{-\pi\lambda_m \left(\frac{C_{\mathrm{l}}^{\beta_m}}{C_{\mathrm{l}}^{\beta_s}} \right)^{2/\alpha_m} x_s^{2\alpha_s/\alpha_m}} e^{-\pi\lambda_s x_s^2} \mathrm{d}x_s$$
$$- \int_0^\infty 2\pi\lambda_s x_s e^{-\pi\lambda_m \left(\frac{C_{\mathrm{h}}^{\beta_m}}{C_{\mathrm{h}}^{\beta_s}} \right)^{2/\alpha_m} x_s^{2\alpha_s/\alpha_m}} e^{-\pi\lambda_s x_s^2} \mathrm{d}x_s. \quad (6.26)$$

If $\alpha_m = \alpha_s = \alpha_{\mathrm{p}}$ then the above expression simplifies to:

$$\Pr(\text{case 2.1}) = \frac{\lambda_s}{\lambda_m \left(\frac{C_{\mathrm{l}}^{\beta_m}}{C_{\mathrm{l}}^{\beta_s}} \right)^{2/\alpha_{\mathrm{p}}} + \lambda_s} - \frac{\lambda_s}{\lambda_m \left(\frac{C_{\mathrm{h}}^{\beta_m}}{C_{\mathrm{h}}^{\beta_s}} \right)^{2/\alpha_{\mathrm{p}}} + \lambda_s}. \quad (6.27)$$

For the special case in which $\alpha_m = 4$ and $\alpha_s = 2$:

$$\Pr\left(\text{case 2.1}\right) = 2\pi\lambda_s \left(\frac{1}{2b} - \frac{a_1 e^{a_1^2/4b}\sqrt{\pi}\text{erfc}\left(a_1/2\sqrt{b}\right)}{4b^{2/3}} \right) - 2\pi\lambda_s \left(\frac{1}{2b} - \frac{a_2 e^{a_2^2/4b}\sqrt{\pi}\text{erfc}\left(a_2/2\sqrt{b}\right)}{4b^{2/3}} \right), \tag{6.28}$$

where $a_1 = \pi\lambda_m \sqrt{\frac{C_{\text{l}}^{\beta_m}}{C_{\text{l}}^{\beta_s}}}$, $a_2 = \pi\lambda_m \sqrt{\frac{C_{\text{h}}^{\beta_m}}{C_{\text{h}}^{\beta_s}}}$, and $b = \pi\lambda_s$. For other values of α_m and α_s the expression in 6.26 must be solved with numerical integration.

The joint UL/DL probability for the association case 2.2 is defined by the following events. For the highest frequency CC:

$$P_m C_{\text{h}}^{\beta_m} \left\|x_m\right\|^{-\alpha_m} > P_s C_{\text{h}}^{\beta_s} \left\|x_s\right\|^{-\alpha_s} \cap P_d C_{\text{h}}^{\beta_m} \left\|x_m\right\|^{-\alpha_m} < P_d C_{\text{h}}^{\beta_s} \left\|x_s\right\|^{-\alpha_s},$$
$$\left\|x_m\right\|^{-\alpha_m} > \frac{P_s}{P_m} \frac{C_{\text{h}}^{\beta_s}}{C_{\text{h}}^{\beta_m}} \left\|x_s\right\|^{-\alpha_s} \cap \left\|x_m\right\|^{-\alpha_m} < \frac{C_{\text{h}}^{\beta_s}}{C_{\text{h}}^{\beta_m}} \left\|x_s\right\|^{-\alpha_s}. \tag{6.29}$$

For the lowest frequency CC:

$$P_m C_{\text{l}}^{\beta_m} \left\|x_m\right\|^{-\alpha_m} > P_s C_{\text{l}}^{\beta_s} \left\|x_s\right\|^{-\alpha_s} \cap P_d C_{\text{l}}^{\beta_m} \left\|x_m\right\|^{-\alpha_m} < P_d C_{\text{l}}^{\beta_s} \left\|x_s\right\|^{-\alpha_s},$$
$$\left\|x_m\right\|^{-\alpha_m} > \frac{P_s}{P_m} \frac{C_{\text{l}}^{\beta_s}}{C_{\text{l}}^{\beta_m}} \left\|x_s\right\|^{-\alpha_s} \cap \left\|x_m\right\|^{-\alpha_m} < \frac{C_{\text{l}}^{\beta_s}}{C_{\text{l}}^{\beta_m}} \left\|x_s\right\|^{-\alpha_s}. \tag{6.30}$$

Given that $C_l/C_h > 1$ and $\beta_s > \beta_m$, it is inferred that $\frac{C_{\text{h}}^{\beta_m}}{C_{\text{h}}^{\beta_s}} > \frac{C_{\text{l}}^{\beta_m}}{C_{\text{l}}^{\beta_s}}$. The joint probability reduces to satisfying the high frequency events.

The resulting probabilities are obtained following the same procedure than in 6.26. If $\alpha_m = \alpha_s = \alpha_{\text{p}}$ then the above expression simplifies to:

$$\Pr\left(\text{case 2.2}\right) = \frac{\lambda_s}{\lambda_m \left(\frac{C_{\text{h}}^{\beta_m}}{C_{\text{h}}^{\beta_s}}\right)^{2/\alpha_{\text{p}}} + \lambda_s} - \frac{\lambda_s}{\lambda_m \left(\frac{C_{\text{h}}^{\beta_m}}{C_{\text{h}}^{\beta_s}} \frac{P_m}{P_s}\right)^{2/\alpha_{\text{p}}} + \lambda_s}. \tag{6.31}$$

For the special case in which $\alpha_m = 4$ and $\alpha_s = 2$:

$$\Pr\left(\text{case 2.2}\right) = 2\pi\lambda_s \left(\frac{1}{2b} - \frac{a_1 e^{a_1^2/4b}\sqrt{\pi}\text{erfc}\left(a_1/2\sqrt{b}\right)}{4b^{2/3}} \right) - 2\pi\lambda_s \left(\frac{1}{2b} - \frac{a_2 e^{a_2^2/4b}\sqrt{\pi}\text{erfc}\left(a_2/2\sqrt{b}\right)}{4b^{2/3}} \right), \tag{6.32}$$

where $a_1 = \pi\lambda_m \sqrt{\frac{C_{\text{h}}^{\beta_m}}{C_{\text{h}}^{\beta_s}}}$, $a_2 = \pi\lambda_m \sqrt{\frac{C_{\text{h}}^{\beta_m}}{C_{\text{h}}^{\beta_s}} \frac{P_m}{P_s}}$, and $b = \pi\lambda_s$.

Case 3: DL connected to SCell and UL connected to MCell

The joint probability for associating the DL of any CC to the SCell and the UL to the MCell is satisfied by the following events. For the frequency CC_i:

$$P_m C_{f_i}^{\beta_m} \|x_m\|^{-\alpha_m} < P_s C_{f_i}^{\beta_s} \|x_s\|^{-\alpha_s} \cap P_d C_{f_i}^{\beta_m} \|x_m\|^{-\alpha_m} > P_d C_{f_i}^{\beta_s} \|x_s\|^{-\alpha},$$
$$C_{f_i}^{\beta_m} \|x_m\|^{-\alpha_m} < \frac{P_s}{P_m} C_{f_i}^{\beta_s} \|x_s\|^{-\alpha_s} \cap C_{f_i}^{\beta_m} \|x_m\|^{-\alpha_m} > C_{f_i}^{\beta_s} \|x_s\|^{-\alpha_s}. \quad (6.33)$$

There is no domain that satisfies both conditions, so the probability that a device selects the SCell in the DL and the MCell in the UL is zero.

Case 4: All carriers associated to the SCell

The joint probability that a device will associate to the SCell in both UL and DL and in all available carriers is defined by the following events. For CC_{h}:

$$P_m C_{\mathrm{h}}^{\beta_m} \|x_m\|^{-\alpha_m} < P_s C_{\mathrm{h}}^{\beta_s} \|x_s\|^{-\alpha_s} \cap P_d C_{\mathrm{h}}^{\beta_m} \|x_m\|^{-\alpha_m} < P_d C_{\mathrm{h}}^{\beta_s} \|x_s\|^{-\alpha_s},$$
$$\|x_s\|^{-\alpha_s} > \frac{P_m}{P_s} \frac{C_{\mathrm{h}}^{\beta_m}}{C_{\mathrm{h}}^{\beta_s}} \|x_m\|^{-\alpha_m} \cap \|x_s\|^{-\alpha_s} > \frac{C_{\mathrm{h}}^{\beta_m}}{C_{\mathrm{h}}^{\beta_s}} \|x_s\|^{-\alpha_m}. \quad (6.34)$$

For the lowest frequency CC:

$$P_m C_{\mathrm{l}}^{\beta_m} \|x_m\|^{-\alpha_m} < P_s C_{\mathrm{l}}^{\beta_s} \|x_s\|^{-\alpha_s} \cap P_d C_{\mathrm{l}}^{\beta_m} \|x_m\|^{-\alpha_m} < P_d C_{\mathrm{l}}^{\beta_s} \|x_s\|^{-\alpha_s},$$
$$\|x_s\|^{-\alpha_s} > \frac{P_m}{P_s} \frac{C_{\mathrm{l}}^{\beta_m}}{C_{\mathrm{l}}^{\beta_s}} \|x_m\|^{-\alpha_m} \cap \|x_s\|^{-\alpha_s} > \frac{C_{\mathrm{l}}^{\beta_m}}{C_{\mathrm{l}}^{\beta_s}} \|x_s\|^{-\alpha_m}. \quad (6.35)$$

Knowing that $P_m > P_s$, $C_l/C_h > 1$ and $\beta_s > \beta_m$, it is inferred that $\frac{C_{\mathrm{h}}^{\beta_m}}{C_{\mathrm{h}}^{\beta_s}} > \frac{C_{\mathrm{l}}^{\beta_m}}{C_{\mathrm{l}}^{\beta_s}}$. The joint probability reduces to satisfying the high frequency events.

The resulting probabilities are obtained following the same procedure than in 6.17. If $\alpha_m = \alpha_s = \alpha_{\mathrm{p}}$ then the above expression simplifies to:

$$\Pr(\text{case 4}) = \frac{\lambda_s}{\left(\lambda_m \left(\frac{P_m}{P_s} \frac{C_{\mathrm{h}}^{\beta_m}}{C_{\mathrm{h}}^{\beta_s}}\right)^{2/\alpha_{\mathrm{p}}} + \lambda_s\right)}. \quad (6.36)$$

For the special case in which $\alpha_m = 4$ and $\alpha_s = 2$:

$$\Pr(\text{case 4}) = 2\pi\lambda_s \left(\frac{1}{2b} - \frac{a e^{a^2/4b} \sqrt{\pi} \operatorname{erfc}\left(a/2\sqrt{b}\right)}{4b^{2/3}}\right), \quad (6.37)$$

where $a = \pi\lambda_m \sqrt{\frac{P_m}{P_s} \frac{C_{\mathrm{h}}^{\beta_m}}{C_{\mathrm{h}}^{\beta_s}}}$ and $b = \pi\lambda_s$.

6.3.3 Spectral Efficiency

Using the previously derived association regions, the distance distributions to the serving eNB in the UL are obtained. All association rules are conditioned to the probability of case 2.1 (full flexibility association from section 6.3.2). From the association probability derivation, the region that corresponds to this access case is:

$$\frac{C_{\mathrm{h}}^{\beta_s}}{C_{\mathrm{h}}^{\beta_m}} \left\|x_s\right\|^{-\alpha_s} < \left\|x_M\right\|^{-\alpha_m} \leq \frac{C_{\mathrm{l}}^{\beta_s}}{C_{\mathrm{l}}^{\beta_m}} \left\|x_s\right\|^{-\alpha_s}. \tag{6.38}$$

The distance to the serving eNB is $X_{v,2.1}$ where $v = m$ for CC_{h} and $v = s$ for CC_{l} in PCD; $v = s$ for both carriers in the suboptimal association case BCD and $v = m$ in the DLRP suboptimal association case; subscript 2.1 describes the conditioning on case 2.1. The complementary distribution function of $X_{s,2.1}$ is derived as:

$$\begin{aligned} F^{c}_{X_{s,2.1}}(x) &= \Pr\left(X_s > x \mid \frac{C_{\mathrm{h}}^{\beta_s}}{C_{\mathrm{h}}^{\beta_m}} \left\|x_s\right\|^{-\alpha_s} < \left\|x_M\right\|^{-\alpha_m} \leq \frac{C_{\mathrm{l}}^{\beta_s}}{C_{\mathrm{l}}^{\beta_m}} \left\|x_s\right\|^{-\alpha_s} \right) \\ &= \frac{\Pr\left(X_s > x; \frac{C_{\mathrm{l}}^{\beta_m\,\frac{1}{\alpha_m}}}{C_{\mathrm{l}}^{\beta_s}} X_s^{\frac{\alpha_s}{\alpha_m}} < X_m \leq \frac{C_{\mathrm{h}}^{\beta_m\,\frac{1}{\alpha_m}}}{C_{\mathrm{h}}^{\beta_s}} X_s^{\frac{\alpha_s}{\alpha_m}} \right)}{\Pr(\text{Case 2.1})} \\ &= \frac{\int_x^{\infty} \left(e^{-\pi\lambda_m \frac{C_{\mathrm{l}}^{\beta_m\,\frac{2}{\alpha_m}}}{C_{\mathrm{l}}^{\beta_s}} x_s^{\,2\frac{\alpha_s}{\alpha_m}}} - e^{-\pi\lambda_m \frac{C_{\mathrm{h}}^{\beta_m\,\frac{2}{\alpha_m}}}{C_{\mathrm{h}}^{\beta_s}} x_s^{\,2\frac{\alpha_s}{\alpha_m}}} \right) f_{X_s}(x)\mathrm{d}x}{\Pr(\text{Case 2.1})}, \end{aligned} \tag{6.39}$$

where $\Pr(\text{Case 2.1})$ simplified expression for the particular case where $\alpha_m = \alpha_s = \alpha_{\mathrm{p}}$ is defined in equation 6.27. By differentiating the cdf it is derived the pdf of the distance to the serving eNB in the low frequency CC:

$$f_{X_{s,2.1}}(x) = \frac{\left(e^{-\pi\lambda_m \frac{C_{\mathrm{l}}^{\beta_m\,\frac{2}{\alpha_m}}}{C_{\mathrm{l}}^{\beta_s}} x^{2\frac{\alpha_s}{\alpha_m}}} - e^{-\pi\lambda_m \frac{C_{\mathrm{h}}^{\beta_m\,\frac{2}{\alpha_m}}}{C_{\mathrm{h}}^{\beta_s}} x^{2\frac{\alpha_s}{\alpha_m}}} \right) f_{X_s}(x)}{\Pr(\text{Case 2.1})}. \tag{6.40}$$

Following the same procedure, the distribution of the distance to the MCell with optimal association in the high frequency CC is:

$$f_{X_{m,2.1}}(x) = \frac{\left(e^{-\pi\lambda_s \frac{C_{\mathrm{h}}^{\beta_s\,\frac{2}{\alpha_m}}}{C_{\mathrm{h}}^{\beta_m}} x^{2\frac{\alpha_s}{\alpha_m}}} - e^{-\pi\lambda_s \frac{C_{\mathrm{l}}^{\beta_s\,\frac{2}{\alpha_m}}}{C_{\mathrm{l}}^{\beta_m}} x^{2\frac{\alpha_s}{\alpha_m}}} \right) f_{X_m}(x)}{\Pr(\text{Case 2.1})}. \tag{6.41}$$

For the BCD association, the distance distribution is the same as in equation 6.40 for both carriers considering a suboptimal association in CC_{h}. In the DLRP association

the distance distribution for both carriers follows the one in equation 6.41.

These distance distributions are useful to derive the UE spectral efficiency. Also, with the aim of comparing the performance of the full flexibility solution, the spectral efficiency derivation is conditioned to the probability of case 2.1. To calculate the aggregated spectral efficiency experienced by a UE transmitting in more than one carrier, this simplifying hypothesis is used:

1. The total bandwidth is the sum of each individual carrier bandwidths

2. The total capacity is the sum of the individual capacities

Given this, the spectral efficiency with PCD is defined as:

$$\begin{aligned} C_{\mathrm{PCD}_{2.1}} &= C_{\mathrm{PCD}_{X_{m,2.1}}} + C_{\mathrm{PCD}_{X_{s,2.1}}} \\ &= \mathbb{E}\left[\log_2\left(1+\gamma_m^{UL}\right) + \log_2\left(1+\gamma_s^{UL}\right)\right]. \end{aligned} \tag{6.42}$$

For $T>0$, $\mathbb{E}[T] = \int_0^\infty \Pr(T>t)\mathrm{d}t$. Applying this property the spectral efficiency for one general case C_{x_v} can be expressed as:

$$\begin{aligned} C_{x_v} &= \frac{1}{\ln(2)} \int_0^\infty \Pr\left(\ln\left(1+\gamma_v^{UL}\right) > t\right) \mathrm{d}t \\ &= \frac{1}{\ln(2)} \int_0^\infty \Pr\left(\gamma_v^{UL} > e^t - 1\right) \mathrm{d}t \\ &= \frac{1}{\ln(2)} \int_0^\infty f_{X_v}(x) \int_0^\infty \Pr\left(\frac{P_d h_{x_v} C_{f_i}^{\beta_v} x_v^{-\alpha_v}}{I_x + \sigma^2} > e^t - 1\right) \mathrm{d}t\mathrm{d}x \\ &= \frac{1}{\ln(2)} \int_0^\infty f_{X_v}(x) \int_0^\infty \Pr\left(h_{x_v} > P_d^{-1} C_{f_i}^{-\beta_v} x_v^{\alpha_v}\left(I_x+\sigma^2\right)\left(e^t-1\right)\right) \mathrm{d}t\mathrm{d}x \\ &= \frac{1}{\ln(2)} \int_0^\infty f_{X_v}(x) \int_0^\infty \mathbb{E}\left[e^{-\frac{C_{f_i}^{-\beta_v} x_v^{\alpha_v}\left(I_x+\sigma^2\right)\left(e^t-1\right)}{P_d}}\right] \mathrm{d}t\mathrm{d}x \\ &= \frac{1}{\ln(2)} \int_0^\infty f_{X_v}(x) \int_0^\infty e^{-\frac{\sigma^2 C_{f_i}^{-\beta_v} x_v^{\alpha_v}\left(e^t-1\right)}{P_d}} L_{I_x}\left(\left(e^t-1\right) C_{f_i}^{-\beta_v} x_v^{\alpha}\right) \mathrm{d}t\mathrm{d}x. \end{aligned} \tag{6.43}$$

where $L_{I_x}\left(\left(e^t-1\right) C_{f_i}^{-\beta_v} x_v^{\alpha}\right)$ is the Laplace transform of the aggregated interference

calculated assuming $\alpha_m = \alpha_s = \alpha_{\mathrm{p}}$:

$$\begin{aligned} L_{I_x}\left((e^t-1)C_{f_i}^{-\beta_v}x_{\mathrm{p}}^{\alpha}\right) &= \mathbb{E}_{I_x}\left[e^{-(e^t-1)C_{f_i}^{-\beta_v}x_v^{\alpha_{\mathrm{p}}}I_x}\right] = \\ &= \mathbb{E}_{\Phi_{I_d}}\left[\prod_{x_j\in\Phi_{I_d}}\mathbb{E}_h\left[e^{-(e^t-1)x_v^{\alpha_{\mathrm{p}}}h_{x_j}x_j^{-\alpha_{\mathrm{p}}}}\right]\right] \\ &= \exp\left(-2\pi\lambda_{I_d}\int_0^{\infty}\left(1-\frac{1}{1+(e^t-1)x_v^{\alpha_{\mathrm{p}}}x_j^{-\alpha_{\mathrm{p}}}}\right)x_j\mathrm{d}x_j\right). \end{aligned} \tag{6.44}$$

applying the change $u = \left[(e^t-1)x_v^{\alpha_{\mathrm{p}}}\right]^{-\frac{2}{\alpha_{\mathrm{p}}}}x_j^2$:

$$L_{I_x}\left((e^t-1)C_{f_i}^{-\beta_v}x_{\mathrm{p}}^{\alpha}\right) = \exp\left(-\pi\lambda_{I_d}x^2\mathcal{K}\left(e^t-1,\alpha_{\mathrm{p}}\right)\right), \tag{6.45}$$

where $\mathcal{K}\left(e^t-1,\alpha_{\mathrm{p}}\right) = (e^t-1)^{2/\alpha_{\mathrm{p}}}\int_0^{\infty}\frac{1}{1+u^{\frac{\alpha_{\mathrm{p}}}{2}}}\mathrm{d}u$.

Capacity evaluation:

The capacity expressions are simplified for the special evaluation where $\alpha_{\mathrm{p}} = 4$. With the aim of clarifying the mathematical expressions $K = \frac{\log_2(e)}{\Pr(\text{Case 2.1})}$ in the rest of the chapter. For the optimal association in case 2.1:

$$\begin{aligned} C_{\mathrm{PCD}_{x_{m,2.1}}} = K\int_0^{\infty}&\left[e^{-\pi\lambda_s\frac{C_{\mathrm{h}}^{\beta_s}}{C_{\mathrm{h}}^{\beta_m}}^{\frac{2}{\alpha_{\mathrm{p}}}}x^2} - e^{-\pi\lambda_s\frac{C_{\mathrm{l}}^{\beta_s}}{C_{\mathrm{l}}^{\beta_m}}^{\frac{2}{\alpha_{\mathrm{p}}}}x^2}\right]e^{-\pi\lambda_m x^2} \\ &\int_0^{\infty}e^{-\frac{\sigma^2C_{\mathrm{h}}^{-\beta_m}x^{\alpha_{\mathrm{p}}}(e^t-1)}{P_d}}L_{I_x}\left((e^t-1)C_{\mathrm{h}}^{-\beta_m}x_{\mathrm{p}}^{\alpha}\right)\mathrm{d}t2\pi\lambda_m x\mathrm{d}x. \end{aligned} \tag{6.46}$$

For this particular evaluation $L_{I_x}\left((e^t-1)C_{\mathrm{h}}^{-\beta_m}x^4\right) = \exp\left(-\frac{\pi^2}{2}\lambda_{I_d}x^2\sqrt{e^t-1}\right)$. For simplicity in the expressions the following substitutions are carried out: $C'^2_{\mathrm{h}} = \frac{C_{\mathrm{h}}^{\beta_s}}{C_{\mathrm{h}}^{\beta_m}}^{\frac{2}{\alpha_{\mathrm{p}}}}$, $C'^2_{\mathrm{l}} = \frac{C_{\mathrm{l}}^{\beta_s}}{C_{\mathrm{l}}^{\beta_m}}^{\frac{2}{\alpha_{\mathrm{p}}}}$.

$$\begin{aligned} C_{\mathrm{PCD}_{x_{m,2.1}}} = K\int_0^{\infty}\int_0^{\infty}&\left[e^{-\pi\lambda_s C'^2_{\mathrm{h}}x^2} - e^{-\pi\lambda_s C'^2_{\mathrm{l}}x^2}\right]e^{-\pi\lambda_m x^2} \\ &e^{-\frac{\sigma^2C_{\mathrm{h}}^{-\beta_m}x^4(e^t-1)}{P_d}}e^{-\frac{\pi^2}{2}\lambda_{I_d}x^2\sqrt{e^t-1}}2\pi\lambda_m x\mathrm{d}x\mathrm{d}t. \end{aligned} \tag{6.47}$$

Applying the variable change $u = \pi x^2$ it is obtained an integral of the form:

$$I = \int_0^\infty e^{-ax} e^{-bx^2} \mathrm{d}x = \sqrt{\frac{\pi}{b}} e^{a^2/4b} Q\left(\frac{a}{\sqrt{2b}}\right), \tag{6.48}$$

where $Q(x) = \frac{1}{2\pi} \int_x^\infty e^{-y^2/2} \mathrm{d}y$. Given this:

$$C_{\mathrm{PCD}_{x_{m,2.1}}} = \lambda_m K \int_0^\infty \sqrt{\frac{\pi}{b(t)}} \left[e^{\frac{a_1(t)^2}{4b(t)}} Q\left(\frac{a_1(t)}{\sqrt{2b(t)}}\right) - e^{\frac{a_2(t)^2}{4b(t)}} Q\left(\frac{a_2(t)}{\sqrt{2b(t)}}\right) \right] \mathrm{d}t, \tag{6.49}$$

where $a_1(t) = \lambda_s C'^2_{\mathrm{h}} + \lambda_m + \frac{\pi}{2}\lambda_{I_d}\sqrt{(e^t - 1)}$, $a_2(t) = \lambda_s C'^2_{\mathrm{l}} + \lambda_m + \frac{\pi}{2}\lambda_{I_d}\sqrt{(e^t - 1)}$, and $b(t) = \frac{\sigma^2 C_{\mathrm{h}}^{-\beta_m}\left(e^t - 1\right)}{P_d \pi}$.

Following the same procedure for the spectral efficiency in the low frequency carrier the expression is simplified to:

$$C_{\mathrm{PCD}_{x_{s,2.1}}} = \lambda_s K \int_0^\infty \sqrt{\frac{\pi}{b(t)}} \left[e^{\frac{a_1(t)^2}{4b(t)}} Q\left(\frac{a_1(t)}{\sqrt{2b(t)}}\right) - e^{\frac{a_2(t)^2}{4b(t)}} Q\left(\frac{a_2(t)}{\sqrt{2b(t)}}\right) \right] \mathrm{d}t, \tag{6.50}$$

where $a_1(t) = \lambda_m C'^{-2}_{\mathrm{l}} + \lambda_s + \frac{\pi}{2}\lambda_{I_d}\sqrt{(e^t - 1)}$, $a_2(t) = \lambda_m C'^{-2}_{\mathrm{h}} + \lambda_s + \frac{\pi}{2}\lambda_{I_d}\sqrt{(e^t - 1)}$ and $b(t) = \frac{\sigma^2 C_{\mathrm{l}}^{-\beta_s}\left(e^t - 1\right)}{P_d \pi}$.

In the BCD case CC_{l} has the exact same distance distribution as in PCD so: $C_{\mathrm{BCD}_{\mathrm{l}x_{s,2.1}}} = C_{\mathrm{PCD}_{x_{s,2.1}}}$. The CC_{h} capacity is calculated as follows:

$$C_{\mathrm{BCD}_{\mathrm{h}x_{s,2.1}}} = \lambda_s K \int_0^\infty \sqrt{\frac{\pi}{b(t)}} \left[e^{\frac{a_1(t)^2}{4b(t)}} Q\left(\frac{a_1(t)}{\sqrt{2b(t)}}\right) - e^{\frac{a_2(t)^2}{4b(t)}} Q\left(\frac{a_2(t)}{\sqrt{2b(t)}}\right) \right] \mathrm{d}t, \tag{6.51}$$

where $a_1(t) = \lambda_m C'^{-2}_{\mathrm{l}} + \lambda_s + \frac{\pi}{2}\lambda_{I_d}\sqrt{(e^t - 1)}$, $a_2(t) = \lambda_m C'^{-2}_{\mathrm{h}} + \lambda_s + \frac{\pi}{2}\lambda_{I_d}\sqrt{(e^t - 1)}$ and $b(t) = \frac{\sigma^2 C_{\mathrm{h}}^{-\beta_s}\left(e^t - 1\right)}{P_d \pi}$.

For the suboptimal association case DLRP, the capacity in CC_{h} equals the one in the PCD being in both cases connected to the MCell: $C_{\mathrm{DLRP}_{\mathrm{h}x_{m,2.1}}} = C_{\mathrm{PCD}_{x_{m,2.1}}}$. On the other hand, the CC_{l} capacity is given by:

$$C_{\mathrm{DLRP}_{\mathrm{l}x_{m,2.1}}} = \lambda_m K \int_0^\infty \sqrt{\frac{\pi}{b(t)}} \left[e^{\frac{a_1(t)^2}{4b(t)}} Q\left(\frac{a_1(t)}{\sqrt{2b(t)}}\right) - e^{\frac{a_2(t)^2}{4b(t)}} Q\left(\frac{a_2(t)}{\sqrt{2b(t)}}\right) \right] \mathrm{d}t, \tag{6.52}$$

where $a_1(t) = \lambda_s C'^2_{\mathrm{h}} + \lambda_m + \frac{\pi}{2}\lambda_{I_d}\sqrt{(e^t-1)}$, $a_2(t) = \lambda_s C'^2_{\mathrm{l}} + \lambda_m + \frac{\pi}{2}\lambda_{I_d}\sqrt{(e^t-1)}$ and $b(t) = \frac{\sigma^2 C_{\mathrm{l}}^{-\beta_m}\left(e^t-1\right)}{P_d \pi}$.

Capacity evaluation:

This evaluation only considers the Signal to Interference Ratio (SIR) on each carrier. Therefore, $\alpha = 4$ and $\sigma^2 = 0$:

$$C_{\mathrm{PCD}_{x_{m,2.1}}} = \lambda_m K \int_0^\infty \frac{1}{\frac{\pi}{2}\lambda_{I_d}\sqrt{e^t-1} + \lambda_s C'^2_{\mathrm{h}} + \lambda_m} \tag{6.53}$$

$$- \frac{1}{\frac{\pi}{2}\lambda_{I_d}\sqrt{e^t-1} + \lambda_s C'^2_{\mathrm{l}} + \lambda_m}\mathrm{d}x, \tag{6.54}$$

$$C_{\mathrm{PCD}_{x_{s,2.1}}} = \lambda_s K \int_0^\infty \frac{1}{\frac{\pi}{2}\lambda_{I_d}\sqrt{e^t-1} + \lambda_m C'^{-2}_{\mathrm{l}} + \lambda_s} \tag{6.55}$$

$$- \frac{1}{\frac{\pi}{2}\lambda_{I_d}\sqrt{e^t-1} + \lambda_m C'^{-2}_{h} + \lambda_s}\mathrm{d}x. \tag{6.56}$$

The capacity in the suboptimal association with BCD is $C_{\mathrm{BCD}_{\mathrm{l}x_{s,2.1}}}, C_{\mathrm{BCD}_{\mathrm{h}x_{s,2.1}}}$. The derivation is the same as in $C_{\mathrm{PCD}_{x_{s,2.1}}}$, given that the distance distribution to the SCell is equal. With BCD association both high and low frequency carriers have the same spectral efficiency given that the Laplace transform of the aggregate interference, derived in 6.45, has no dependency with the frequency dependent path-loss. The same argument is applied for the DLRP case.

Capacity evaluation:

This evaluation only considers the noise power on each carrier, $\alpha = 2$, $\sigma^2 \neq 0$ and $I_{x_v} = 0$:

$$C_{\mathrm{PCD}_{x_{m,2.1}}} = \lambda_m K \int_0^\infty \frac{1}{\frac{\sigma^2 C_{\mathrm{h}}^{-\beta_m}(e^t-1)}{P_d} + \pi\left(\lambda_s C'^2_{\mathrm{h}} + \lambda_m\right)} \tag{6.57}$$

$$- \frac{1}{\frac{\sigma^2 C_{\mathrm{h}}^{-\beta_m}(e^t-1)}{P_d} + \pi\left(\lambda_s C'^2_{\mathrm{l}} + \lambda_m\right)}\mathrm{d}x, \tag{6.58}$$

$$C_{\mathrm{PCD}_{x_s,2.1}} = \lambda_s K \int_0^\infty \frac{1}{\frac{\sigma^2 C_{\mathrm{l}}^{-\beta_s}(e^t-1)}{P_d} + \pi\left(\lambda_m C'^{-2}_{\mathrm{l}} + \lambda_s\right)} \tag{6.59}$$

$$- \frac{1}{\frac{\sigma^2 C_{\mathrm{l}}^{-\beta_s}(e^t-1)}{P_d} + \pi\left(\lambda_m C'^{-2}_{h} + \lambda_s\right)} \mathrm{d}x. \tag{6.60}$$

The CC_{h} spectral efficiency simplified expression for the BCD association is:

$$C_{\mathrm{BCD}_{\mathrm{h}}x_{s,2.1}} = \lambda_s K \int_0^\infty \frac{1}{\frac{\sigma^2 C_{\mathrm{l}}^{-\beta_s}(e^t-1)}{P_d} + \pi\left(\lambda_m C'^{-2}_{\mathrm{l}} + \lambda_s\right)} \tag{6.61}$$

$$- \frac{1}{\frac{\sigma^2 C_{\mathrm{h}}^{-\beta_s}(e^t-1)}{P_d} + \pi\left(\lambda_m C'^{-2}_{\mathrm{h}} + \lambda_s\right)} \mathrm{d}x. \tag{6.62}$$

As for the DLRP association, the low frequency carrier simplified expression is:

$$C_{\mathrm{DLRP}_{\mathrm{h}}x_{m,2.1}} = \lambda_m K \int_0^\infty \frac{1}{\frac{\sigma^2 C_{\mathrm{l}}^{-\beta_m}(e^t-1)}{P_d} + \pi\left(\lambda_s C'^{2}_{\mathrm{h}} + \lambda_m\right)} \tag{6.63}$$

$$- \frac{1}{\frac{\sigma^2 C_{\mathrm{l}}^{-\beta_m}(e^t-1)}{P_d} + \pi\left(\lambda_s C'^{2}_{\mathrm{l}} + \lambda_m\right)} \mathrm{d}x. \tag{6.64}$$

6.3.4 Outage Probability

The outage probability is defined as the probability that the instantaneous SINR of a randomly located UE is less than the target SINR. The outage calculation follows a similar derivation to the spectral efficiency one in section 6.3.3:

$$\begin{aligned} O_{X_{v,2.1}} &= \mathbb{E}\left[\gamma_v^{UL} < \tau\right] \\ &= 1 - \int_0^\infty \Pr\left(\gamma_v^{UL} > \tau\right) f_{X_v}(x)\mathrm{d}x \\ &= 1 - \int_0^\infty \Pr\left(\frac{P_d h_{x_v} C_{f_i}^{\beta_v} x_v^{-\alpha_v}}{I_x + \sigma^2} > \tau\right) f_{X_v}(x)\mathrm{d}x, \end{aligned} \tag{6.65}$$

where $f_{X_v}(x)$ is the distance distribution to the serving cell. The probability is expressed as:

$$\Pr\left(\gamma_v^{UL} > \tau\right) = \int_0^\infty e^{-\frac{\sigma^2 C_{f_i}^{-\beta_v} x_v^{\alpha_v} \tau}{P_d}} L_{I_x}\left(\tau C_{f_i}^{-\beta_v} x_v^{\alpha}\right) f_{X_v}(x)\mathrm{d}x. \tag{6.66}$$

Given this, the resulting outage probability is expressed as:

$$O_{X_{v,2.1}} = 1 - \int_0^{\infty} e^{-\frac{\sigma^2 C_{f_i}^{-\beta_v} x_v^{\alpha_v} \tau}{P_d}} L_{I_x}\left(\tau C_{f_i}^{-\beta_v} x_v^{\alpha}\right) f_{X_v}(x)\mathrm{d}x. \tag{6.67}$$

6.4 Numerical Results

Results for the association probabilities, spectral efficiency and outage are provided. All three association processes are compared to each other and the analysis provided in the previous section is validated by numerical results and a PPP based Matlab Monte-Carlo simulation. Table 6.2 summarizes the parameters configuration.

6.4.1 Association Probability

Following the derivations in section 6.3.2, figure 6.2 depicts the analytical and the simulated results for the association probability. In the figure, the line corresponds to the simulated result and the bullets are the probabilities obtained analytically. Recall that the different cases represent:

- Case 1: No decoupling. All CCs are connected to the MCell.
- Case 2: Decoupling
  - Case 2.1: Frequency dependent decoupling. Low CC decoupled, UL in SCell and DL in MCell. High CC not decoupled, UL and DL in MCell.
  - Case 2.2: Full decoupling. No matter the carrier, UL in SCell and DL in MCell
- Case 4: No decoupling. All CCs in SCell.

Table 6.2: Parameters configuration

Parameter	Value
P_m	43 dBm
P_s	20 dBm
P_d	23 dBm
λ_m	5 MCells/A
λ_d	10^4 UEs/A
Scenario layout	100 m x 100 m
Simulation iterations	10000

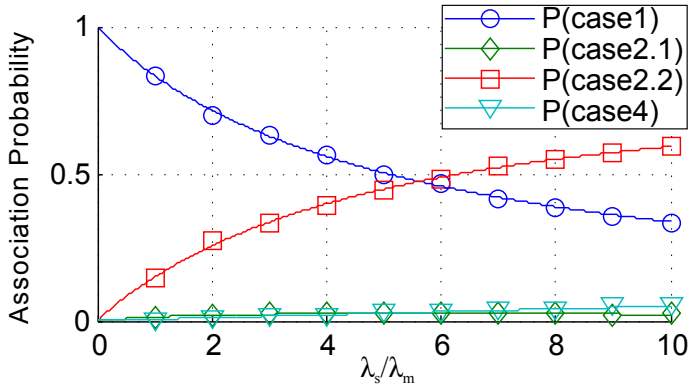

Figure 6.2: Association probability with PCD. Inter-band CA [2, 2.6] GHz, $\alpha_m = \alpha_s = 3$, $\beta_m = 2$, $\beta_s = 2.55$

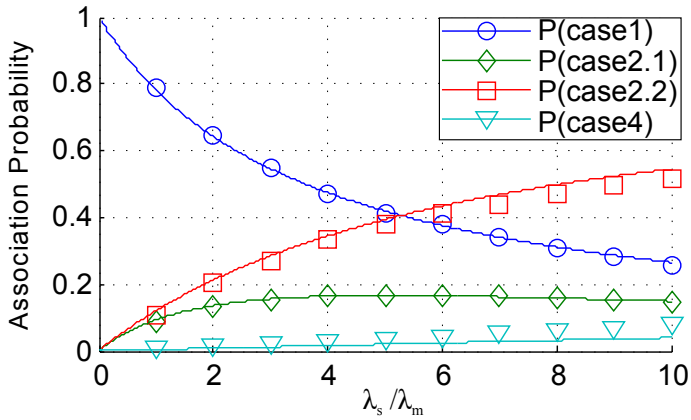

Figure 6.3: Association probability with PCD. Inter-band CA [800 MHz 5 GHz], $\alpha_m = \alpha_s = 3$, $\beta_m = 2$, $\beta_s = 2.55$

Results are very much aligned with the ones obtained in the literature for single carrier DUDe: as the density of the SCells increases the probability of decoupling one or both UL carriers is higher. However, note that per-carrier decoupling is very unlikely. This is because both frequency carriers are very close in band, so propagation losses are very similar. Figure 6.3 shows the case in which CCs are in very separated bands and then, it is remarkable the change in the association probabilities and in particular the per-carrier decoupling. The low frequency coverage grows, while the high frequency coverage shrinks, therefore the probability of each carrier having different optimal serving cells increases. This is an important observation given the disjoint pieces of spectrum that operators usually have in very different bands and the new for spectrum aggregation.

However, not only the frequency carrier affects the frequency dependent path-loss, it is also affected by β_v, the frequency dependent path-loss exponent. Based on the

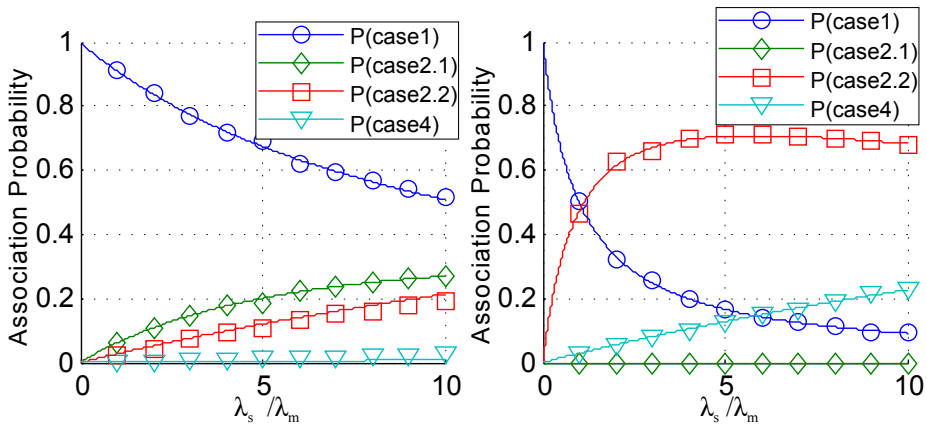

(a) $\beta_m = 2$, $\beta_s = 3$ (b) $\beta_m = \beta_s = 2$

Figure 6.4: Association probability with PCD. Inter-band CA [800 MHz 5 GHz], β_v impact $\alpha_m = \alpha_s = 3$

3GPP models it is assumed that $\beta_m < \beta_s$. Figure 6.4(a) shows the association when $\beta_s = 3$. When the propagation conditions in the SCell are deteriorated because of the increase of the frequency dependent path-loss exponent, the probability of having only the lowest frequency decoupled increases (case 2.1), and it overpasses the probability of having both carriers decoupled. To have both UL carriers connected to the SCell, case 2.2, the events on the high frequency CC must be satisfied, according to the analysis in section 6.3.2. Therefore, if the SCell provides a higher source of loss (owing to the rise of β_s) less UEs will decouple both carriers. Instead they will remain connected to the MCell, as it is the optimal option in terms of UL received power. On the other hand, if both cells provide the same frequency dependent path-loss because $\beta_m = \beta_s$, the probability of frequency dependent decoupling is nonexistent, as shown in figure 6.4(b). In this situation both frequency dependent path-loss components are equal generating the same coverage footprint, thus, when one CC is decoupled the other is also. In this sense, there are no events that satisfy the probability of case 2.1.

6.4.2 Distance distribution to serving cell

Figure 6.5 shows the distance distribution to the serving cell derived in section 6.3.3. The distribution is conditioned to the probability of case 2.1. To satisfy that the received power in the low frequency accomplishes $S_s^{\mathrm{UL}} > S_m^{\mathrm{UL}}$, the typical device must be closer to the SCell than to the MCell. This way, the distance dependent path-loss can overcome the frequency dependent path-loss gain with respect to the MCell, given that $C_{\mathrm{h}}^{\beta_m} > C_{\mathrm{h}}^{\beta_s}$ because $\beta_m < \beta_s$. This is also noted in figure 6.6(a), where $C_{\mathrm{h}}^{\beta_m} >> C_{\mathrm{h}}^{\beta_s}$ because β_s is higher. The distance distribution to the SCell is narrower as the difference in frequency path-loss exponent increases, which means

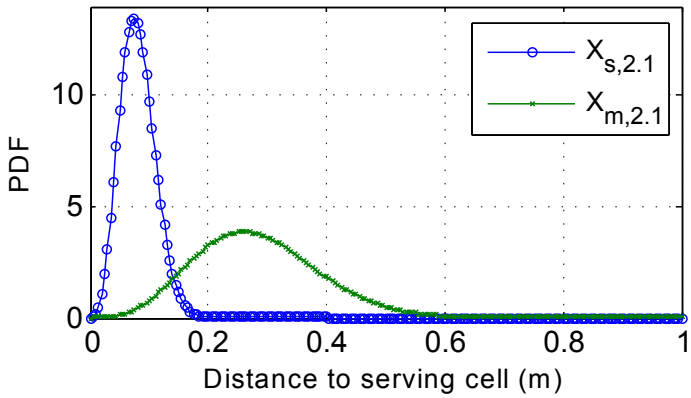

Figure 6.5: Distance distribution to serving cell. Inter-band CA, two CC [800 MHz 2.6 GHz], $\alpha_m = \alpha_s = 4$, $\beta_m = 2$, $\beta_s = 2.55$, $\lambda_s/\lambda_m = 5$

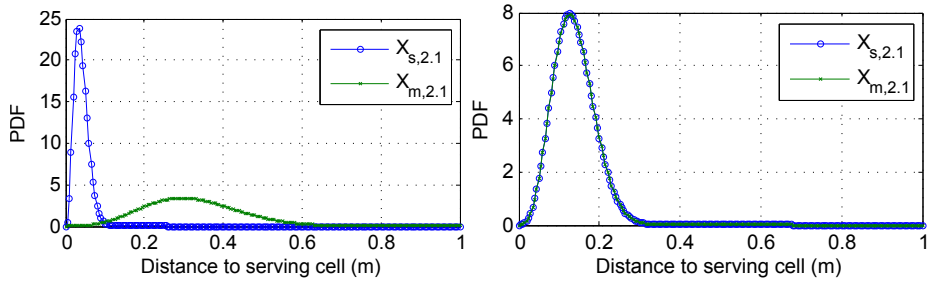

(a) $\beta_m = 2$, $\beta_s = 3$ (b) $\beta_m \approx \beta_s$

Figure 6.6: Distance distribution to serving cell. Inter-band CA, two CC [800 MHz 5 GHz], β_v impact, $\alpha_m = \alpha_s = 3$

that, as the difference in β_s and β_m is higher, the UE has to be nearer the SCell to satisfy case 2.1 events. On the contrary, when $\beta_m \approx \beta_s$ both cells share roughly the same coverage. Given this, the distance distribution that satisfies the events in case 2.1 is equal, as shown in figure 6.6(b).

6.4.3 Spectral Efficiency and Outage Probability

First, results for the suboptimal association rule with DLRP are compared with the PCD association case. Owing to the different propagation conditions, because $\beta_m \neq \beta_s$, the path-loss experienced CC_h is lower to the MCell and the path-loss perceived in CC_l is lower to the SCell. In this regard, in CC_l, the suboptimal association following DLRP would be to the MCell. Based on the distance distribution to both cells for case 2.1, immediate gains can be inferred when decoupling, because the UE transmits to the cell which is the nearest. Figure 6.7(a) compares the path-loss of the typical device to the associated cell in CC_l for both strategies. The linear

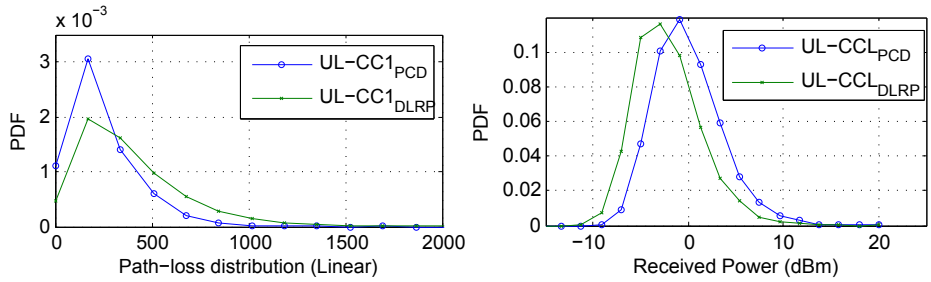

(a) Path-loss distribution to serving cell

(b) Received power at serving cell

Figure 6.7: Path-loss and Received power, PCD vs DLRP. Inter-band CA [800 MHz 5 GHz], $\alpha_m = \alpha_s = 2$, $\beta_m = 2$, $\beta_s = 2.55$, $\lambda_s/\lambda_m = 5$

path-loss distribution is represented to better observe the difference between both cases. The suboptimal association provides a much poorer connection, essentially because the distance dependent path-loss is much lower towards the SCell than to the MCell. As a result the overall path-loss to the SCell is lower though the frequency dependent one is higher (because $\beta_s > \beta_m$). All this is translated into a higher received power compared to the suboptimal association, as shown in figure 6.7(b). Note that in both cases, path-loss and received power, the absolute values correspond to very short distances to the serving cell, given the high density and the small scenario layout. However, it is particularly interesting to observe the difference between both distributions. Note also that the area of simulation does not affect the statistics of the final results, but a small area lets simulations last shorter.

Figure 6.8 compares the UL achieved throughput with PCD association and the suboptimal DLRP association for a range of SCell densities. Each marker represented in the curve is the resulting throughput with each association rule, and goes from a less to a more dense network ($\lambda_s = \lambda_m$, $\lambda_s = 30\lambda_m$). UL throughput is calculated by multiplying the spectral efficiency derived in section 6.3.3 by B/N_a, where B is the carrier bandwidth and N_a corresponds to the average number of associated users. Recall that the spectral efficiency and hence the achieved throughput is conditioned to the probability of case 2.1. There is a constant, almost linear, improvement when decoupling. This is given by two main reasons: improvement in distance dependent path-loss and also lower congestion in the SCell. Significant gains in outage can also be noted, as shown in figure 6.9.

Full flexibility is understood as the possibility of decoupling the UL carriers separately. The PCD association is compared to the BCD one, in which both carriers are decoupled to the SCell based on the low frequency CC. As shown in figure 6.5, the distance distribution in case 2.1 is lower to the SCell. However, because of the frequency dependent path-loss difference between both cells, the overall resulting path-loss to the MCell is lower for the high frequency CC (shown in figure 6.10(a)), and hence, the received power in the MCell is higher with PCD association than with BCD association, as depicted in figure 6.10(b). This increase in received power brings improvement to the SNR. Figure 6.11 shows the gain in UL throughput for

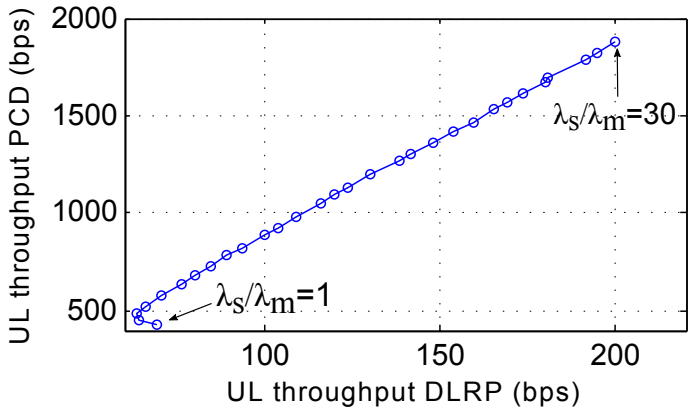

Figure 6.8: Analytical UL Throughput, PCD vs DLRP. Inter-band CA [800 MHz 5 GHz] $B_{CC} = 20\,\text{MHz}$, $\alpha_m = \alpha_s = 4$, $\beta_m = 2$, $\beta_s = 2.55$

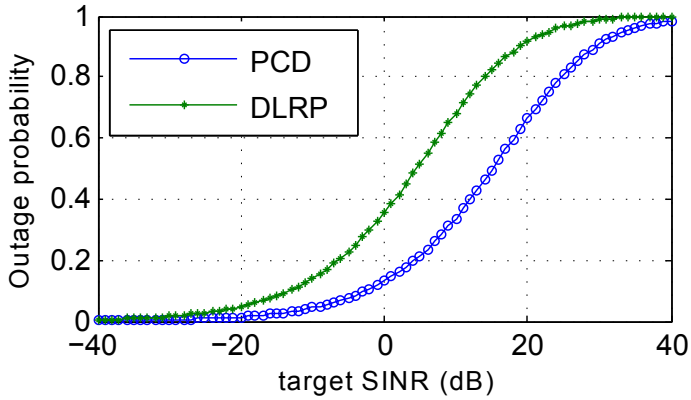

Figure 6.9: Analytical Outage, PCD vs DLRP. Inter-band CA [800 MHz 5 GHz], $\alpha_m = \alpha_s = 4$, $\beta_m = 2$, $\beta_s = 2.55$, $\lambda_s/\lambda_m = 5$

the analytical special case derived in 6.3.3, where only noise power is considered, $\sigma^2 \neq 0$ and $I_{x_v} = 0$. Again, each marker represented in the curve corresponds to the gain obtained in throughput for one particular SCell density; λ_s varies from λ_m to $30\,\lambda_m$. Small gains are brought when associating the high frequency to the MCell, this is because although $C_{\text{h}}^{\beta_m} > C_{\text{h}}^{\beta_s}$ the distance to the serving cell $X_m > X_s$.

Results in terms of UL throughput and outage for the special case derived in 6.3.3 considering an interference limited case are shown in figures 6.12(a) and 6.12(b), respectively. According to the definition of the SINR in equation 6.8, the average SIR can be simplified as in equation 6.68:

$$SIR_{\text{UL}} = \frac{\|x_v\|^{-\alpha_v}}{\sum\limits_{x_j \in \Phi_{I_d}} \|x_j\|^{-\alpha_v}}. \tag{6.68}$$

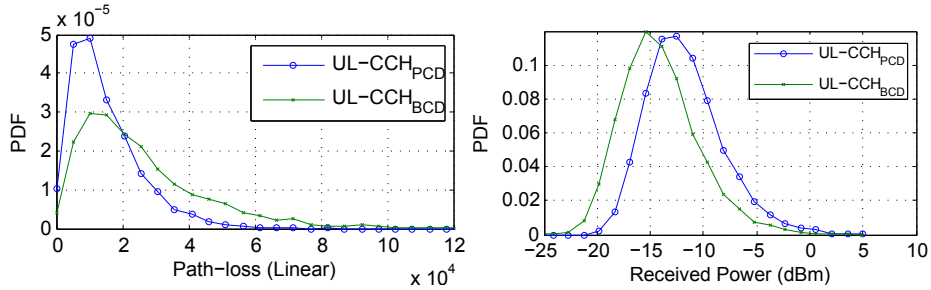

(a) Path-loss distribution to serving cell

(b) Received power at serving cell

Figure 6.10: Path-loss and Received power, PCD vs BCD. Inter-band CA [800 MHz 5 GHz], $\alpha_m = \alpha_s = 2$, $\beta_m = 2$, $\beta_s = 2.55$, $\lambda_s/\lambda_m = 5$

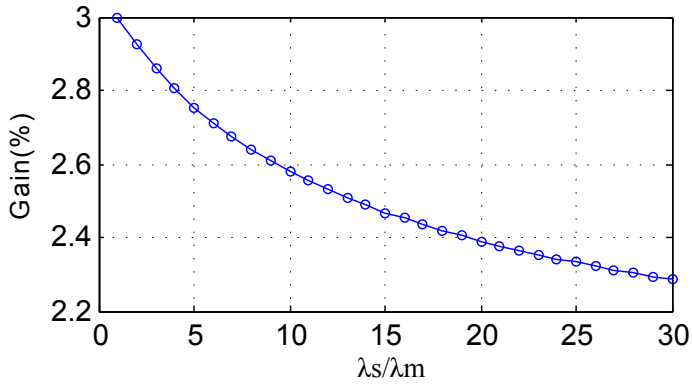

Figure 6.11: Gain in UL Throughput, PCD vs BCD. Inter-band CA [800 MHz 5 GHz], $B_{CC} = 20\,MHz$, $\alpha_m = \alpha_s = 2$, $\beta_m = 2$, $\beta_s = 2.55$

Given that $\sigma^2 << I_{x_v}$ then, $\gamma_v^{\mathrm{UL}} \approx SIR_{\mathrm{UL}}$. When the aggregate interference experienced on each cell is considered, I_{x_v}, the BCD association obtains higher throughput levels against the PCD association, despite the higher UL power received in the MCell. Even though BCD association is supposed to be suboptimal in path-loss terms, it results better in terms of SIR. Given equation 6.68, and under the assumption of equal P_d, the SIR basically depends on the distance distribution to the associated cell, which also depends on $C_{f_i}^{\beta_v}$ (frequency dependent path-loss) of both cells when conditioned to case 2.1; it also depends on the distance distribution of the interferers. Statistically, the distance distribution of the interferers to the desired cell (MCell or SCell) is equal, and it does not depend on the type. Given the the discussion done in previous paragraphs about the distance distribution (see section 6.4.2), when $\beta_m < \beta_s$ the SIR is always higher in the SCell than in the MCell for case 2.1. According to this, in terms of throughput gains it is better to decouple all carriers to the SCell when the distance to it is smaller and the low frequency carrier received power is higher. Providing full flexibility and associating in terms of path-loss minimizes the SIR regarding its dependence with the distance distribution and also because of the small gain in received power.

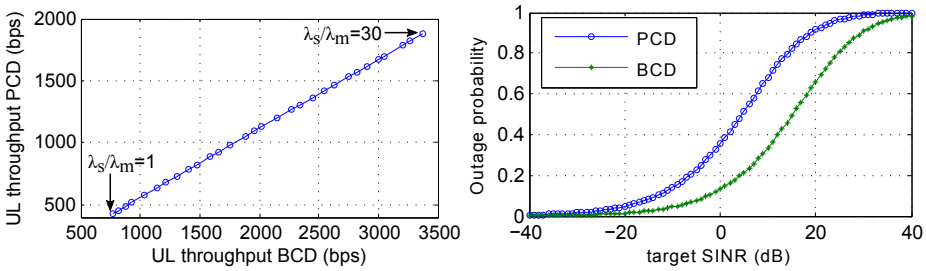

(a) Analytical UL Throughput

(b) Analytical Outage. $\lambda_s/\lambda_m = 5$

Figure 6.12: Analytical UL Throughput, PCD vs BCD. Inter-band CA [800 MHz 5 GHz], $B_{CC} = 20\,MHz$, $\alpha_m = \alpha_s = 4$, $\beta_m = 2$, $\beta_s = 2.55$

6.5 System level simulations and Discussions

The proposed model of UL decoupling with CA is verified in a realistic scenario. The same association rules previously analysed with stochastic geometry are tested in a dynamic system level simulator that considers a realistic HetNet. Performance results are discussed and compared in the following paragraphs.

6.5.1 Simulation setup

The scenario considered in this evaluation largely follows the MCell-only one described in appendix A, however, SCells are randomly placed along the simulation area; specific information about the scenario layout can be consulted in section A.2 of appendix A. As for the simulation conditions, a fixed number of UEs are uniformly distributed along the network, and each UE associates to the eNB following the three studied rules: DLRP, BCD and PCD. An inter-band CA environment is considered, and given the results provided in the previous section, two largely separated frequencies are considered. With the aim of not jeopardizing the power limited UEs, CC selection algorithm described in chapter 4 is applied, thus, non-CA UEs are also considered. Power control considerations for the HetNet scenario are different, given the higher interference. In this sense, the adjustment of power control parameters largely follows the work in [84], and it is equal in all cells. Specific simulation parameters are expanded in table 6.3. Note that different SRS bandwidths are considered, in particular for the DLRP association strategy, a moderate value of sounded bandwidth is necessary given the higher load of cells and the maximum number of UEs allowed to be multiplexed in sounding transmissions.

6.5.2 Simulation results

Figure 6.13 shows the association probability for different inter-band CA configurations, the first case (plotted in figure 6.13(a)) has a lower frequency separation

Table 6.3: DUDe: Simulation scenario assumptions

Parameter	Value
Bandwidth	2 x 80 PRBs
Carrier Frequency	800 MHz and 2.6 GHz
SRS BW DLRP	8 PRBs
SRS BW DUDe	16 PRBs
Number of UEs served	10
Number of UEs connected	1000
PRBs allocated	2 clusters of 4 PRBs x CC
Simulation time	15 kTTI
$\alpha_s = \alpha_m$	3
β_s	2.55
β_m	2
λ_s/λ_m	5

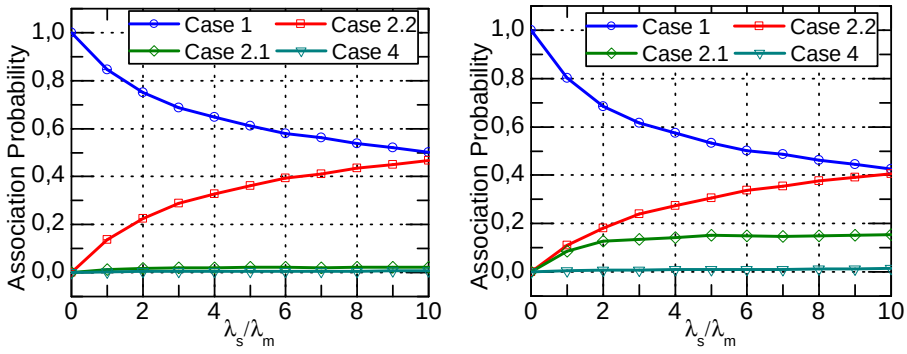

(a) Inter-band CA 2 GHz 2.6 GHz

(b) Inter-band CA 800 MHz 5 GHz

Figure 6.13: Association probabilities for different frequency separation $B_{CC} = 20\,MHz$, $\alpha_m = \alpha_s = 3$, $\beta_m = 2$, $\beta_s = 2.55$, $\lambda_s/\lambda_m = 5$

than the second, figure 6.13(b). These figures show the final association following the PCD rule for different SCells densities. Same trends as in the analytical results can be confirmed for the probability. When comparing the performance changes due to more separated frequencies, case 1 drops up to 8% with respect to the case in which both frequency carriers are close to each other. This is because of the increase in case 2.1, where the user decouples the low CC to the SCell given the improvement in path-loss, up to 13%. The same happens in case 2.2, where a reduction of 3% to 7% in the association probability occurs when increasing the frequency separation. Nearly the same drop can be observed in the analytical results previously discussed.

The influence of the frequency dependent path-loss exponent on the association

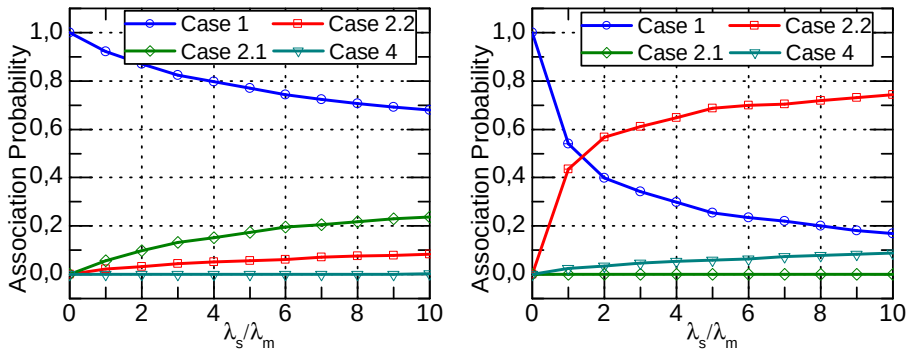

(a) $\beta_m = 2$, $\beta_s = 3$ (b) $\beta_m = \beta_s = 2$

Figure 6.14: Association probabilities, $beta_v$ impact, $\alpha_m = \alpha_s = 3$

probability also follows very similar trends, as shown in 6.14. With the increase of β_s, users are less likely to decouple given that path-loss towards the SCell increases, so case 1 probability is higher than any decoupling event. When $\beta_m = \beta_s$, the probability of case 2.1 is again zero, given that there are no propagation differences between both cells, and when one carrier has better coverage to the SCell the other CC does as well.

It is interesting to recognise the difference in the absolute values of the probabilities. In all the network configurations presented, the case 1 association probability is higher when compared to the mathematical analysis. This is because the system level simulator considers realistic antennas for both type of cells. The MCells have more directive antennas given its tri-sectorial deployment, which provide larger gains than the omnidirectional ones used in the SCells. The antenna gain and pattern has an evident impact on the user received power, which is also translated into a change in the association probability. None the less, it is worth stressing that the association trend is equal despite the difference in scenario layout and antenna considerations.

The distance to the serving cell distributions conditioned to case 2.1 are shown in figure 6.15 for different β configurations. In the realistic simulation, the distributions for different values of frequency dependent path-loss exponent, shown in figure 6.15(a), follow the same trend as in the analytical results shown in section 6.4.2. The distance to the MCell is larger than the distance to the SCell; again, the rationale behind this is that to achieve the events in case 2.1 the distance dependent path-loss has to overcome the difference in frequency dependent path-loss. However, in figure 6.15(b) where close values of β are considered, the distribution is different from the mathematical analysis. Because of the already mentioned antenna gain impact, having the same received power in both SCell and MCell allows to have higher distances to the MCell, given that the antenna compensates the distance loss. In fact, introducing the effect of the antenna gain into the equations is not complicated and would add an extra gain of realism to the analysis.

Cell association determines which eNB is serving the UE, when the eNB is closer

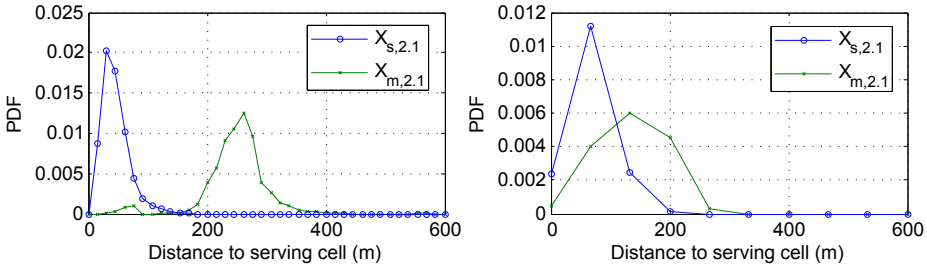

(a) $\beta_m = 2$, $\beta_s = 2.55$ (b) $\beta_m \approx \beta_s$

Figure 6.15: Simulated distance distributions, $\alpha_m = \alpha_s = 3$

Table 6.4: Percentage of UEs transmitting in CA

Strategy	CA Users
DLRP	48.7%
BCD	72.7% dBm
PCD	72.4% dBm

to the UE means that less power is needed to transmit data in a given piece of bandwidth. Results presented in previous chapters have shown that, to assure a correct performance of the aggregated bandwidth transmissions, it is crucial to account for the UE maximum transmit power. In MCell-only deployments, cell edge UEs are less likely to transmit in CA, however in heterogeneous deployments, the distance to the eNB is shorter given the higher cell density. In such a context, if UEs are associated based on the DL RSRP, the UL CA transmission is going to be restricted. Table 6.4 shows the percentage of UEs that are allowed to transmit in CA given their power limitations. In the PCD case, the full flexibility case is also accounted for. Both decoupling strategies are more lax in adopting aggregated transmissions; in the main, this is owed to the improvement in UL power availability brought by decoupled associations. This is an important observation, since CA is intended to be applied in both UL and DL, and with traditional DLRP association rules, the UL is seriously impaired. As seen in previous chapters, the inclusion of CA in the UL allows to improve the UE data rate performance and also the energy efficiency.

The throughput results of all the association rules is shown in figure 6.16. In this case, performance is not conditioned to case 2.1, and results considering all UEs are provided. There is a high improvement in the entire cdf for both decoupling strategies BCD and PDC. Decoupling the UL increases the scheduling opportunity of UEs because the load is better shared among cells, if less UEs compete to access the scheduler, then the buffer can be emptied faster, resulting in an improved data rate. Also, as shown in table 6.4, a minimum path-loss association policy increases

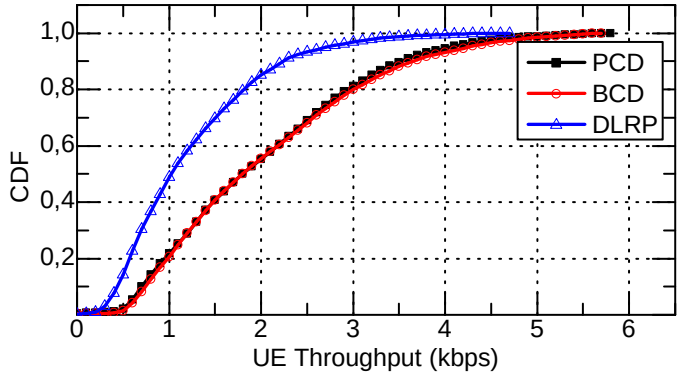

Figure 6.16: cdf of UE throughput distribution for PDC, BCD and DLRP association strategies

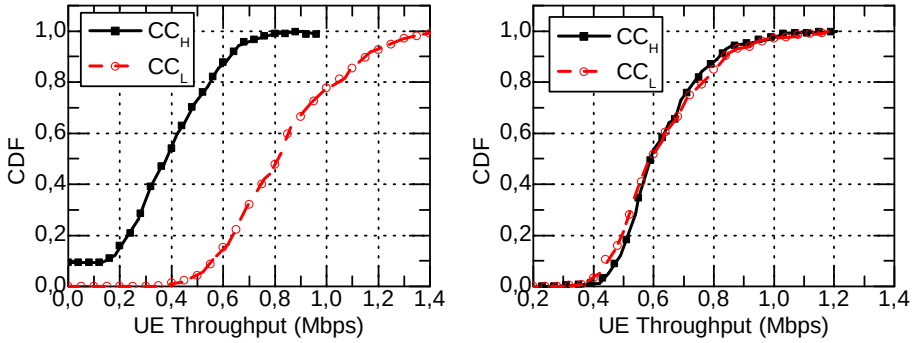

(a) Throughput in both carriers for PCD association rule

(b) Throughput in both carriers for BCD association rule

Figure 6.17: cdf of UE throughput distribution for PDC and BCD association strategies

the number of UEs that are eligible of transmitting in CA, which also allows to further improve the data rate of those UEs that are deprived of it with the DLRP association rule.

Given the low probability of having a case 2.1 event with PCD association in the studied scenario, less than 10%, the impact of PCD with respect to BCD is hardly represented. With the aim of evaluating the performance of BCD and PCD, the data rate of each carrier is analysed separately, figure 6.17. The high load condition of the MCell implies a straightforward throughput reduction in PCD for the highest frequency CC. The scheduling opportunity reduces when connected to the MCell given the higher load, and the loss in throughput overcomes the gains of being connected to the cell that offers less path-loss.

In the realistic simulation, the SIR difference in both PCD and BCD is not as abrupt as in the mathematical analysis. There are many other aspects in the signal

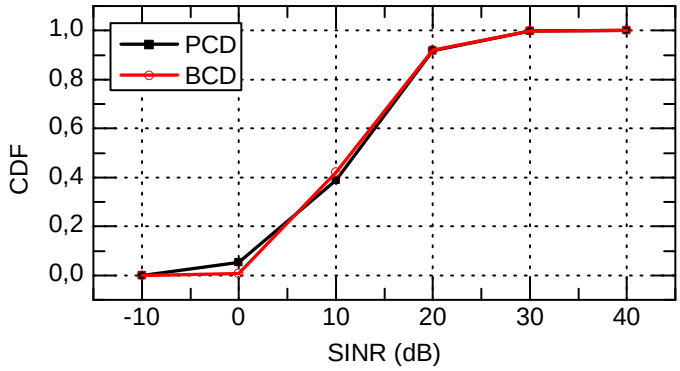

Figure 6.18: cdf of SINR for PDC and BCD association strategies

transmission that affect the SIR, but in the main, the power control formula, that automatically adjusts the UE transmit power. In this sense, the exclusive dependency of the SIR with the UE distance distribution is no longer kept, and the distribution in both association rules is much closer, as shown in figure 6.18.

6.6 Conclusions

This chapter has gone one step further in improving the UL with CA by studying its performance in a new system deployment as it is the HetNet. In this new paradigm of system design, low power eNBs are overlaid with high power MCells and interesting challenges are opened to assure the correct functioning of the entire system. Traditional eNB selection strategies are based on the DL RSRP, however in a HetNet setting, where the different nodes radiate with significant power differences, the DL selection may not be the optimal for the UL transmissions. Thus, an UL/DL imbalance problem arises. With the aim of improving the UL communications in a CA context it has been proposed to include DUDe association rules in co-channel HetNets using intra-band CA. In particular, maximum flexibility in carrier association is allowed introducing the use of inter-site CA. By adopting DUDe, it is assured that the UE is always associated to the eNB that receives the highest power. Based on the 3GPP path-loss models, the frequency propagation losses in both SCells and MCells are different; SCells present a worse behaviour of losses with frequency than MCells. In this sense, there is a certain likelihood that one UE has better coverage to the SCell in the low frequency carrier and to the MCell in the high frequency carrier. In the following, the evaluations provided and its conclusions are detailed:

- Mathematical analysis with stochastic geometry modelling. Performances in terms of association probabilities, capacity and outage have been derived, for the minimum path-loss association, PCD, and two suboptimal association strategies BCD and DLRP.
- Numerical results that validate the mathematical analysis and also a stochastic

geometry simulation is provided to compare the theoretical performance. The conclusions of this evaluation can be summarized as:

1. The association probability strongly depends on the path-loss. In this sense, a change in the frequency separation or the frequency dependent path-loss exponent can alter the performance results. Trends are maintained, and even with high frequency separation, as the eNB density increases UEs are more likely to decouple at least one of the CCs.
2. The distance distribution conditioned to the inter-site CA shows that UEs that decouple the lowest frequency carrier have a higher probability to be placed near a SCell. This provides a lower distance dependent path-loss, and therefore a higher received power in the eNB. When the difference in coverage between both tiers is smaller, the distance distribution is equal to both cells. If both cells have the same frequency propagation loss, the probability of a PCD (termed as case 2.1) event is non-existent, given that the difference in received power is mainly ruled by the distance.
3. The UL throughput performance with decoupled associations strongly improves the performance with respect to DLRP rules, which stems from the load sharing among cells and also from the higher received power at the eNB side. However, when BCD and PCD association rules are compared in terms of throughput, it results more profitable to decouple both carriers than to allow full flexibility. The SIR mainly depends on the UE distance distribution to the serving eNB, and this is proven to be statistically smaller to the SCell in the full flexibility event (case 2.1). In this sense, associating based on minimum path-loss or maximum received power is not always beneficial in inter-band CA scenarios, where strong differences in frequencies generate differences in coverage footprints.

- System level simulations that consider imperfect CSI, a CC selection strategy and scheduling. These results complement the mathematical analysis with a realistic point of view. Conclusions regarding this evaluation are:

  1. The association probabilities and distance distributions have some dependency with the antenna gain, which impacts directly the received power. However, despite the difference in absolute values, general trends are equal in the realistic simulation than in the analytical evaluation.
  2. The DLRP association is detrimental for the UL CA performance. Based on the results obtained, there is a higher probability of transmitting in aggregated carriers when decoupling events are allowed.
  3. In the BCD association case, higher throughput is served when compared to PCD. SCells are less loaded than the MCells, therefore, even though in PCD the UE is associated to the cell that receives the highest power, the scheduling opportunity is lower, resulting in a lower average throughput in the carrier connected to the MCell.

Chapter 7

Conclusions and Future Works

Data centric UEs are currently not only demanding more capacity from wireless networks, but also service oriented QoS and comparable QoE in both DL and UL. With the introduction of internet of things, machine to machine communications, cloud services and the widely-used social media, UEs and devices in general are increasingly more content generators than they were before. As a consequence, the new generations of mobile communications must devise strategies that improve the experience in the data uploading. With the aim of improving spectral efficiency, attending to high bandwidth demands and improving the spectrum usage, LTE-A introduces CA, a new technique that allows to transmit in separated pieces of spectrum, even in different bands.

The use of CA in the UL enables a broad range of new RRM design options, and several open challenges are detected to assure its correct implementation. **This PhD dissertation has pursued the objective of designing original CA strategies so that RRM procedures in the UL can positively contribute to the enhancement of the UE experience.** To this end, research opportunities and open challenges have been identified through the study of the state of the art, and consequently, new methods, strategies for implementation and guidelines have been proposed from a system level point of view. The current research has contributed to the evaluation of the practicality of CA in the UE side, with solid arguments and realistic considerations. To achieve this, the research carried out is supported by system level simulations in the main and mathematical modeling and analysis with the use of stochastic geometry.

Power considerations and resource management procedures based on power capabilities

Power control mechanisms in LTE-A introduce specific rules to control the UE power and improve the system performance by adding a novel capability: the FPC. To avoid high power transmissions in the cell edge, UEs compensate only a fraction of their path-loss generating less interference. In the main, power issues in the UL constitute the most serious constraint for allowing increased bandwidth transmissions, which essentially relies on the UE power availability. To allow CA and non-contiguous allocations in the UL, changes in the access technology must be carried out which lead to increased PAPR in transmissions. To contain the out of band emissions, a spectrum mask is recommended. In this sense, non-contiguous transmissions imply a reduction of the maximum power, thus, adding further challenges to the UE power capabilities.

The research presented in this dissertation started by investigating the power control method proposed for the UL. Two parameters are of utmost importance when designing the OLPC performance, the fractional path-loss compensation factor and the SINR control level. The study of the impact of both parameters revealed that fairness, cell average throughput and transmit power are constantly compromised. Each combination of both parameters constitute an operation point, and with the aim of evaluating the differences that may arise given the evaluation environment, two very different scenarios are tested: a synthetic deployment and a realistic one. No rule of thumb can be proposed for the parameters adjustment, given that the OLPC turns to be very dependent on the environment and layout deployment. So, a case by case evaluation is recommended to make the most of the FPC feature.

The research thereupon focuses specifically on the implementation of CA in the UL context, where power capabilities of the UEs constitute the most limiting constraint. Prior work addressing CA issues is observed to be centred in the DL rather than in the UL, and works that do focus in the UL hardly consider cell edge UEs as capable of transmitting in aggregated carriers. It is noted that UEs are most likely to be power limited when situated in the cell edge, however, depriving them from CA may result in a loss of gain in terms of user and cell throughput. Thus, two resource allocation mechanisms are proposed that introduce individual assessments of improvements or deteriorations brought by non-contiguous transmissions. First, a novel JCS strategy that considers MPR information opportunistically in the scheduling decisions is designed; it quantifies the gains or losses brought by non-contiguous allocations, and selects the configuration that results in higher throughput. Second, a CC selection process addressed for ICS schemes that considers the UE power limitations when assessing the UE CA eligibility; it accounts for the frequency selective gain brought by flexible allocations in wider bandwidths. Both proposed strategies require a previous knowledge of the UE channel state, and to provide this information sounding reference signals are considered.

The performance of multi-cluster allocations has been analysed for different transmit bandwidths and ISDs. It is observed that the potential gains of multi-cluster transmissions are strongly related to the power demanded, which essentially

depends on the bandwidth allocations and UE path-loss. In this sense, the proposed JCS solution reacts to the lack of power and dynamically allocates resources in a contiguous or non-contiguous manner, assuring always the highest performance. It is worth stressing that the permissiveness of opportunistic non-contiguous transmissions in the cell edge results in significant data rate improvements. This throughput increase stems from the increased bandwidth and also from the frequency diversity gain introduced by scheduling flexibility.

The proposed JCS strategy has to deal with increased assessments, since every TTI the entire scheduling process needs to be reevaluated. In this manner, it is proposed to select UEs at an RRC level and perform ICS, each UE is selected for CA based on a CC selection condition that allows for an increased power demand introduced by an acceptance margin. This margin is fundamentally considered bearing in mind that CA transmissions bring an intrinsic frequency diversity gain. A simple mathematical model based on the throughput gains makes possible a theoretical derivation of such acceptance margin. This novel proposal provides significant gains in terms of cell-edge improvement; again, allowing power limited UEs to transmit in aggregated carriers contributes with performance gains, and no impairment has been observed in the average UE throughput.

The CA feasibility study in the UL is completed with a detailed comparison between aggregated and single carrier transmissions. The focus of this study has been to evaluate this new feature in terms of energy efficiency, throughput and fairness. Results show that CA improves the energy efficiency of the UE because more bits per unit of energy are sent when higher bandwidth allocations take place, communications can finish faster and less allocations are required. Based on the different performance analysis carried out, the following conclusions can be summarized:

- Despite the higher probability of power limitation, cell edge UEs are as eligible as cell centre UEs for CA transmissions.
- To assure no loss is provided by aggregated transmissions, the RRM procedures of scheduling and CC selection must consider the UE PHRs and CQIs, to be obtained from SRSs.
- CA not only provides higher throughput performance, but also improves the energy efficiency of UEs. With moderate bandwidth transmissions, assuring that the PSD remains maximum, CA allows for faster communications and higher bit/power efficiency.
- The reliability of the CSI available in the eNB is of paramount importance when deciding the CA eligibility.

On the improvement of CSI acquisition

The results of the first study suggested that the performance of the RRM strategies strongly depends on a good knowledge of the UE channel conditions. This information

is sent by the UE in the form of reference signals (SRSs) and it is used by the eNB to perform opportunistic scheduling and also helping link adaptation. It has been argued that high bandwidth soundings may provide wrong channel measurements because of the increased power demands to cover the entire system bandwidth; thus, small bandwidth soundings are preferred, which becomes challenging in CA scenarios where the available bandwidth is increased. The impact of several variables that affect the CQI acquisition has been studied, and the following challenges are observed when facing UL channel measurement:

- Sounding delay, which is influenced by numerous variables. A short delay is desired to better capture the channel information, however the selected sounding bandwidth, the number of UEs sharing the spectrum and the system bandwidth directly impact the delay.
- Interference variability is very high in UL because allocations change in every scheduling opportunity. Scheduling decisions alter the interferer position in a TTI basis.
- The total number of UEs connected to the cell and the RU directly affect over the generation of interference. A higher number of UEs increases the variability due to the larger probability of having different interference sources; a higher RU particularly affects the aggregate interference generated.

To address this UL problem the use of prediction techniques is proposed; by employing past sounding signals, scheduling decisions and link adaptation are based on future predictions of the signal to be. An in depth study of the most relevant prediction techniques is carried out, mainly contemplating those that the literature has yet proposed to address problems of the same nature. The UL presents mainly two constraints to this problem: the difficulty to estimate error measurements, given the rapid SINR variability, and the contiguous time formulation, where the predicted CQI may be needed by the scheduler on any TTI. The prediction strategy that better suits the UL problem and its constraints is the mathematical pice-wise interpolation method, known as splines.

The proposed solution is tested under different number of active connections and RU conditions. It is observed that the performance of the spline extrapolation method in the absence of interference outperforms the CSI with acquisition just based on the last reported SRS. When realistic interferences are considered, very poor performance of both splines and SRSs are obtained, this motivates the inclusion of IC techniques that suppresses one or more interference sources. In this sense, an evaluation of the number of sources required to improve the SRS performance is carried out. It is observed that under diverse interference conditions the cancellation required is different: the more variant the interference map is, the more interference sources must be suppressed. An important observation noted in this study is that no matter how many interference sources are cancelled that the performance with SRS-only is hardly improved when it arrives to its upper bound limit, which is basically similar to the performance results obtained under no interference conditions. This upper bound limit recognised with the SRS CQI acquisition process is very

much related to the sounding delay. As the delay increases there is less room for improvement with prediction techniques, even in the absence of interference, which mainly stems from the poor information provided by the SRS itself. Essentially, it is verified that large delays in measurement impair the CSI as much as strong interference variations.

With the aim of specifically addressing the sounding delay issue, it is proposed to introduce well-known ICIC techniques in the sounding process with a twofold advantage: shorten the available bandwidth and control the interference. Two ICIC strategies are tested and compared, SFR and FFR. Both provide less sounding delay, but FFR provides a shorter available bandwidth and a reduced delay than SFR. Again, the strategy proposed is tested in different interference conditions, in particular diverse values of RU and number of active connections. SFR provides the highest performance in terms of SINR misalignment reduction and consequently BLER improvements; the FFR scheme allows very reduced number of UEs in the ICIC band, which also reduces the occurrences of the set of UEs placed in the cell edge. It is observed that under less interference variability the benefits brought by the delay reduction are more prominent. When the scheduling is more competitive to access (i.e low RU) the cell edge UEs have lower probability of being scheduled than with higher RU, therefore, it is observed that for low RU the FFR solution performs closer to the baseline solution. The SFR solution adds flexibility to the scheduling process which is a result of the higher number of cell edge UEs allowed to be scheduled. This flexibility allows to exploit better the interference management solution without jeopardizing the cell edge performance by limiting their access to the scheduler. In this sense, SFR solutions are preferred, since improve the system performance allowing both BLER and throughput enhancements.

As a general conclusion of this study, it is important to address the efforts in improving the interference management in the UL to provide more reliable CSI. However, it is also important to provide shorter sounding delays to those UEs whose channel variations are below the maximum MCS. With lower delays and a better interference management CSI can be improved and the performance of RRM algorithms can be maximized.

One step forward in UL improvement with new system designs

As a final objective of research, this dissertation studies the UL CA performance performance under a HetNet deployment. Networks composed out of different cell types are gaining popularity lately, and it is well-known that it is one of the operators choice to improve the QoE of UEs along the MCell coverage. By adding SCells, coverage holes can be better covered and also, load balancing can be provided. The research community and standardization bodies are designing the new trends of what the new generation 5G will be. In particular, to further improve the UE performance in SCells the idea of dual connectivity has been already introduced in Release 12, which allows more than one eNB to simultaneously serve one UE. With this, several new design options arise, and specially attractive options for CA; in a dual connectivity framework where eNBs have access to more than one CC,

coordinated RRM can be carried out in the UL, where the different CCs may be managed by more than one eNB simultaneously.

The UL/DL imbalance problem may be one of the most important limitations of UL transmissions in HetNets. Cell selection based on DLRP impairs the UL performance provided that the best cell selected may not be the optimal one in the UL. Thus, with the aim of maximizing the UL and not jeopardizing the DL, it is proposed to introduce the DUDe association rule in HetNets transmitting in inter-band CA. The evaluation of this new system design is done with stochastic geometry, and system level simulations are provided to support the conclusions drawn. Three association rules are studied: PCD, BCD and DLRP. It is verified that both decoupling solutions improve the average and cell edge UE performance, an important observation is that with DLRP the probability of accessing to CA is reduced when compared to DUDe. This is, in the main, owing to the shorter path-loss to the eNB selected. In MCell-only deployments DLRP association or minimum path-loss association is not an issue, when all cells transmit the same power level, the selected one is always going to be the nearest one. In this sense, to capitalize the gains brought by CA, is essential that UEs transmit to the closest eNB (radio-electrically speaking) where power limitations are less likely. A study comparing the two DUDe solutions is conducted, the full flexibility strategy, PCD, that allows for inter-site CA, is compared to BCD, where both carriers are decoupled when the lowest frequency carrier has smaller path-loss to the SCell. Intuitively, staying connected to the cell that offers lower propagation losses provides the highest performance. However, not only propagation conditions are determinant on the system performance. In the mathematical analysis it is shown that a better UL performance is obtained in terms of SIR with BCD; in this sense, remaining connected to the nearest cell rather than the one that offers better propagation conditions is the solution that provides better performance. In the system level simulations, the SIR is not only dependent on the distance distribution, given that OLPC rules the received power in the eNB. Moreover, the scheduling opportunity of UEs with both carriers connected to the SCell is higher, because MCells are most likely to be overloaded. It is worth mentioning that the mathematical model and the system level simulations have very close trends in the performance results. In general, the assumptions that have been proved to have an impact are the path-loss models, mainly affected by the antenna radiation pattern.

Future research lines

CA was first standardized in Release 10 and, since then, it has been one of the most attractive LTE-A features. As explained in the introduction of this dissertation, CA constitutes one of the most transversal features to improve spectral efficiency and system performance. Given this, new releases (12 and beyond) are continuously adopting CA in the new innovative features and study items. The new dual connectivity concept has enabled several design options and further research can be conducted in:

- Devise strategies to reduce interferences and increase system performance in the context of HetNets.
- Centralised backhaul architectures where multi-site CA can improve mobility across the MCell. Items such as coordination, multiple timing advance, fronthaul capacity limitations are of special interest.
- Carrier selection in the context of fronthaul and backhaul limited cells in centralised architectures.
- CA flexibility to effectively support dual connectivity.

The research community is recently introducing the idea of CA with *licensed assisted access* that uses part of the unlicensed spectrum for mobile communications. It is thought to be initially deployed in SCells, given the strong power limitations in these bands. The CA capability can ease this new technology by allowing the control data being transmitted in the licensed band and the data information in the unlicensed spectrum. This LTE carrier can be used as a supplemental DL carrier or can be used for UL and DL transmissions.

Appendices

Appendix A

Simulation Environment

This annex explains the simulation environment used throughout the completion of the research presented in this document. First, the scenarios are described and all the simulation assumptions regarding the modeling of the network deployment are also included. Two main scenarios have been used in this dissertation, a Macro-case scenario, used for simulations in chapters 3, 4 and 5 and a HetNet scenario designed for chapter 6. Specific information about each particular case are explained in the corresponding section, however, general assumptions have been maintained to allow for the consistency of this work.

To simulate a 4G mobile network the development of a simulation platform was required. In particular, a dynamic UL system level simulator has been developed during the process of this Ph.D thesis. The last part of this annex is devoted to the detailed description of this simulator.

A.1 Macro-case Scenario

This scenario is a 3GPP based, urban macro-case that follows the guidelines in [19, 30]. It is composed of 14 sites and 3 sectors per site, a total of 42 Macro eNBs, scattered in a regular hexagonal layout. The ISD is considered to be 500 m in general, however a proportional noise-limited scenario of 1732 m has also been used. The propagation model considered is a COST231-Hata model for the different frequencies studied; in general the carrier frequency is 2 GHz unless contrary is indicated. Realistic long and short term fading is considered. Spatially correlated log-normal variations are introduced, based on the two dimensional correlated shadowing model presented in [116]. This model does not consider a shadowing component independently for each user, and nearby ones have related values, situation that closely resembles reality. An extended pedestrian B power delay profile is assumed considering a UE speed of 3 km/h based on the guidelines of [117]. The fast fading channel used is a binary file created by an external channel simulator, it has a time

Table A.1: Parameters common to all studies

Parameter	Value
Carrier frequency	2 GHz
ISD	500 m
ISD	1732 m
Pixel resolution	5 m/pixel
Bandwidth	2x20 MHz
Power delay profile	Extended pedestrian B
Doppler model	Young and Beaulieu [117] 3 km/h
Shadowing correlation distance	50 m
Shadowing deviation	6 dB [115]
UE Buffer size	1 Mb
RTT	8 ms
Target BLER	10 %
SRS periodicity	2 TTI
SRS information expiration	10 TTI
Maximum UE transmission power	23 dBm
MCell transmission power	43 dBm
Termal noise power(σ^2)	-174 dBm/Hz
Distance dependent path-loss	128.1+3.76log(d)[1]

[1] d: distance in km

dimension large enough to spread users in different starting time instants, assuring that all their channels are uncorrelated.

The simulator is dynamic, which means that the system is evaluated during a certain observation time and with a time resolution of 1 TTI, and all metrics are obtained with this resolution. Users are randomly scattered in the simulation area. The wireless access network is considered to have a RTT of 8 ms. Finite buffer communications are assumed and, as soon as the buffer is entirely transmitted, the UE is automatically reconnected in another position, as a new user. This keeps a constant number of interference sources during the simulation time. General specifications of the scenario are detailed in table A.1.

Figure A.1 represents the minimum attenuation map and depicts the network layout. Antennas considered in this scenario are placed at a height of 25 m and radiation patterns from commercial antennas [118] have been used. In particular, the model considered follows the specifications in table A.2. This antenna has a 0-10° electric tilt adjustment. By changing the elevation angle, energy can be concentrated in the target area and interferences towards (and from) other cells can be reduced. That is why it is considered a cost effective method to provide both coverage improvement and interference reduction. In this work fixed downtilt angles of 10° have been introduced for all the sites in the scenario.

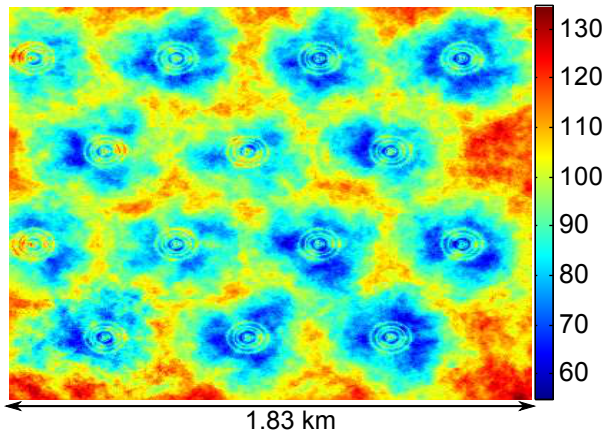

Figure A.1: Minimum attenuation in macro-case synthetic scenario (dB)

Table A.2: Macro antenna specifications

Parameter	Value
Frequency range	[1920-2170] MHz
Gain	18 dBi
Horizontal half power beam	63°
Vertical half power beam	6.5°

A.2 HetNet Scenario

The HetnNet scenario largely follows the macro cellular scenario previously described. It has 14 tri-sectorial sites with 42 MCells and SCells are randomly placed along the area under study. The SCell deployment considers a minimum ISD between them and the MCells which is detailed in table A.3. Antennas are placed at a height of 25 m in MCells and 10 m in the SCells, radiation patterns for MCells are the same as in the previous description and antennas considered for the SCells are omnidirectional antennas with 5 dBi gain. Figure A.2 represents the minimum attenuation map and depicts the network layout.

Table A.3: HetNet: Simulation scenario assumptions

Parameter	Value
MCell ISD	500 m
SCell minimum distance	25 m
SCell-MCell minimum distance	75 m
MCell transmission power	43 dBm
SCell transmission power	20 dBm

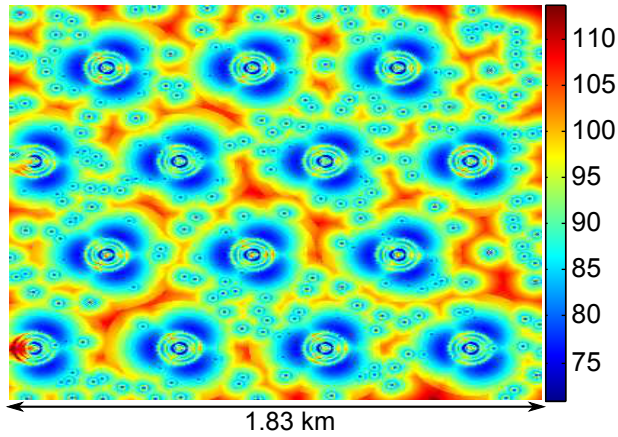

Figure A.2: Minimum attenuation in HetNet synthetic scenario (dB)

A.3 Simulation Platform

In the software tool all the main RRM functionalities have been implemented in a simple but yet realistic way. This section goes through the architecture of the software and details the main LTE-A features included.

A.3.1 Architecture

The simulator is completely developed in C# object-oriented programming language in a .NET framework. The diagram in figure A.3 depicts the simulator structure. The program feeds from configuration documents that provide all the information related to the scenario and simulation parameters that are susceptible of change, thereupon the scenario is created. The main program of the simulation directly calls the scenario, where the dynamic sequential simulation takes place. Complementary functions run in other classes, for example, the CSI class is in charge of allocating sounding resources, calculating the SINR of the entire scenario and deriving UEs to the HARQ process of each eNB.

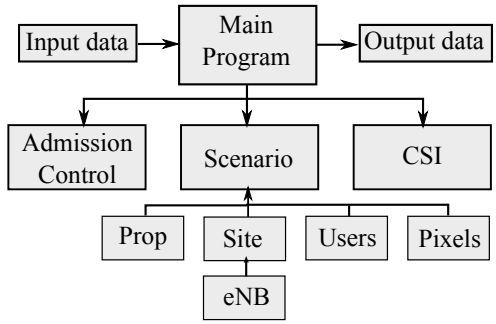

Figure A.3: Software tool diagram

One pixel is the smallest unit in the scenario. It saves all the information regarding the path-loss, shadowing losses and distances, i.e. the static information. In this manner, when UEs move from one pixel to another all the information regarding the scenario can be automatically gathered by updating the pixel in which the UE is placed.

A.3.2 Main features

The platform has been developed with the objective of providing a realistic simulation tool to validate the proposals presented in this document. Therefore the main RRM processes at a system level are modelled and implemented:

- Synchronisation. The eNBs deployed in the scenario are not synchronised. Indeed, all eNBs are randomly set an initial time in the frame. In this manner, SRS and PUSCH transmissions may interfere one another and a more realistic perspective of interference is considered.

- CSI procedure: The eNB allocates the SRSs to the UEs. The SRS allocation process initiates with the UEs multiplex and cyclic prefix assignment. Then, based on the sounding bandwidth selected for the simulation, resources are allocated sequentially. The CSI manager is in charge of gathering the SRS information and calculating the sounding SINR which is handed to the scheduling unit for opportunistic decisions. A RTT different than zero is considered in the simulation. Thus, since the eNB decides the sounding resource allocation and the UE transmits the subsequent sounding signal, a delay of 1RTT (i.e. 8 ms) is considered.

- Packet scheduling: Opportunistic scheduling is carried out every TTI. Based on the information provided by the CSI manager and the past acknowledged throughput, the eNB allocates resources in a PF manner. The scheduler is detailed in 4 and is a HARQ based scheduler that operates in two steps: a time domain, where UEs are ordered based on throughput fairness conditions, and a frequency domain step, where resources are allocated to UEs with the aim

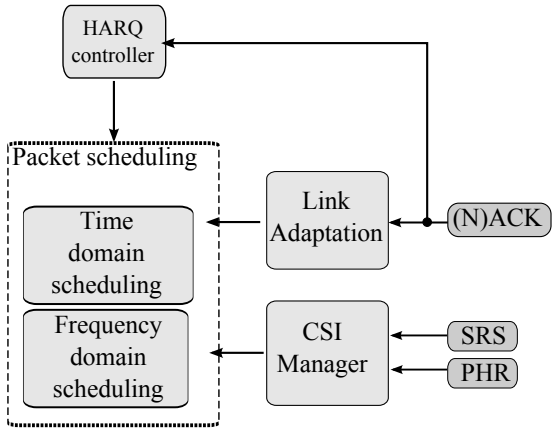

Figure A.4: Information flow in the RRM processes

of maximizing the spectral efficiency in the scheduling process. Sounding SRSs are an input for the frequency division step, where decisions are conditioned to the SINR calculated based on the reference signals. Not to impair the scheduling process, sounding signals are considered to be outdated 20 ms after the reception. As in the sounding allocation process, 1 RTT is considered between the PUSCH scheduling and the reception. As specified in [19] the number of allocable clusters per CC is two, and the number of PRBs per cluster depends on the system bandwidth.

- Link adaptation process: Based on the scheduling decision and the sounding signal information, the most suitable MCS is selected to target a BLER of 10% in the first transmission attempt. The link to system level abstraction follows the guidelines in [98], table A.4 provides the MCS with the SINR target obtained from the link level simulation.
- HARQ process: Is in charge of modeling the error control on each cell. The BLER of each received packet is evaluated, and in case of failure up to three retransmissions are done. Since the HARQ performs incremental redundancy, the relationship between the average BLER value and the measured SINR changes with every retransmission.
- Power control setting: OLPC parameters are configured as described in chapter 3. Power headroom information is considered to be available at the eNB for opportunistic scheduling decisions.

The SINR model calculation is the average received power over the transmission bandwidth (i.e., the sum of power over the different PRBs, divided by the number of PRBs) divided by the average interference over the transmission bandwidth. This is an accurate model as in SC-FDMA each data symbol is spread over the whole allocated bandwidth. So, even though every sub carrier experiences a different channel gain, the differences are averaged out over a sufficiently large bandwidth. Figure A.4 summarizes the information flow in the main RRM processes.

Table A.4: Modulations and Coding schemes and SINR threshold

Index	**Modulation**	**Coding rate**	**SINR (dB)**
0	QPSK	0.12	-4.7
1	QPSK	0.16	-3.4
2	QPSK	0.19	-2.7
3	QPSK	0.25	-1.7
4	QPSK	0.30	-1
5	QPSK	0.37	0
6	QPSK	0.44	1
7	QPSK	0.52	2
8	QPSK	0.59	2.9
9	QPSK	0.67	3.8
10	16QAM	0.33	4
11	16QAM	0.37	4.4
12	16QAM	0.43	5.4
13	16QAM	0.48	6.4
14	16QAM	0.54	7.4
15	16QAM	0.60	8.2
16	16QAM	0.64	8.9
17	64QAM	0.43	9.7
18	64QAM	0.46	10.3
19	64QAM	0.51	11.3
20	64QAM	0.55	12.1
21	64QAM	0.60	13
22	64QAM	0.65	14
23	64QAM	0.70	15
24	64QAM	0.75	15.9
25	64QAM	0.80	16.7
26	64QAM	0.85	17.9
27	64QAM	0.89	18.8

Bibliography

[1] 3GPP, "Requirements for Evolved UTRA (E-UTRA) and Evolved UTRAN (E-UTRAN)," TR 25.913, 3rd Generation Partnership Project (3GPP), Mar. 2006.

[2] R1-072261, "LTE Performance Evaluation - Uplink Summary," Tech. Rep. R1-072261, 3GPP TSG-RAN 50, May 2007.

[3] ITU-R, "Requirements Related to Technical Performance for IMT-Advanced Radio Interface(s)," tech. rep., ITU-R, Nov. 208.

[4] S. Sesia, I. Toufik, and M. Baker, *LTE The UMTS Long Term Evolution, from Theory to Practice*. Wiley Online Library, 2009.

[5] G. Yuan, X. Zhang, W. Wang, and Y. Yang, "Carrier Aggregation for LTE-Advanced Mobile Communication Systems," *IEEE Communications Magazine*, vol. 48, pp. 88 –93, february 2010.

[6] M. Iwamura, K. Etemad, M.-H. Fong, R. Nory, and R. Love, "Carrier Aggregation Framework in 3GPP LTE-Advanced [WiMAX/LTE Update]," *IEEE Communications Magazine*, vol. 48, pp. 60 –67, august 2010.

[7] A. Roessler and S. Merkel, "Carrier Aggregation: A Key Enabler for LTE-Advanced." Microwave Journal Frequency Matters, November 2012.

[8] Z. Shen, A. Papasakellariou, J. Montojo, D. Gerstenberger, and F. Xu, "Overview of 3GPP LTE-Advanced Carrier Aggregation for 4G Wireless Communications," *IEEE Communications Magazine*, vol. 50, pp. 122 –130, february 2012.

[9] K. Pedersen, F. Frederiksen, C. Rosa, H. Nguyen, L. Garcia, and Y. Wang, "Carrier Aggregation for LTE-Advanced: Functionality and Performance Aspects," *IEEE Communications Magazine*, vol. 49, pp. 89 –95, june 2011.

[10] L. Chen, W. Chen, X. Zhang, and D. Yang, "Analysis and Simulation for Spectrum Aggregation in LTE-Advanced System," in *2009 IEEE 70th Vehicular Technology Conference Fall (VTC)*, pp. 1 –6, sept. 2009.

[11] Y. Wang, K. Pedersen, P. Mogensen, and T. Sorensen, "Carrier Load Balancing Methods with Bursty Traffic for LTE-Advanced Systems," in *2009 IEEE 20th International Symposium on Personal, Indoor and Mobile Radio Communications (PIMRC)*, pp. 22 –26, sept. 2009.

[12] L. Zhang, Y. Y. Wang, L. Huang, H. L. Wang, and W. B. Wang, "QoS Performance Analysis on Carrier Aggregation based LTE-A Systems," in *2009 IET International Communication Conference on Wireless Mobile and Computing (CCWMC)*, pp. 253 –256, dec. 2009.

[13] L. Zhang, F. Liu, L. Huang, and W. Wang, "Traffic Load Balance Methods in the LTE-Advanced System with Carrier Aggregation," in *2010 International Conference on Communications, Circuits and Systems (ICCCAS)*, pp. 63 –67, july 2010.

[14] H. Gao, J. Zhang, L. Zhang, and J. Zhang, "Semi-JUS Method for Carrier Aggregation in LTE-Advanced Systems," in *2012 3rd IEEE International Conference on Network Infrastructure and Digital Content (IC-NIDC)*, pp. 631 –635, sept. 2012.

[15] H. Wang, C. Rosa, and K. Pedersen, "Performance Analysis of Downlink Inter-Band Carrier Aggregation in LTE-Advanced," in *2011 IEEE Vehicular Technology Conference (VTC Fall)*, pp. 1 –5, sept. 2011.

[16] H. Tian, S. Gao, J. Zhu, and L. Chen, "Improved Component Carrier Selection Method for Non-Continuous Carrier Aggregation in LTE-Advanced Systems," in *2011 IEEE Vehicular Technology Conference (VTC Fall)*, pp. 1 –5, sept. 2011.

[17] C. Li, B. Wang, W. Wang, Y. Zhang, and X. Chang, "Component Carrier Selection for LTE-A Systems in Diverse Coverage Carrier Aggregation Scenario," in *2012 IEEE 23rd International Symposium on Personal Indoor and Mobile Radio Communications (PIMRC)*, pp. 1004–1008, IEEE, 2012.

[18] Z. Ji-hong, L. Hui, and Q. Hua, "A SPF-PF Crossing Component Carrier Joint Scheduling Algorithm," in *2012 14th International Conference on Advanced Communication Technology (ICACT)*, pp. 173–177, 2012.

[19] 3GPP, "User Equipment (UE) Radio Transmission and Reception (Release 11)," TS 36.101, 3rd Generation Partnership Project (3GPP), Sept. 2012.

[20] H. Wang, C. Rosa, and K. Pedersen, "Performance of Uplink Carrier Aggregation in LTE-Advanced Systems," in *2010 IEEE 72nd Vehicular Technology Conference Fall (VTC 2010-Fall)*, pp. 1 –5, sept. 2010.

[21] H. Wang, C. Rosa, and K. Pedersen, "Uplink Component Carrier Selection for LTE-Advanced Systems with Carrier Aggregation," in *2011 IEEE International Conference on Communications (ICC)*, pp. 1 –5, june 2011.

[22] H. Wang, H. Nguyen, C. Rosa, and K. Pedersen, "Uplink Multi-cluster Scheduling with MU-MIMO for LTE-Advanced with Carrier Aggregation," in *2012 IEEE Wireless Communications and Networking Conference (WCNC)*, pp. 1202 –1206, april 2012.

[23] R. Sivaraj, A. Pande, K. Zeng, K. Govindan, and P. Mohapatra, "Edge-Prioritized Channel and Traffic-Aware Uplink Carrier Aggregation in LTE-Advanced Systems," in *IEEE International Symposium on a World of Wireless, Mobile and Multimedia Networks (WoWMoM)*, pp. 1–9, IEEE, 2012.

[24] Y. Wang, K. Pedersen, P. Mogensen, and T. Srensen, "Resource Allocation Considerations for Multi-Carrier LTE-Advanced Systems Operating in Backward Compatible Mode," in *2009 IEEE 20th International Symposium on Personal, Indoor and Mobile Radio Communications (PIMRC)*, pp. 370 –374, sept. 2009.

[25] Y. Wang, K. Pedersen, T. S andrensen, and P. Mogensen, "Carrier Load Balancing and Packet Scheduling for Multi-Carrier Systems," *IEEE Transactions on Wireless Communications*, vol. 9, pp. 1780 –1789, may 2010.

[26] Y. Wang, K. Pedersen, T. Sorensen, and P. Mogensen, "Utility Maximization in LTE-Advanced Systems with Carrier Aggregation," in *2011 IEEE 73rd Vehicular Technology Conference (VTC Spring)*, pp. 1 –5, may 2011.

[27] L. Liu, M. Li, J. Zhou, X. She, L. Chen, Y. Sagae, and M. Iwamura, "Component Carrier Management for Carrier Aggregation in LTE-Advanced System," in *2011 IEEE 73rd Vehicular Technology Conference (VTC Spring)*, pp. 1 –6, may 2011.

[28] F. Liu, K. Zheng, W. Xiang, and H. Zhao, "Design and Performance Analysis of An Energy-Efficient Uplink Carrier Aggregation Scheme," *IEEE Journal on Selected Areas in Communications*, vol. 32, pp. 197–207, February 2014.

[29] T. Iwai, A. Matsumoto, S. Takaoka, Y. Ogawa, A. Nishio, and D. Imamura, "System Performance of Clustered DFT-S-OFDM Considering Maximum Allowable Transmit Power," in *2011 IEEE International Conference on Communications (ICC)*, pp. 1 –5, june 2011.

[30] 3GPP, "Physical Layer Procedures," TS 36.213, 3rd Generation Partnership Project (3GPP), Sept. 2009.

[31] 3GPP, "Evolved Universal Terrestrial Radio Access (E-UTRA); Physiscal Channels and Modulation," TS 36.211, 3rd Generation Partnership Project (3GPP), Sept. 2007.

[32] A. Ghosh and R. Ratasuk, *Essentials of LTE and LTE-A*. Cambridge University Press, 2011.

[33] M. Ni, X. Xu, and R. Mathar, "A Channel Feedback Model with Robust SINR Prediction for LTE Systems," in *7th European Conference on Antennas and Propagation (EuCAP)*, pp. 1866–1870, IEEE, 2013.

[34] H. Dai, Y. Wang, K. Zhang, and C. Shi, "Link Adaptation Algorithms for Channel Estimation Error Mitigation in LTE Systems," in *Global Communications Conference (GLOBECOM)*, pp. 1835–1840, Dec 2012.

[35] H. Dai, Y. Wang, C. Shi, and W. Zhang, "The Evaluation of CQI Delay Compensation Schemes Based on Jakes' Model and ITU Scenarios," in *2012 IEEE Vehicular Technology Conference (VTC Fall)*, pp. 1–5, Sept 2012.

[36] J. Heo, Y. Wang, and K. Chang, "A Novel Two-Step Channel-Prediction Technique for Supporting Adaptive Transmission in OFDM/FDD System," *IEEE Transactions on Vehicular Technology*, vol. 57, pp. 188–193, Jan 2008.

[37] D. Martin-Sacristan, J. Cabrejas, D. Calabuig, and J. Monserrat, "MAC Layer Performance of Different Channel Estimation Techniques in UTRAN LTE Downlink," in *IEEE 69th Vehicular Technology Conference*, pp. 1–5, April 2009.

[38] S. Falahati, A. Svensson, T. Ekman, and M. Sternad, "Adaptive Modulation Systems for Predicted Wireless Channels," *IEEE Transactions on Communications*, vol. 52, pp. 307–316, Feb 2004.

[39] H. Sahlin, "Channel Prediction for Link Adaptation in LTE Uplink," in *Vehicular Technology Conference (VTC Fall)*, pp. 1–5, Sept 2012.

[40] J.-Y. Wu and W.-M. Lee, "Optimal Linear Channel Prediction for LTE-A Uplink Under Channel Estimation Errors," *IEEE Transactions on Vehicular Technology*, vol. 62, pp. 4135–4142, Oct 2013.

[41] X. Xu, M. Ni, and R. Mathar, "Improving qos by predictive channel quality feedback for lte," in *Software, Telecommunications and Computer Networks (SoftCOM), 2013 21st International Conference on*, pp. 1–5, Sept 2013.

[42] F. Wang, T. Zhang, C. Feng, R. Li, and Yu-Ngok, "Limited Feedback Scheme in the Presence of Feedback Delay using Kalman Filter," in *IET International Conference on Communication Technology and Application (ICCTA 2011)*, pp. 253–257, Oct 2011.

[43] R. Akl, S. Valentin, G. Wunder, and S. Stanczak, "Compensating for CQI Aging by Channel Prediction: The LTE Downlink," in *2012 IEEE Global Communications Conference (GLOBECOM)*, pp. 4821–4827, Dec 2012.

[44] K. Leung, "Power Control by Interference Prediction for Broadband Wireless Packet Networks," *IEEE Transactions on Wireless Communications*, vol. 1, pp. 256–265, Apr 2002.

[45] F. Diehm and G. Fettweis, "Cooperative Interference Prediction for Enhanced Uplink Link Adaptation under Backhaul Delays," in *IEEE 23rd International Symposium on Personal Indoor and Mobile Radio Communications (PIMRC)*, pp. 173–177, Sept 2012.

[46] 3GPP, "Non-Contiguous UL Resource Allocation: Throughput Performance," Tech. Rep. R1-091910, 3GPP TSG-RAN, Jan. 2010.

[47] 3GPP, "Necessity of Multiple Bandwidths for Sounding Reference Signals," Tech. Rep. R1-074807, 3GPP TSG-RAN, Nov. 2007.

[48] 3GPP, "SRS for Carrier Aggregation in LTE-Advanced," Tech. Rep. R1-100458, 3GPP TSG-RAN, Jan. 2010.

[49] Y. Leost, M. Abdi, R. Richter, and M. Jeschke, "Interference Rejection Combining in LTE Networks," *Bell Labs Technical Journal*, vol. 17, no. 1, pp. 25–49, 2012.

[50] A. Simonsson and A. Furuskar, "Uplink Power Control in LTE-Overview and Performance, Subtitle: Principles and Benefits of Utilizing rather than Compensating for SINR Variations," in *IEEE 68th Vehicular Technology Conference VTC 2008-Fall*, pp. 1–5, IEEE, 2008.

[51] C. Castellanos, D. Villa, C. Rosa, K. Pedersen, F. Calabrese, P. Michaelsen, and J. Michel, "Performance of Uplink Fractional Power Control in UTRAN LTE," in *IEEE Vehicular Technology Conference, 2008. VTC Spring 2008.*, pp. 2517–2521, IEEE, 2008.

[52] D. GonzÃ¡lez G, M. GarcÃa-Lozano, S. Ruiz, and J. Olmos, "On the Need for Dynamic Downlink Intercell Interference Coordination for Realistic Long Term Evolution Deployments," *Wireless Communications and Mobile Computing*, vol. 14, no. 4, pp. 409–434, 2014.

[53] X. Mao, A. Maaref, and K. H. Teo, "Adaptive Soft Frequency Reuse for Inter-Cell Interference Coordination in SC-FDMA Based 3GPP LTE Uplinks," in *2008 IEEE Global Telecommunications Conference*, pp. 1–6, Nov 2008.

[54] S. Liu, Y. Chang, G. Wang, and D. Yang, "Distributed Resource Allocation with Inter-Cell Interference Coordination in OFDMA Uplink," in *2012 IEEE Vehicular Technology Conference (VTC Fall)*, pp. 1–5, Sept 2012.

[55] M. Al-Shalash, F. Khafizov, and Z. Chao, "Interference Constrained Soft Frequency Reuse for Uplink ICIC in LTE Networks," in *2010 IEEE 21st International Symposium on Personal Indoor and Mobile Radio Communications (PIMRC)*, pp. 1882–1887, Sept 2010.

[56] 3GPP, "Study on Network-Assisted Interference Cancellation and Suppression (NAIC) for LTE," TS 36.814, 3rd Generation Partnership Project (3GPP), Mar. 2014.

[57] 3GPP, "Enhanced Performance Requirement for LTE User Equipment (UE)," TS 36.814, 3rd Generation Partnership Project (3GPP), Jan. 2013.

[58] J. Andrews, "Seven Ways that HetNets are a Cellular Paradigm Shift," *IEEE Communications Magazine*, vol. 51, pp. 136–144, March 2013.

[59] 4GAmericas, "Developing and Integrating a High Performance HET-NET," tech. rep., October 2012.

[60] S. Tombaz, P. Monti, F. Farias, M. Fiorani, L. Wosinska, and J. Zander, "Is Backhaul Becoming a Bottleneck for Green Wireless Access Networks?," in *2014 IEEE International Conference on Communications (ICC)*, pp. 4029–4035, June 2014.

[61] C. Ranaweera, M. Resende, K. Reichmann, P. Iannone, P. Henry, B.-J. Kim, P. Magill, K. Oikonomou, R. Sinha, and S. Woodward, "Design and Optimization of Fiber Optic Small-Cell Backhaul based on an Existing Fiber-to-the-Node Residential Access Network," *IEEE Communications Magazine*, vol. 51, pp. 62–69, September 2013.

[62] Ericsson, "It all Comes Back to Backhaul," tech. rep., August 2014.

[63] D. Lopez-Perez, I. Guvenc, and X. Chu, "Mobility Management Challenges in 3GPP Heterogeneous Networks," *IEEE Communications Magazine*, vol. 50, pp. 70–78, December 2012.

[64] D. Lopez-Perez, I. Guvenc, and X. Chu, "Mobility Enhancements for Heterogeneous Networks through Interference Coordination," in *2012 IEEE Wireless Communications and Networking Conference Workshops (WCNCW)*, pp. 69–74, April 2012.

[65] M. Joud, M. Garcia-Lozano, and S. Ruiz-Boque, "Selective C-/U-plane split and CoMP to improve moderate speed users performance in small cell deployments," in *"Proc. of IEEE Wireless and Mobile Computing, Networking and Communications WIMOB"*, (Larnaca (Cyprus)), pp. 697–702, 2014.

[66] M. Joud, M. Garcia-Lozano, and S. Ruiz-Boque, "On the Mobility of Moderate Speed Users in Ultra Dense Small Cell Deployments with mmW," in *"Proc. of IEEE Vehicular Technology Conference Spring (VTC-Spring)"*, (Glasgow (UK)), 2015.

[67] 3GPP, "Study on Small Cell Enhancements for E-UTRA and E-UTRAN; Higher Layer Aspects," TR 36.842, 3rd Generation Partnership Project (3GPP), Sept. 2014.

[68] S. Ericsson, "Physical Layer Aspects of Dual Connectivity," Tech. Rep. R1-130566, 3GPP TSG-RAN, Feb. 2013.

[69] DOCOMO, "DOCOMO 5G White Paper," tech. rep., July 2014.

[70] E. Seidel, "LTE-A HetNets using Carrier Aggregation," tech. rep., June 2013.

[71] 3GPP, "Technical Specification Group Radio Access Network; Evolved Universal Terrestrial Radio Access (E-UTRA) and Evolved Universal Terrestrial Radio Access Network (E-UTRAN); Overall description; Stage 2(Release 11)," TS 36.300, 3rd Generation Partnership Project (3GPP), Sept. 2012.

[72] B. Soret, H. Wang, K. Pedersen, and C. Rosa, "Multicell Cooperation for LTE-Advanced Heterogeneous Network Scenarios," *IEEE Wireless Communications*, vol. 20, pp. 27–34, February 2013.

[73] 4GAmericas, "LTE Carrier Aggregation. Technology Developement and Deployment Worldwide," tech. rep., October 2014.

[74] H. Wang, C. Rosa, and K. Pedersen, "Dedicated Carrier Ceployment in Heterogeneous Networks with Inter-Site Carrier Aggregation," in *2013 IEEE Wireless Communications and Networking Conference (WCNC)*, pp. 756–760, April 2013.

[75] H. Wang, C. Rosa, and K. Pedersen, "Uplink Inter-Site Carrier Aggregation between Macro and Small Cells in Heterogeneous Networks," in *2014 IEEE 80th Vehicular Technology Conference (VTC Fall)*, pp. 1–5, Sept 2014.

[76] I. Guvenc, M.-R. Jeong, I. Demirdogen, B. Kecicioglu, and F. Watanabe, "Range Expansion and Inter-Cell Interference Coordination (ICIC) for Picocell Networks," in *2011 IEEE Vehicular Technology Conference (VTC Fall)*, pp. 1–6, Sept 2011.

[77] A. Daeinabi, K. Sandrasegaran, and X. Zhu, "Performance Evaluation of Cell Selection Techniques for Picocells in LTE-Advanced Networks," in *2013 10th International Conference on Electrical Engineering/Electronics, Computer, Telecommunications and Information Technology (ECTI-CON)*, pp. 1–6, May 2013.

[78] X. Lin, J. Andrews, R. Ratasuk, B. Mondal, and A. Ghosh, "Carrier Aggregation in Heterogeneous Cellular Networks," in *2013 IEEE International Conference on Communications (ICC)*, pp. 5199–5203, June 2013.

[79] X. Lin, J. Andrews, and A. Ghosh, "Modeling, Analysis and Design for Carrier Aggregation in Heterogeneous Cellular Networks," *IEEE Transactions on Communications*, vol. 61, pp. 4002–4015, September 2013.

[80] S. Ericsson, "Further Discussions on UL/DL Split," Tech. Rep. R2-131678, 3GPP TSG-RAN, May 2013.

[81] H. Elshaer, F. Boccardi, M. Dohler, and R. Irmer, "Downlink and Uplink Decoupling: a Disruptive Architectural Design for 5G Networks," 2014. 2014 IEEE Global Telecommunications Conference (GLOBECOM 2014).

[82] K. Smiljkovikj, P. Popovski, and L. Gavrilovska, "Analysis of the Decoupled Access for Downlink and Uplink in Wireless Heterogeneous Networks," 2014. Available online at http://arxiv.org/abs/1407.0536.

[83] K. Smiljkovikj, H. Elshaer, P. Popovski, F. Boccardi, M. Dohler, L. Gavrilovska, and R. Irmer, "Capacity Analysis of Decoupled Downlink and Uplink Access in 5G Heterogeneous Systems," 2014. Available online at http://arxiv.org/abs/1410.7270.

[84] H. Elshaer, F. Boccardi, M. Dohler, and R. Irmer, "Load & Backhaul Aware Decoupled Downlink/Uplink Access in 5G Systems," 2014. Available online at http://arxiv.org/abs/1405.1853.

[85] S. Singh, X. Zang, and J. Andrews, "Joint Rate and SINR Coverage Analysis for Decoupled Uplink-Downlink Biased Cell Associations in HetNets," 2014. Available online at http://arxiv.org/abs/1412.1898.

[86] R. Verdone and H. Buehler, "MORANS White Paper," Tech. Rep. available as TD(03)057, COST-237, Jan. 2003.

[87] C. 231, "Propagation prediction models," in *COST-231 Final Rep*, pp. 17–22.

[88] 3GPP, "Evolved Universal Terrestrial Radio Access (E-UTRA); Long Term Evolution (LTE) physical layer; General description," TS 36.201, 3rd Generation Partnership Project (3GPP), Dec. 2007.

[89] 3GPP, "System Level Performances of Non-contiguous RB Assignment for LTE-Advanced Uplink," Tech. Rep. R1-090020, 3GPP TSG-RAN, Jan. 2008.

[90] 3GPP, "PAPR of UL Access Schemes," Tech. Rep. R1-083780, 3GPP TSG-RAN, Oct. 2008.

[91] G. Berardinelli, T. Sorensen, P. Mogensen, and K. Pajukoski, "Transmission over Multiple Component Carriers in LTE-A Uplink," *IEEE Wireless Communications*, vol. 18, pp. 67 –73, august 2011.

[92] 3GPP, "MPR for Non-contiguous Allocation," Tech. Rep. R4-110265, 3GPP TSG-RAN, Jan. 2011.

[93] 3GPP, "MPR for LTE Multi Cluster Transmission," Tech. Rep. R4-110955, 3GPP TSG-RAN, Feb. 2011.

[94] 3GPP, "LTE-A MC RF Requirements for Contiguous Carriers," Tech. Rep. R4-091910, 3GPP TSG-RAN, May 2009.

[95] 3GPP, "PUSCH Power Control for LTE-Advanced," Tech. Rep. R1-092574, 3GPP TSG-RAN, July 2009.

[96] H. H and A. Toskala, *LTE-A 3GPP Solution for IMT-Advanced*. Wiley Online Library, 2012.

[97] A. Pokhariyal, K. Pedersen, G. Monghal, I. Kovacs, C. Rosa, T. Kolding, and P. Mogensen, "HARQ Aware Frequency Domain Packet Scheduler with Different Degrees of Fairness for the UTRAN Long Term Evolution," in *IEEE 65th Vehicular Technology Conference, 2007. VTC2007-Spring*, pp. 2761 –2765, april 2007.

[98] J. Olmos, S. Ruiz, M. Garcia, and D. Martin, "Link Abstraction Models Based on Mutual Information for LTE Downlink," Tech. Rep. available as TD(10)11052, Cost 2100, 2010.

[99] A. Ambrosy, O. Blume, H. Klessig, and W. Wajda, "Energy Saving Potential of Integrated Hardware and Resource Management Solutions for Wireless Base Stations," in *2011 IEEE 22nd International Symposium on Personal Indoor and Mobile Radio Communications (PIMRC)*, pp. 2418–2423, 2011.

[100] M. Lauridsen, A. Jensen, and P. Mogensen, "Reducing LTE Uplink Transmission Energy by Allocating Resources," in *2011 IEEE Vehicular Technology Conference (VTC Fall),*, pp. 1–5, 2011.

[101] N. Mai, Y. Zakharov, and A. Burr, "Iterative B-spline Channel Estimation for Space-Time Block Coded Systems in Fast Flat Fading Channels," in *IEEE 61st Vehicular Technology Conference*, vol. 1, pp. 476–480 Vol. 1, May 2005.

[102] G. Boudreau, J. Panicker, N. Guo, R. Chang, N. Wang, and S. Vrzic, "Interference Coordination and Cancellation for 4G Networks," *IEEE Communications Magazine*, vol. 47, pp. 74–81, April 2009.

[103] M. Wildemeersch, T. Quek, M. Kountouris, and C. Slump, "Successive Interference Cancellation in Uplink Cellular Networks," in *2013 IEEE 14th Workshop on Signal Processing Advances in Wireless Communications (SPAWC)*, pp. 310–314, June 2013.

[104] F. Capozzi, D. Laselva, F. Frederiksen, J. Wigard, I. Kovacs, and P. Mogensen, "UTRAN LTE Downlink System Performance under Realistic Control Channel Constraints," in *IEEE 70th Vehicular Technology Conference Fall (VTC 2009-Fall), 2009*, IEEE, 2009.

[105] K. Pedersen, Y. Wang, B. Soret, and F. Frederiksen, "eICIC Functionality and Performance for LTE HetNet Co-Channel Deployments," in *2012 IEEE Vehicular Technology Conference (VTC Fall)*, pp. 1–5, Sept 2012.

[106] X. Gu, X. Deng, Q. Li, L. Zhang, and W. Li, "Capacity Analysis and Optimization in Heterogeneous Network with Adaptive Cell Range Control," *International Journal of Antennas and Propagation*, vol. 2014, p. 10, April 2014.

[107] F. Baccelli and B. Blaszczyszyn, "Stochastic Geometry and Wireless Networks: Volume I Theory," *Foundations and Trends in Networking*, vol. 3, no. 3â€"4, pp. 249–449, 2010.

[108] H. ElSawy, E. Hossain, and M. Haenggi, "Stochastic Geometry for Modeling, Analysis, and Design of Multi-Tier and Cognitive Cellular Wireless Networks: A Survey," *IEEE Communications Surveys Tutorials*, vol. 15, pp. 996–1019, Third 2013.

[109] J. Andrews, F. Baccelli, and R. Ganti, "A Tractable Approach to Coverage and Rate in Cellular Networks," *IEEE Transactions on Communications*, vol. 59, pp. 3122–3134, November 2011.

[110] S. Singh, H. Dhillon, and J. Andrews, "Offloading in Heterogeneous Networks: Modeling, Analysis, and Design Insights," *IEEE Transactions on Wireless Communications*, vol. 12, pp. 2484–2497, May 2013.

[111] H.-S. Jo, Y. J. Sang, P. Xia, and J. Andrews, "Heterogeneous Cellular Networks with Flexible Cell Association: A Comprehensive Downlink SINR Analysis," *IEEE Transactions on Wireless Communications*, vol. 11, pp. 3484–3495, October 2012.

[112] T. Novlan, H. Dhillon, and J. Andrews, "Analytical Modeling of Uplink Cellular Networks," *IEEE Transactions on Wireless Communications*, vol. 12, pp. 2669–2679, June 2013.

[113] X. Lin, J. Andrews, and A. Ghosh, "Modeling, Analysis and Design for Carrier Aggregation in Heterogeneous Cellular Networks," *IEEE Transactions on Communications*, vol. 61, pp. 4002–4015, September 2013.

[114] S. Puthenpura, "Understanding the Science Behind Small Cell Deployment." AT&T Researchers, November 2013.

[115] 3GPP, "Further Advancements for E-UTRA; Physical Layer Aspects," TS 36.814, 3rd Generation Partnership Project (3GPP), Mar. 2010.

[116] R. Fraile, O. Lazaro, and N. Cardona, "Two Dimensional Shadowing Model," Tech. Rep. available as TD(03)171, COST 273, 2003.

[117] D. Young and N. Beaulieu, "The Generation of Correlated Rayleigh Random Variates by Inverse Discrete Fourier Transform," *IEEE Transactions on Communications*, vol. 48, pp. 1114 –1127, jul 2000.

[118] "Kathrein Website." `http://www.kathrein.com/en/`.